

Response to Reviewers

The authors would like to thank Dr. M. E. Koukouli and another anonymous reviewer for their comprehensive review and for giving us the opportunity to change/clarify various things in the revised version of our manuscript. Below, please find attached our response to each one of the reviewers' comments:

Dr. M. E. Koukouli

1. Line 9, Page 1: Maybe you can use : "also in", because being a two places at the same time sort of defies many major laws of physics. :)

We agree with the reviewer that the use of two current addresses may be confusing. We have only one current address in the revised manuscript.

2. Line 15, Page 1: I am rather concerned about this precise phrasing and would prefer to alter it, it gives an erroneous first impression on how this "corrected" dataset is all about.

We agree with the reviewer. We have rephrased this in the revised manuscript: "...*The GOME and GOME-2 data are "corrected" relative to the SCIAMACHY to produce a self-consistent dataset that covers the period 4/1996-9/2017...*".

3. Line 18, 19 and 21, Page 1: I do not think that you can use e.g. here since the numerical findings you quote are the results of your work, right? I would delete the e.g. from this location and the others also highlighted.

We agree with the reviewer. We have removed "e.g." in the revised manuscript.

4. Line 32, Page 2: Maybe you can update with this: Munro, R., Lang, R., Klaes, D., Poli, G., Retscher, C., Lindstrot, R., Huckle, R., Lacan, A., Grzegorski, M., Holdak, A., Kokhanovsky, A., Livschitz, J., and Eisinger, M.: The GOME-2 instrument on the Metop series of satellites: instrument design, calibration, and level 1 data processing – an overview, *Atmos. Meas. Tech.*, 9, 1279-1301, <https://doi.org/10.5194/amt-9-1279-2016>, 2016.

The paper of Munro et al. (2016) is now cited.

5. Line 5, Page 3: This is not such a general reference to use for describing the two sensors, you could you the Munro et al., 2016, reference or also:

Hassinen, S., Balis, D., Bauer, H., Begoin, M., Delcloo, A., Eleftheratos, K., Gimeno Garcia, S., Granville, J., Grossi, M., Hao, N., Hedelt, P., Hendrick, F., Hess, M., Heue, K.-P., Hovila, J., Jønch-Sørensen, H., Kalakoski, N., Kauppi, A., Kiemle, S., Kins, L., Koukouli, M. E., Kujanpää, J., Lambert, J.-C., Lang, R., Lerot, C., Loyola, D., Pedernana, M., Pinardi, G., Romahn, F., van Roozendaal, M., Lutz, R., De Smedt, I., Stammes, P., Steinbrecht, W., Tamminen, J., Theys, N., Tilstra, L. G., Tuinder, O. N. E., Valks, P., Zerefos, C., Zimmer, W., and Zyrichidou, I.: Overview of the O3M SAF GOME-2 operational atmospheric composition and UV radiation data products and data availability, *Atmos. Meas. Tech.*, 9, 383-407, <https://doi.org/10.5194/amt-9-383-2016>, 2016.

We thank the reviewer for her suggestion. We replace the Wang et al. (2017) paper with Munro et al. (2016) which is a more general reference.

6. Line 17, Page 3: The wording "first time" refer to the usage of the four specific sensors or the technique? I would be a bit weary in using such a phrase after spending a whole paragraph above stating other relevant efforts.

We agree with the reviewer, the phrase "for the first time" has been removed in the revised manuscript.

7. Line 19, Page 3: Updated also,

Levelt, P. F., Joiner, J., Tamminen, J., Veefkind, J. P., Bhartia, P. K., Stein Zweers, D. C., Duncan, B. N., Streets, D. G., Eskes, H., van der A, R., McLinden, C., Fioletov, V., Carn, S., de Laat, J., DeLand, M., Marchenko, S., McPeters, R., Ziemke, J., Fu, D., Liu, X., Pickering, K., Apituley, A., González Abad, G., Arola, A., Boersma, F., Chan Miller, C., Chance, K., de Graaf, M., Hakkarainen, J., Hassinen, S., Ialongo, I., Kleipool, Q., Krotkov, N., Li, C., Lamsal, L., Newman, P., Nowlan, C., Suleiman, R., Tilstra, L. G., Torres, O., Wang, H., and Wargan, K.: The Ozone Monitoring Instrument: overview of 14 years in space, *Atmos. Chem. Phys.*, 18, 5699-5745, <https://doi.org/10.5194/acp-18-5699-2018>, 2018.

We thank the reviewer for noting that, the Levelt et al (2006) reference has been replaced from Levelt et al. (2018).

8. Line 8, Page 4: I assume that there exists a main paper that describes the algorithm? please add the reference here.

We cite the Boersma et al. (2004) paper here in the revised manuscript.

9. Line 23, Page 4: Is there a report/paper that details this methodology? for e.g. is there a minimum of days that are required for the equivalent month to be calculated? is there an effective day consideration? also, where all SZs there a report/paper that details this methodology? for e.g. is there a minimum of days that are required for the equivalent month to be calculated? is there an effective day consideration? also, where all SZAs used? how about locations with high albedo? was the associated error included in the averaging? how about negative trop NO₂ columns which are also reported in the nominal data? and so on. As used? how about locations with high albedo? was the associated error included in the averaging? how about negative trop NO₂ columns which are also reported in the nominal data? and so on.

We thank the reviewer for giving us the opportunity to clarify this. In the end of Sect. 2.1 we added the following phrase in the revised manuscript describing the method that was followed and the various filters that were applied when averaging.

"...When averaging, each observation is weighted by its fractional area (%) within the grid cell. For each valid observation, the cloud radiance fraction has to be less than 50% (cloud fraction less than about 20%) and the surface albedo not higher than 0.3, while observations with a solar zenith angle higher than 80° are filtered-out. In addition, there is no limitation in the number of observations used, negative columns are taken into account, and the observational error is ignored in the averaging process (e.g. Schneider et al., 2015)...."

10. Line 24, Page 4: Have these datasets been used previously in similar studies, or validation studies, or trend studies, or intercomparison campaigns, etc? if so, a brief mention is worth here.

This is the standard averaging method has been applied in a number of studies in the past. Here we cite Schneider et al. (2015) who used the same averaging method for the same version (TM4NO₂A v.2.3) of data.

11. Line 25, Page 4: I have a major concern regarding the methodology provided below, which I am sure stems from the fact that the authors have not wished to increase their article in length by explaining in detail but I consider it paramount: since they already work on monthly mean gridded data, i.e. 0.25x0.25 deg, how do they justify in post-correcting for the different pixel sizes of the original instantaneous measurements? isn't this correction already taken care of by the original gridding where "When averaging, the observations were weighted by the size of the overlapping surface defined by the pixel and the corresponding grid cell." [verbatim from page 4, line 22.]

I am guessing that the first correction, CF1, has more to do in harmonising the datasets not in spatial resolution [horizontal resolution as the authors state] but in general differences due to observation geometry, spectrometric/radiometric differences, FWHM differences, etc.

I expect this topic to be discussed clearly and explained adequately in the next version of the manuscript.

We thank the reviewer for giving us the opportunity to clarify this. Indeed, when gridding the data, the original swath measurements are weighted according to the size of the overlapping surface defined by the pixel and the corresponding grid cell (see details in the answers above). However, this does not impact the fact that the information included in a larger swath corresponds to a larger area. Hence, the gridded data which are produced from larger pixels (e.g. 320 x 40 km² for GOME) will be of "lower resolution" than the ones produced from smaller pixels (e.g. 60 x 30 km² for SCIAMACHY) and the resulting maps will be much smoother, despite the fact that the grid cell size is the same (0.25° x 0.25°). As the GOME nominal resolution is nearly 3 times lower than that of SCIAMACHY at the horizontal dimension, we may assume that each grid cell of the GOME gridded data despite having the same size with SCIAMACHY grid cells, will correspond to an area nearly 3 times larger. The latitudinal dimension is considered to be close in both the datasets (40 km vs 30 km) and also close to the latitudinal dimension of the gridded data (0.25°). This is why we used a boxcar algorithm with an averaging window of 13 x 0.25° (3.25°) in the longitudinal direction only, similarly to Geddes et al. (2016) to smooth the SCIAMACHY data (CF1). Our results are very close to the ones seen in Hilboll et al. (2013) where a more detailed pixel by pixel approach was followed. Taking into account this and the discussion above we prefer to preserve the term "spatial resolution correction" in the revised version of the manuscript. A paragraph explaining the whole reasoning has been added in the revised manuscript.

12. Line 1, Page 5: Also at this location, I suggest you alter this phrase. No one can really reproduce what an instrument would have seen where it in orbit, and functioning, longer.

We agree with the reviewer. We have removed this phrase in the revised manuscript.

13. Line 4, Page 5: What does this VCDsc stand for?

We mention in the revised manuscript: "...the SCIAMACHY monthly gridded VCD data (VCD_{SC}) were smoothed..."

14. Line 7, Page 5: It would be beneficial to explain why this correction is performed in the horizontal resolution only, since the satellite pixels are not entirely aligned in the east-west direction but, depending on the sensor, have a different geospatial direction.

We understand fully the reviewer's point. However, the fact that satellite pixels are not entirely aligned in the east-west direction having a different geospatial direction is ignored following Hilboll

et al. (2013) and Geddes et al. (2016), considering this of minor importance compared to the correction that has to be applied in the horizontal direction.

The following phrase is added in the revised manuscript: *The correction is applied in the horizontal dimension only as the along track dimensions are close in the two datasets (40 km vs 30 km) and also close to the latitudinal dimension of the gridded dataset (0.25°).*

Please also look into our answer No.11 above and the corresponding paragraph we added in the revised manuscript.

15. Line 9, Page 5: I am assuming that this factor is calculated on molec/cm². Which means that, for small changes in absolute numbers between VCD_{sc} and VCD_{sc-sm}, this may result in a rather un-physically large number. How do you deal with this issue? any limits imposed?

So, you are basically saying that you spread the SCIAMACHY observations to a pseudo-GOME pixel size and then you de-seasonalise them and then you multiply the CF1 factor to the GOME data in order to create a pseudo-GOME product on the SCIAMACHY pixel size?

We thank the reviewer for giving us the opportunity to improve our manuscript here. CF1 is dimensionless as it is the ratio of VCD_{SC} and VCD_{SCsm} on a climatological monthly basis. As discussed in the revised manuscript to avoid having unreasonably large CF1 values due to very low tropospheric NO₂ levels, CF1 was set equal to 1, in cases of VCD^{SCsm} lower than 0.1 x 10¹⁵ molecules cm⁻² which corresponds to SCIAMACHY's precision.

Indeed, this is the general idea.

Line 14, Page 5: I understand why you would have to show these maps in the supplement, instead of the main text, however you definitely have to discuss them, explain what is seen, what was found, was there a seasonal pattern [which is not shown in these annual averages, for e.g. that summertime was systematically over or wintertime was over.] Since you are applying this technique on a species that has a very clear seasonal variability, such discussion is paramount. Also, in the legend of Fig S1, you note:

"A value of 1 was used in cases where the mean tropospheric NO₂ VCD was lower than SCIAMACHY's precision (0.1 x 10¹⁵ molecules cm⁻²)."

This is information that should appear in the text, alongside a comprehensive discussion on what a less than unity value signifies. I suggest that you can add one of these four figures in the main text.

Also, I was surprised to see patterns in the CF1 that appear to alter in the latitudinal direction and not the longitudinal direction, which is the one "corrected" for. How do you discuss this? please add in the text.

We added a new figure (Fig. 1) where we show the changes that the original GOME data undergo from step to step and discuss the correction factor patterns trying to connect them with areas of high and low tropospheric NO₂. This is a large improvement in our paper. In addition, the CF1 patterns have been plotted on a global and regional basis on a monthly and annual basis. Now the reader may get an idea about the seasonal variability of the CF patterns which are pretty persistent throughout the year as discussed in the revised manuscript. The CF1 patterns are given in high resolution in the supplement along with similar figures for CF2 and CF3. The paragraph has been enhanced so that the readers can find various important details about our method.

For the limit value of 1, please see our answer above.

As discussed in the revised manuscript CF1 exhibits characteristic spatial patterns with values greater than and lower than 1 over and adjacent to pollution hotspots, respectively. The CF1 patterns are pretty persistent throughout the year.

16. Line 14, Page 5: Do you apply the CF1 to GOME-2 as well? I am guessing not. Then maybe you should not mention GOME-2 here as it appears slightly confusing.

We agree. We refer to the GOME period only in the revised manuscript.

17. Line 19, Page 5: Shift correction due to which SCIA/GOME difference? more detail is needed here to explain why this CF2 is applied and what exactly it is.

The details are given in a couple of lines below that point "*...The shift correction factor (CF2: 1 value for each grid cell) is equal to the difference between the two datasets for the common period and was calculated on a grid cell basis (Eq. 4) similarly to Geddes et al. (2016)...*". However, we added a few lines connecting this correction with the work of Hilboll et al. (2013). Following, Hilboll et al. (2016) who used a trend model that explicitly accounts for a level shift between the two instruments and for a change in the amplitude of the seasonal variation, we applied a shift correction (step 2) and a seasonal amplitude correction (step 3) successively, on top of the spatial resolution correction (step 1). The goal here is to account for instrumental biases that were not corrected with the spatial resolution correction. The method follows the reasoning of Geddes et al. (2016) who applied a shift correction but for annual data.

18. Line 20, Page 5: Which two datasets? SCIA VCDsc and GOME VCDcg1? SCIA VCDscsm and GOME VCDcg1? ... and GOME VCDg?

These two paragraphs have proven quite difficult to follow, since the reader has to go back and forth between this part of the paper, Appendix A and the supplement. I strongly suggest to the authors to move the equations here, and at least one of the Figs S1 to S4 and Figs S5 to S8 in this part of the text so that the reader can follow seamlessly the methodology and benefit from its discussion.

We added VCD_{SC} after SCIAMACHY: "*...were compared against SCIAMACHY data (VCD_{sc})...*" and the corresponding equations from the Appendix were placed at the end of the paragraph.

The equations that correspond to each correction step are now at the end of the corresponding paragraphs within the text and not in an Appendix.

19. Line 25, Page 5: Normalized to what?

We rephrase this paragraph also including the equations in the text.

20. Line 27, Page 5: Normalized to what?

The same as above.

21. Line 33, Page 5: As you know, GOME2A has been suffering from degradation effects and shows different levels for its atmospheric retrievals than GOME2B. Also the GOME2A pixel size has changed during the time period chosen. How are these issues dealt with/compensated for?

The GOME-2A and GOME-2B data were assumed to be of equal quality and resolution within the calculations. As $80 \times 40 \text{ km}^2$ (GOME-2A before July 2013 and GOME-2B) is equally different to the SCIAMACHY resolution like $40 \times 40 \text{ km}^2$ (GOME-2A after July 2013) the authors decided not to apply any corrections and the GOME-2A and GOME-2B data were averaged on a monthly basis. We mention that in the revised version of the manuscript.

22. Line 6, Page 6: Due to the systematic lack of....

Corrected.

23. Line 13, Page 6: What constitutes a major trend reversal as far as NO₂ is concerned? this is a very important detail which have to be discussed and the choice explained.

We acknowledge that this phrase might be puzzling for the reader and hence we decided to omit it. The method reports only one reversal (where $S(t)$ minimizes). There is not much possibility that there were more than one significant reversals (secondary $S(t)$ minima) within the period studied here. However, in the future when there will be three or four decades of data there may be a need for the detection of more than one reversals. This is why in the last sentence of the paper we write: *"...the need to develop similar methods in the future that will be able to incorporate both morning and afternoon measurements (e.g. from OMI and TROPOMI) and detect more than one trend reversal points in improved tropospheric NO₂ products (e.g. QA4ECV v.1.1, Zara et al., 2018 and references therein) is acknowledged..."*

Also, the trend reversal method is now described in more details and it is placed within the text and not in an Appendix.

24. Line 16, Page 6: A general comment on the discussion of the methodology: even though the authors mention that they chose to have the equations and such like in the appendix so that the text quickly enters the results section, I find it very hard to follow [and be convinced by] the methodology since it is a constant back and forth to the appendix and the supplement. I strongly suggest that they re-think this strategy, that they add the equations in the main text, and also include an example of how the GOME [for e.g.] VCD alters between the nominal and the corrected levels for the three corrected VCDs. The annual CFs may not be so important, especially since the authors simply give the plot without discussion, but for the reader [and potential user of this new dataset] it is important to see how the original satellite data alter.

We thank the reviewer for giving us the opportunity to do this change in the revised manuscript. As discussed above, the detailed description of the method has been placed in the Methodology Section within the text. We agree that this will make it easier for the reader to follow the various changes that the data undergo within each step of the method. In addition, a figure (Fig. 1) has been added with the tropospheric NO₂ patterns for the whole GOME period from the original (VCD_G) data (a), from the corrected in step 1 (VCD_{GC1}) data (b), from the corrected in step 2 (VCD_{GC2}) data (c) and from the corrected in step 3 (VCD_{GC3}) data (d).

25. Line 19, Page 6: The multi year average tropospheric...

Corrected.

26. Line 19, Page 6: -GOME-2 dataset ... [space missing]

Corrected.

27. Line 21, Page 6: I am afraid that the choice of colour bar does not permit such a careful look, or it is a problem of providing the figure with sufficient analysis. I suggest you change the colour bar to the more typical, for e.g., http://www.temis.nl/airpollution/no2col/no2month_tropomi.php?Region=9&Year=2018&Month=02 which allows for the shipping tracks to show clearly.

We agree with the reviewer and hence we have changed our colobar. Now, the ship tracks can be seen more clearly. Our original figures are in high resolution and we will make sure in close collaboration with the copyediting department of the Copernicus that they will appear perfectly in the final version of the paper.

28. Line 25, Page 6: Maybe you could also add other works such as: <https://www.nature.com/articles/srep35912>; Krotkov, N. A. et al. Aura OMI observations of regional SO₂ and NO₂ pollution changes from 2005 to 2015. *Atmos. Chem. Phys.* 16, 4605–4629 (2016); <https://www.tandfonline.com/doi/full/10.1080/01431161.2018.1430402>; <https://agupubs.onlinelibrary.wiley.com/doi/full/10.1002/2017GL076788>; <https://www.atmos-chemphys.net/17/9261/2017/>

We also cite the works of de Foy et al. (2016) and Krotkov et al. (2016) which refer directly to the three urban clusters.

29. Line 28, Page 6: I also suggest that you add references to other works that have observed these hotspots from space, a short review of ScopuS results would provide you with numerous choices.

We have added some references here including global maps with tropospheric NO₂ also suggesting that one should also look into the references given there.

30. Line 1, Page 7: maybe you can write "various socioeconomic changes", if you do not wish to mention specifically what types of changes.

We added "socioeconomic"

31. Line 5, Page 7: If the reason you are showing both these figures is to compare to the work of Schneider et al. then you definitely need to add a nice long comparison between your work and theirs. IF you do not plan to add such a comparison, then I would exclude Fig2a and add zoomed-in plots showing Europe/Africa/East Asia/etc, i.e. so that one can see also visually the findings you have in your tables.

Furthermore, since you have already discussed the trend reversal, how do you justify showing this Figure? for e.g. at locations where you found a trend reversal which trend do you depict in this plot?

We thank the reviewer for giving us the opportunity to clarify this. First of all, our goal is not to compare our results with Schneider et al. (2015); however, it is important that our results are similar to that of Schneider et al. (2015) despite the fact that we use a much longer period in our analysis and not a single sensor like they did. This is indicative of the fact that the sources are persistent during the period we study and despite the trend reversal that some regions experienced, the sign of the trends for the whole satellite period has not yet changed (the significance has changed in some cases).

As this is the first global map presented using more than two decades of tropospheric NO₂ from satellites we prefer to keep this figure as is. We have produced regional plots with the trends but we believe that it is better for the reader to have the whole picture.

When preparing the manuscript we also thought of keeping only the second panel (Fig. 3b) with the statistically significant results. However, we decided that we should include the non-statistically significant trends which they still show a kind of tendency. In addition, we have gone through comparisons of the trends with data from the recently released QA4-ECV product (<http://www.qa4ecv.eu>). We have seen that despite the fact that the trends are largely similar in the two datasets, the QA4-ECV, trends are much smoother over the oceans and in some cases the tendencies are opposite (see Deliverable 6.3: <http://www.qa4ecv.eu/node/9>). As this new dataset is going to be used in the future for trend analysis studies, we believe it is very important to include a map with the all the trends regardless of their significance. Unfortunately, keeping the Fig. 3a and indicating statistical significance (like e.g. in Pozzer et al., 2015) with a symbol (e.g. + or ·) is not possible due to the high resolution of the data.

When writing the paper at first place we decided to show the full period trends regardless of the fact that there may be a reversal. The calculation of the trends for a 2-decades period that we focus here period is not wrong, it gives us an indication of the general tendency of the tropospheric NO₂ levels during the whole period of measurements. However, the detection of trend reversals and the calculation of the trend for the period before and after is just more accurate. We strongly believe that the presentation of the full-period trends and then the trend reversals is the optimal way of stating that our results are similar to previous studies with shorter periods (and maybe one single sensor), but now it is time to start taking into account the trend reversals. With our approach one may also see that despite the fact that a trend appears to be insignificant there are two different periods (before and after the reversal) with significant trends of opposite sign.

We will make sure that the figure appears large enough and in high resolution in the final manuscript so that each detail can be seen.

32. Line 8, Page 7: Shouldn't the precision of the GOME and GOME2 sensors also worry you? what levels are those at? maybe 0.1×10^{15} is a bit too optimistic?

We decided to keep a uniform precision of 0.1×10^{15} molecules cm⁻² as the SCIAMACHY data are used as the GOME and GOME-2 data are "corrected" relative to the SCIAMACHY data. The same reasoning was followed by Hilboll et al. (2013).

33. Line 8, Page 7: It would also be interesting if you were to actually compare you work with that of Hilboll et al., 2013, since you actually used their technique.

We agree with the reviewer that a detailed comparison would be very interesting; however, this is not within the scope of the current paper. Here, we compare our findings with Hilboll et al. (2013) qualitatively rather than quantitatively and our results are indeed close to theirs. However, taking into account that we did not apply the same method but our method was based on their reasoning there may be differences.

34. Line 9, Page 7: I am not sure I follow your mathematical knowledge here, why does the cut-off value of 0.1×10^{15} mol/cm² mean 2 decimal places for the trend result and not 1 decimal place, for e.g.?

The 2 decimal places refer to the -0.0037×10^{15} molecules cm⁻² yr⁻¹ value that is well above the precision value (0.1×10^{15} molecules cm⁻²). So, any trend above this "background" trend of our self-consistent dataset may be considered "real" and the use of two decimal places definitely ensures that.

35. Line 12, Page 7: Add here the actual numbers, I assume that they appear on one of the Tables further below, but it useful to have them here. Also, how do your trends compare to other trend studies? in numerics.

We have added the required information in the text.

"...America (the region of Mexico city). The trend values over these areas are higher than 0.05×10^{15} molecules $\text{cm}^{-2} \text{yr}^{-1}$, with a maximum value of 2.18×10^{15} molecules $\text{cm}^{-2} \text{yr}^{-1}$ appearing within the BTH urban cluster in eastern China. On the contrary, strong statistically significant negative trends appear over the largest part of the U.S. (especially the eastern U.S. and the state of California), western and central Europe, Japan and Taiwan in south-eastern Asia and the region around the Johannesburg-Pretoria conurbation in South Africa. The absolute trend values over these areas are higher than 0.05×10^{15} molecules $\text{cm}^{-2} \text{yr}^{-1}$, with a maximum value of 1.40×10^{15} molecules $\text{cm}^{-2} \text{yr}^{-1}$ appearing close to Los Angeles city in the eastern U.S..."

36. Line 20, Page 7: You definitely need numerics here, I am sorry to have to say. How similar is similar?

We refer here to the patterns and not the trend values per se. We acknowledge that the use of word "similar" here is not proper and hence we rephrased this sentence. Comparing the trend values with values from other studies quantitatively is not as trivial as it may seem because they refer to different periods. We therefore did not proceed to a quantitative comparison here.

"...In general, the trend patterns here resemble the ones appearing in previous satellite-based studies for shorter periods (e.g. van der A et al., 2008; Schneider et al., 2012; Hilboll et al., 2013; Krotkov et al., 2016)..."

37. Line 24, Page 7: Is this per annum or per decade? please specify.

This is the percentage decrease or increase (relative to the fitted mean for the first year) for the whole period. We give this information in the revised manuscript wherever these values appear.

38. Line 27, Page 7: Please compare these findings to other major works in literature, either satellite works or ground-based/in situ findings.

The % changes given here are not directly comparable to that of other works. This has to do with the fact that the trends are calculated relative to a different period. E.g. our % trends are calculated relative to the fitted mean for the first year (see van der A et al., 2006) while Schneider et al. (2015) used the whole period of SCIAMACHY as a base period and Hilboll et al. (2013) used 1996 as a base year. Taking this into account and our answers to comment 33 and 36 we refrained from comparing quantitatively these results with results from other works.

39. Line 29, Page 7: Indeed, which is now worrying that you are moving into stating that the trend already shown is not one trend but two. How do you explain this?

As discussed above we decided to show the full period trends regardless of the fact that there may be a reversal. The calculation of the trends for a 2-decades period that we focus here period is not wrong, it gives us an indication of the general tendency of the tropospheric NO₂ levels during the whole period of measurements. However, the detection of trend reversals and the calculation of the trend for the period before and after is just more accurate. We strongly believe that the presentation of the full-period trends and then the trend reversals is the optimal way of stating that our results are

similar to previous studies with shorter periods (and maybe one single sensor), but now it is time to start taking into account the trend reversals. With our approach one may also see that despite the fact that a trend appears to be insignificant there are two different periods (before and after the reversal) with significant trends of opposite sign.

40. Line 4, Page 8: I strongly suggest you break down these figures into sub-figures that show zoomed-in, as was shown for e.g. in Schneider and van der A, 2012. That way you can also discuss them more easily.

We thank the reviewer for giving us the opportunity to improve our figures. Zoomed-in global figures are provided in the revised manuscript. We excluded areas that did not present any reversals and at the same time we preserved all the interesting information into two single panels. As this is a highlight figure of the paper we will make sure in close collaboration with the copyediting department of the Copernicus that it will appear large and clear enough in the final version of the paper. All the figures are plotted in high resolution and we will make sure they appear perfectly.

41. Line 8, Page 8: This is precisely the point I cannot follow, how do you show the positive trend in Fig 2a and then in Fig 3a show the trend reversal?

Please see our answers to comment 39 and comment 31.

42. Line 17, Page 8: between

Corrected

43. Line 21, Page 8: What do these standards mean, in numbers, i.e. what are the new levels of emissions permitted?

The maximum allowed amount of on-road vehicle NO_x emissions was reduced by 50%. This information is included in the revised manuscript.

44. Line 21, Page 8: This refers to NO_x? VOC? particles?

This refers to a number of restrictions (e.g. a ban on older polluting cars) that were implemented in specific cities in China (e.g. Beijing) rather than to specific emissions. We have rephrased this in the revised version of the manuscript.

"...Stricter regulations were implemented on a city level for on-road vehicles (e.g. a ban on older polluting cars in Beijing)..."

45. Line 25, Page 8: (see Fig 3a.)

This was changed.

46. Line 26, Page 8: Maybe the quotes are not necessary.

Quotes were removed.

47. Line 28, Page 8: ... China, large....

Corrected.

48. Line 28, Page 8: I think that you have to discuss a bit on India's air quality here, and not to assume that all readers are well-versed in the details of the air over there. Much like you did for China, even though India does not have a five-year plan. What are the sources of pollution over there? what is already known? does this add to you finding a trend reversal in all those locations? Hilboll et al., 2017, cannot be the only source of reference in this point.

We thank the reviewer for giving us the opportunity to enhance this paragraph in the revised manuscript (see below). In addition, a number of additional papers are now cited.

"... Similarly to eastern China, large parts of India experienced a reversal from positive to negative trends mostly in 2011. On the contrary, areas in central-southern India experienced a reversal from negative to positive trends at some point in the period 2000-2006. India experienced a population growth of ~37% (relative to 1996) during the period 1996-2017, mostly in urban areas, which was accompanied by a gross domestic product (GDP) increase of ~29% (World Bank, 2019). NO_x emissions generally increased as a result of large-scale urbanization (rural population decreased from ~73% of the total population in 1996 to ~66% in 2017), industrialization and economic growth, energy production, industry and transportation being the main contributors to the emissions (Ghude et al., 2013 and references therein). The Indian economy started developing at much higher rates after 2002 (World Bank, 2019) which might explain the observed negative to positive trend reversals appearing in the years 2000-2006 over specific regions (e.g. increase of tropospheric NO₂ in the greater Ballari region due to the rapid growth of the steel industry, especially after 2006). India's economic growth experienced a slow-down after 2011 (GDP still increased but at a lower rate) which might explain part of the observed positive to negative trend reversals over specific areas. Hilboll et al. (2017) also observed a stagnation of tropospheric NO₂ over India, attributing it to a combination of a slow-down in Indian economic development, the implementation of cleaner technology (e.g. Bansal and Bandivadekar, 2013), meteorological factors (see Voulgarakis et al., 2010) and changes in tropospheric chemistry. However, it has to be noted that the way all these parameters may influence the tropospheric NO₂ levels and trends over India is pretty complicated and should be studied in more detail in the future..."

49. Line 31, Page 8: So you mean that somewhere in those six years some areas in C-SE India showed a trend reversal? is this significant? is this something one may use? How much did the population increase within the ~21 years you are studying? how about demographics? how many farmers turned into city people? and so on.

We have rephrased that (see answer to comment 48). We mean that there is a reversal at some point within the period 2000-2006. As discussed several times in the manuscript we report a trend reversal only when the trend for the whole period before the reversal year or the trend for the whole period after the reversal year is statistically significant at the 95% confidence level. So, yes the result is statistically significant. Several numbers concerning the population statistics are given in the revised manuscript (see previous answer).

50. Line 32, Page 8: You mean that the steel industry became as stronger presence in that region? please re-phrase and also explain the steel industry emissions of NO_x.

Yes, we have rephrased this sentence (see answer to comment 48). To manufacture steel requires very high temperatures for smelting and processing and the related combustion processes lead to emissions of NO_x.

51. Line 2, Page 9: You definitely need to expand on a few more details on this study, what does "in accordance" mean? numerics on the trend reversals from the in situ measurements are definitely a good idea to strengthen your case.

We have added a sentence here: "...which is in accordance to NO₂ ground concentration measurements. More specifically, in Cuevas et al. (2014) a continuous drop of surface NO₂ is seen after 1999-2000 over the two cities..."

52. Line 6, Page 9: Investigate further in either scientific references or policy making reports and add your sources to this statement.

We have added a sentence here and two related reports.

"...(EEA-APFS-Spain., 2014). Following the European Union directives, Spain introduced its First National Emission Reduction Program in 2003 setting stringent combustion emission standards (IEA, 2017). This was afterwards updated and revised leading to the Second National Emission Reduction Program in 2008."

53. Line 7, Page 9: Investigate further in either scientific references or policy making reports and add your sources to this statement.

The same as above.

54. Line 8, Page 9: Maybe there are other, more appropriate references to add here for the economic crisis of 2008 over Spain?

This is a highlight paper that discusses the effect of economic crisis on Spain NO₂ levels and it is the most appropriate for what we discuss here.

55. Line 9, Page 9: Any explanations on this fact?

We cite here a report (EEA-APFS-Portugal., 2014) where it is shown that the NO_x emissions decline after 2005 in line with our findings. The trends are similar to that of Spain. So it is probably the compliance with the EU environmental directives that explain the 2004-2005 trend reversals while the reversals in late 2000s- early 2010s are probably related to the financial recession.

56. Line 11, Page 9: ... the whole of Syria...

Corrected.

57. Line 13, Page 9: I am sorry to repeat myself, but you are not doing yourself justice with this Figure. Again I urge you to break it down to sub-figs, and change the colour bar.

We have addressed that issue by providing zoomed-in global figures (see answer to comment 40). Prior choosing the trend reversal colorbar we did several tests using different colors and combinations and this one was found to be the most appropriate. Probably the conversion to pdf affected the colors. Our original figures are in high resolution and we will make sure they appear perfectly in the final article.

58. Line 15, Page 9: Why should this be?

The emissions in neighbouring countries (Syria, Iraq) have decreased due to warfare and hence transported pollution is expected to be less. We decided to remove the sentence about the political/financial involvement of Iran as it is difficult to explain it in a line. We have rephrased

accordingly: "...while a decrease of transboundary transport of NO₂ from neighbouring countries due to the warfare cannot be ruled out..."

59. Line 21, Page 9: Which year? which magnitude of trend reversal? why? and so on...

The trend reversals appear in the early 2000s and are statistically significant. The reasons are probably the same with the regions mentioned in the sentence above. We have rephrased accordingly.

"...Within the Middle East there are also sporadic areas (e.g. in Iran, in Iraq, areas around the Persian Gulf, and areas around the east coast of the Red Sea in Saudi Arabia and the Nile River in Egypt) with a trend reversal from negative to positive in the early 2000s (2000-2003) probably due to changes in power generation, industrial, transport and shipping emissions (Krotkov et al., 2016) (Fig. 4b)..."

60. Line 23, Page 9: Are you not going to discuss this finding further? I would assume that there exists a wealth of references and relevant studies for the US at least.

We prefer to refrain from reaching conclusions about the reversals in Mexico and Africa as there could be a number of different reasons (from environmental policies to land use changes, see e.g. Andela and van der Werf, 2014, doi: 10.1038/nclimate2313). A discussion about the U.S. is given in Sect. 3.4 mostly focusing on California and Los Angeles.

61. Line 2, Page 10: This Figure is very informative and shares a wealth of information extracted from your study, however:

1. Avoid the use of special text effects [for e.g. shadow] for the titles/legends/etc of the figures. In my humble opinion it makes reading the text very difficult, see for e.g. the trend information on the upper right plot. I suggest you remove all these effects and add the plots using the highest resolution possible. For the final version of the article, I of course highly recommend you provide ACP proof teams with *eps versions of your plots.

2. You have to explain the following at this point [it could have been done further up in the text of course]:

a. why did you choose to calculate trends on normal monthly mean time series and not the de-seasonalised monthly means?

b. how do you actually prove that the separation of trends results [right plots] is correct and not the full time series trend [left plots.]? you truly have to actually show this somehow mathematically. Or statistically. Or otherwise, but in actual numerics.

1. We have updated the figure as requested. Such changes have been applied on similar figures in the manuscript. As discussed above, probably the conversion to pdf affected the colors. Our original figures are in high resolution and we will make sure they appear perfectly in the final article.

2a. All the trends are calculated using the Fourier-based method described in detail in the manuscript. The method accounts for the seasonal variability using a Fourier-based seasonal component and hence there is no meaning in deseasonalizing the data before the application of the method as the method more or less "deseasonalizes" the data before calculating the linear trends.

2b. As discussed in previous comments the calculation of the trends for a 2-decades period that we focus here period is not wrong, it gives us an indication of the general tendency of the tropospheric NO₂ levels during the whole period of measurements. The detection of trend reversals and the

calculation of the trend for the period before and after is just more accurate. Hence, the use of a "correctness index" is not within the scope of the current study.

62. Line 28, Page 10: Again, it is not clear to me why both these figures are needed.

Our reasoning is discussed several times above. We want to show that despite there may be a statistically significant trend during the last 2 decades in the meantime there was a trend reversal. It is not wrong to calculate the trend for the whole period, it is just more accurate to break it into two trends and we believe these comparisons are indeed very informative. With the passing of the years and if the reversal continues the trend for the whole period may not be statistically significant any more. We believe our findings would be valuable for future trend studies including 3 or even more decades of satellite data.

63. Line 5, Page 11: This paragraph is rather difficult to read. I suggest a Table with in this information at this point. Table S1 is fine left in the Supplement.

We agree with the reviewer that this paragraph is very informative. In order to save space only countries that exhibit a trend reversal are shown in Table 2, while results for all the world countries are given in Table S1 of the Supplement. Some of these values appear in Table 2 and all of them in Table S1 so putting one more Table that will share values with Table 2 would be too much. As these might be very useful not only for scientists but also for journalists, media or other users we prefer to keep these numbers here.

64. Line 17, Page 11: You had a small phrase here which I wanted to highlight, but deleted by mistake. In any case, my recommendation is to delete it.

Corrected.

65. Line 5, Page 12: As above, please make all the letters/numbers/texts in this figure normal letters and not shadowed/text effects.

Corrected.

66. Line 12, Page 12: You had only one for Spain, so please enhance this.

As discussed above more citations are given in the revised manuscript for Spain.

67. Line 13, Page 12: By how much?

The decline was by 18% relative to 2008 levels. This is given in the revised manuscript.

68. Line 14, Page 12: Annual?

We refer to the annual mean levels. We have corrected accordingly.

69. Line 19, Page 12: Which economic recession is this? the pre-2000 one? is it referred to by a specific name, like the 2008 one is called, the economic crisis of 2008 [for e.g.?)

Details are given in Sect. 3.2. For Argentina we may refer to it as the 1998-2002 great depression, while for Brazil, there is not any specific name. We changes "*economic recession*" to "*economic recessions*" to make clear that we had two different crises.

70. Line 21, Page 12: I find it a bit hard to believe that the Brazilian Government started working towards the Rio Games from year 2000... :)

It should not be necessarily connected to the years around 2000. The preparations started gradually the years after 2009 and this could enhance the positive trend appearing after 2000.

71. Line 32, Page 12: Again, as discussed a number of times already previously, I fail to see the reasoning behind showing the trend for the total period since you are planning on showing trend reversals. You could split this map into two, and show trends for the locations without trend reversal for the entire period and then a two-panel plot for the other locations giving both a negative and positive trend and then year of reversal you find. Furthermore, I suggest you do not use an infinite colour bar here but one with say, 34 or 68 colours, so that the actual differences between locations can be seen with the naked eye.

Please see our answers above. The use of less colors did not change the figure drastically. Hence, we prefer to keep it as is in order to be consistent with the trend maps on a global and country basis.

72. Line 4, Page 13: Comment as per the similar paragraph above.

As discussed above we agree with the reviewer that this paragraph is very informative. However, we believe that such statistics are very useful not only for scientists but also for journalists, media or other users and hence we strongly believe they should be included in the text.

73. Line 14, Page 14: Comment as above.

Corrected.

74. Line 8, Page 16: Unless you can verify this with financial figures [e.g. GDP, plant emission increases, vehicle numbers increasing], it does seem a bit extreme, a positive trend starting in 2000.

Details are given in the text. The GDP decreased after 1998 and started increasing in 2002.

75. Line 22, Page 16: Reference missing.

We have corrected this. Actually the reference is Zara et al. (2018).

76. Line 22, Page 16: Maybe better to say "strengthened"?

We decided to keep "acknowledged" here.

Anonymous Reviewer #2

Major comments

1. I agree with the other reviewer that having all the equations in the Appendices is not optimal, also one would indeed like to see the result of each step on the data.

We thank the reviewer for giving us the opportunity to improve substantially our manuscript by putting the equations in Section 2.2 (Methodology). This Section has been enhanced with details

about the method we followed and we also include a new plot that shows how the NO₂ patterns changed from step to step (Fig. 1 in the revised manuscript).

2. I do not understand why CF1 has these specific systematic ‘worm-like’ patterns. Please explain. As discussed in the revised manuscript CF1 exhibits characteristic spatial patterns with values greater than and lower than 1 over and adjacent to pollution hotspots, respectively. This leads to the worm-like patterns which are pretty persistent throughout the year. Now, the reader may get an idea about the seasonal variability of the CF patterns. The CF1 patterns are given in high resolution in the supplement along with similar figures for CF2 and CF3.
3. Why would CF2 (and CF3) be (so) different for each grid cell around the world. Please explain why that is. And can we then understand the observed patterns/behaviour ?

The purpose of using CF2 and CF3 is to correct possible over and under corrections inserted during step 1 (resolution correction) which depends on the tropospheric NO₂ levels. Within the revised manuscript (Section 2.2) we give several details about the methodology and discuss about the observed CF patterns. As discussed there, CF2 takes higher positive and negative values over several pollution hot spots (absolute values higher than 0.5) pointing towards an under or overcorrection, respectively, during step 1. The CF3 patterns are pretty patchy and cannot be connected to areas with low or high tropospheric NO₂ like in the case of CF1 and CF2. CF3 accounts for the amplitude and shape of the seasonal variability and takes values that generally vary significantly from month to month over each grid cell.

Minor comments

1. What is the expected effect of the max 1 hour difference in local overpass time between the NO₂ measurements from various satellites ?

Studies around the world do not give large differences around the overpass time of the morning satellites we study here (e.g. Boersma et al., 2009; Kanaya et al., 2014; Hendrick et al., 2014; Drosoglou et al., 2018). The reported differences are expected to be lower than the differences stemming from the special characteristics of each instrument and this is why we did not mention it in the text. The difference between morning and noon is definitely much larger and explains part of e.g. SCIAMACHY-GOME difference.

- Boersma, K. F., Jacob, D. J., Trainic, M., Rudich, Y., DeSmedt, I., Dirksen, R., and Eskes, H. J.: Validation of urban NO₂ concentrations and their diurnal and seasonal variations observed from the SCIAMACHY and OMI sensors using in situ surface measurements in Israeli cities, *Atmos. Chem. Phys.*, 9, 3867-3879, <https://doi.org/10.5194/acp-9-3867-2009>, 2009.

- Hendrick, F., Müller, J.-F., Clémer, K., Wang, P., De Mazière, M., Fayt, C., Gielen, C., Hermans, C., Ma, J. Z., Pinardi, G., Stavrou, T., Vlemmix, T., and Van Roozendaal, M.: Four years of ground-based MAX-DOAS observations of HONO and NO₂ in the Beijing area, *Atmos. Chem. Phys.*, 14, 765-781, <https://doi.org/10.5194/acp-14-765-2014>, 2014.

- Kanaya, Y., Irie, H., Takashima, H., Iwabuchi, H., Akimoto, H., Sudo, K., Gu, M., Chong, J., Kim, Y. J., Lee, H., Li, A., Si, F., Xu, J., Xie, P.-H., Liu, W.-Q., Dzholia, A., Postlyakov, O., Ivanov, V., Grechko, E., Terpugova, S., and Panchenko, M.: Long-term MAX-DOAS network observations of NO₂ in Russia and Asia (MADRAS) during the period 2007-2012: instrumentation, elucidation of climatology, and comparisons with OMI satellite observations and global model simulations, *Atmos. Chem. Phys.*, 14, 7909-7927, <https://doi.org/10.5194/acp-14-7909-2014>, 2014.

- Drosoglou, T., Koukouli, M. E., Kouremeti, N., Bais, A. F., Zyrichidou, I., Balis, D., van der A, R. J., Xu, J., and Li, A.: MAX-DOAS NO_2 observations over Guangzhou, China; ground-based and satellite comparisons, *Atmos. Meas. Tech.*, 11, 2239-2255, <https://doi.org/10.5194/amt-11-2239-2018>, 2018.

2. What is the uncertainty on all these CF1s, for example stdv on the 12 CF1s for each month ? I have no idea how well you can determine these CF1s.

By applying error propagation we found that CF1 could be calculated with a relative error of around 20%. This is a very conservative calculation as the SCIAMACHY precision 0.1×10^{15} molecules cm^{-2} is taken into account in the standard deviations per se. Hence, the uncertainty is expected on a global scale to be well below this value.

3. Same question for CF2.

Similar as above.

4. P6, 18, 'shown below' should be 'shown'

Corrected.

5. P6.110 'to one' should be 'to the one'

Corrected.

6. Looking at Fig. 4 it looks like the yearly variation is much better fitted in the b) curves than in the a) curves. In fact it looks like the seasonal amplitudes are more or less fixed in the single linear trend analysis (a). Is that really a direct consequence of the reversal trend fit and not something prescribed in the linear trend fit ? I find the difference strikingly large.

The grey lines are just connecting the monthly values (grey points). The black lines in the first column panels depict the seasonal component which is fitted to the data. In the second column panels we did not plot the fitted seasonal component because there would be two seasonal components for the year of trend reversal with different amplitudes (as the trends are calculated for the years before and after the reversal but include the reversal year in both cases) and the figure would be very noisy. Hence, we decided to plot only the trend lines (blue or red) and connect the grey points with a grey line in order to get a better idea of the seasonal variability.

Georgoulas_et_al_Two_decades_of_continuous_tropospheric_NO2_recording_from_satellites_v4_track_changes (Last saved by user) [Compatibility Mode]

Main document changes and comments

Page 1: Deleted User 2/1/2019 12:03:00 PM

.b

Page 1: Deleted User 2/1/2019 12:03:00 PM

^acurrent address: Institute for Astronomy, Astrophysics, Space Application and Remote Sensing, National Observatory of Athens, Athens, Greece

^b

Page 1: Inserted User 2/1/2019 12:03:00 PM

^a

Page 1: Deleted User 2/1/2019 12:16:00 PM

self-consistent

Page 1: Inserted User 3/23/2019 10:17:00 AM

data

Page 1: Deleted User 2/1/2019 12:17:00 PM

data in order to reproduce what SCIAMACHY would measure if it was in orbit for

Page 1: Inserted User 2/1/2019 12:17:00 PM

to produce a self-consistent

Page 1: Inserted User 2/1/2019 12:17:00 PM

dataset that covers

Page 1: Deleted User 3/18/2019 5:06:00 PM

e.g. average

Page 1: Inserted User 3/18/2019 5:06:00 PM

a total

Page 1: Deleted User 3/18/2019 5:06:00 PM

e.g. average

Page 1: Inserted User 3/18/2019 5:06:00 PM

a total

Page 2: Inserted User 3/23/2019 10:21:00 AM

,

Page 2: Deleted User 3/23/2019 10:21:00 AM

the

Page 2: Deleted User 2/1/2019 12:26:00 PM

Callies et al., 2000

Page 2: Inserted User 2/1/2019 12:26:00 PM

Munro et al., 2016

Page 2: Inserted	User	3/23/2019 10:23:00 AM
Page 2: Inserted	User	2/1/2019 12:30:00 PM
Munro et al., 2016		
Page 2: Deleted	User	2/1/2019 12:30:00 PM
Wang et al., 2017		
Page 3: Deleted	User	2/1/2019 12:38:00 PM
for the first time		
Page 3: Deleted	User	2/1/2019 12:41:00 PM
2006		
Page 3: Inserted	User	2/1/2019 12:41:00 PM
2018		
Page 3: Deleted	User	3/14/2019 4:52:00 PM
and Appendix A		
Page 3: Deleted	User	3/14/2019 4:52:00 PM
All the methods used in this work are described comprehensively in the Appendix in order to make it easier for the reader to focus on the results and the discussion.		
Page 3: Deleted	User	3/14/2019 4:53:00 PM
and Appendix B for details about the trend calculations		
Page 3: Deleted	User	3/14/2019 4:53:00 PM
and Appendix C for details		
Page 4: Inserted	User	2/1/2019 1:28:00 PM
(Boersma et al., 2004)		
Page 4: Deleted	User	3/19/2019 12:00:00 PM
15		
Page 4: Inserted	User	3/19/2019 12:00:00 PM
19		
Page 4: Deleted	User	3/19/2019 12:00:00 PM
September		
Page 4: Inserted	User	3/19/2019 12:00:00 PM
March		
Page 4: Deleted	User	3/19/2019 12:00:00 PM
2018		
Page 4: Inserted	User	3/19/2019 12:00:00 PM
2019		

Page 4: Inserted **User** **3/7/2019 11:31:00 AM**

each observation is weighted by its fractional area (%) within the grid cell. For each valid observation, the cloud radiance fraction has to be less than 50% (cloud fraction less than about 20%) and the surface albedo not higher than 0.3, while observations with a solar zenith angle higher than 80° are filtered-out. In addition, there is no limitation in the number of observations used, negative columns are taken into account, and the observational error is ignored in the averaging process (e.g. Schneider et al.. 2015).

Page 4: Formatted **User** **3/7/2019 11:37:00 AM**

Superscript

Page 4: Deleted **User** **2/1/2019 3:23:00 PM**

(from

Page 4: Inserted **User** **2/1/2019 3:23:00 PM**

for the period

Page 4: Inserted **User** **2/1/2019 3:26:00 PM**

,

Page 4: Deleted **User** **3/23/2019 10:35:00 AM**

like in

Page 4: Inserted **User** **3/23/2019 10:35:00 AM**

contrary to

Page 4: Deleted **User** **2/1/2019 3:22:00 PM**

This way, we managed to reproduce what SCIAMACHY would measure if the sensor was in orbit for ~21 years (from 4/1996 to 9/2017).

Page 4: Inserted **User** **3/7/2019 2:20:00 PM**

Of course the grid cell size is the same ($0.25^\circ \times 0.25^\circ$) for the GOME and SCIAMACHY monthly datasets; however, this does not impact the fact that the information included in a larger swath corresponds to a larger area. Hence, the gridded data which are produced from larger pixels ($320 \times 40 \text{ km}^2$ for GOME) will be of "lower resolution" than the ones produced from smaller pixels ($60 \times 30 \text{ km}^2$ for SCIAMACHY) and the resulting maps will be much smoother. As the GOME nominal resolution is nearly 3 times lower than that of SCIAMACHY at the horizontal dimension, following the reasoning of Geddes et al. (2016), we may assume that each grid cell of the GOME gridded dataset will correspond to an area nearly 3 times larger. Hence,

Page 5: Deleted **User** **3/7/2019 2:32:00 PM**

To

Page 5: Inserted **User** **3/7/2019 2:35:00 PM**

in step 1

Page 5: Deleted **User** **3/7/2019 2:35:00 PM**

do

Page 5: Inserted User 3/7/2019 2:35:00 PM

,

Page 5: Deleted User 3/7/2019 2:32:00 PM

so

Page 5: Inserted User 3/7/2019 1:28:00 PM

VCD

Page 5: Inserted User 3/7/2019 2:35:00 PM

first

Page 5: Deleted User 3/7/2019 1:28:00 PM

A

Page 5: Deleted User 3/7/2019 2:33:00 PM

Page 5: Inserted User 3/7/2019 2:33:00 PM

The correction is applied in the horizontal dimension only as the along track dimensions are close in the two datasets (40 km vs 30 km) and also close to the latitudinal dimension of the gridded dataset (0.25°).

Page 5: Formatted User 3/7/2019 3:55:00 PM

English (U.K.)

Page 5: Deleted User 3/7/2019 1:28:00 PM

A

Page 5: Inserted User 3/7/2019 3:27:00 PM

(see also Hilboll et al., 2013)

Page 5: Inserted User 3/21/2019 3:37:00 PM

To avoid having unreasonably large CF1 values due to very low tropospheric NO₂ levels, CF1 was set equal to 1, in cases of VCD_{SCSM} lower than 0.1 x 10¹⁵ molecules cm⁻² which corresponds to SCIAMACHY's precision.

Page 5: Formatted User 3/21/2019 3:38:00 PM

Subscript

Page 5: Formatted User 3/21/2019 3:47:00 PM

Subscript

Page 5: Inserted User 3/22/2019 5:11:00 PM

total and the monthly mean

Page 5: Deleted User 3/21/2019 3:33:00 PM

annual mean

Page 5: Deleted User 3/22/2019 5:17:00 PM

China

Page 5: Inserted **User** **3/22/2019 5:17:00 PM**

south-eastern Asia

Page 5: Inserted **User** **3/21/2019 4:37:00 PM**

s

Page 5: Deleted **User** **3/21/2019 4:37:00 PM**

, S2, S3 and

Page 5: Inserted **User** **3/21/2019 4:37:00 PM**

-

Page 5: Deleted **User** **3/21/2019 4:37:00 PM**

S4

Page 5: Inserted **User** **3/21/2019 4:37:00 PM**

S8

Page 5: Deleted **User** **3/21/2019 4:37:00 PM**

, respectively

Page 5: Inserted **User** **3/22/2019 4:08:00 PM**

.

Page 5: Deleted **User** **3/21/2019 4:39:00 PM**

. attern of positive and negative

Page 5: Inserted **User** **3/21/2019 3:59:00 PM**

CF1 is unitless and exhibits characteristic spatial patterns with values greater than and lower than 1 over and adjacent to pollution hotspots, respectively. The CF1 patterns are pretty persistent throughout the year.

Page 5: Deleted **User** **3/7/2019 1:29:00 PM**

A

Page 5: Deleted **User** **3/7/2019 1:29:00 PM**

and GOME-2

Page 5: Deleted **User** **3/7/2019 1:29:00 PM**

s

Page 5: Inserted **User** **3/21/2019 5:00:00 PM**

The VCD_G and VCD_{GCI} patterns for the whole GOME period are shown in Fig. 1a and Fig. 1b, respectively.

$$VCD_{SCsm}(x, y, t) = \frac{1}{13} \left(\sum_{w=-6}^6 (VCD_{SC}(x + w \times 0.25, y, t)) \right)$$

(1)

where x and y are the central longitude and latitude of a grid cell in degrees and t is the time in one month steps (from 1/2003 to 12/2011), ..., while $w=-6, -5, \dots, 0, \dots, 5, 6$ (a total of 13 values).

$$CFI(x, y, m) = VCD_{SC}(x, y, m) / VCD_{SCsm}(x, y, m)$$

(2)

where $m=1, 2, \dots, 12$ is the month for which the climatological monthly values $VCD_{SC}(x,y,m)$ and $VCD_{SCsm}(x,y,m)$ are calculated.

$$VCD_{GCI}(x, y, t) = VCD_G(x, y, t) \times CFI(x, y, m)$$

(3)

Page 5: Formatted	User	3/7/2019 1:26:00 PM
Left		
Page 5: Formatted	User	3/7/2019 1:26:00 PM
Left		
Page 5: Deleted	User	3/7/2019 2:33:00 PM
Page 5: Deleted	User	3/13/2019 3:14:00 PM
had to		
Page 5: Inserted	User	3/13/2019 3:14:00 PM
were		
Page 5: Deleted	User	3/23/2019 10:45:00 AM
be		
Page 5: Inserted	User	3/13/2019 3:15:00 PM
.		
Page 5: Inserted	User	3/13/2019 3:16:00 PM
Following,		
Page 5: Deleted	User	3/13/2019 3:15:00 PM
(
Page 5: Deleted	User	3/13/2019 3:15:00 PM
”		
Page 5: Inserted	User	3/13/2019 3:15:00 PM
.(
Page 5: Deleted	User	3/23/2019 10:46:00 AM
2016		
Page 5: Inserted	User	3/23/2019 10:46:00 AM
2013		
Page 5: Inserted	User	3/13/2019 3:15:00 PM

who used a trend model that explicitly accounts for a level shift between the two instruments and for a change in the amplitude of the seasonal variation, we applied a shift correction (step 2) and a seasonal amplitude correction (step 3) successively, on top of the spatial resolution correction (step 1)

Page 6: Inserted User 3/13/2019 3:21:00 PM

More specifically,

Page 6: Deleted User 3/13/2019 3:21:00 PM

The

Page 6: Inserted User 3/13/2019 3:21:00 PM

the

Page 6: Inserted User 3/23/2019 10:51:00 AM

GOME-SCIAMACHY common

Page 6: Inserted User 3/13/2019 3:59:00 PM

(VCDsc)

Page 6: Deleted User 3/13/2019 2:50:00 PM

A

Page 6: Inserted User 3/22/2019 3:43:00 PM

CF₂ (in 10¹⁵ molecules cm⁻²) takes higher positive and negative values over several pollution hot spots (absolute values higher than 0.5) showing that further corrections should be applied on the data.

Page 6: Formatted User 3/22/2019 3:58:00 PM

Superscript

Page 6: Formatted User 3/22/2019 3:58:00 PM

Superscript

Page 6: Inserted User 3/22/2019 5:17:00 PM

south-eastern Asia

Page 6: Deleted User 3/22/2019 5:17:00 PM

China

Page 6: Deleted User 3/21/2019 5:00:00 PM

S5

Page 6: Inserted User 3/21/2019 5:00:00 PM

S9

Page 6: Deleted User 3/21/2019 5:00:00 PM

S6

Page 6: Inserted User 3/21/2019 5:00:00 PM

S10

Page 6: Deleted User 3/21/2019 5:01:00 PM

S7

Page 6: Inserted User 3/21/2019 5:01:00 PM

S11

Page 6: Deleted User 3/21/2019 5:01:00 PM

S8

Page 6: Inserted User 3/21/2019 5:01:00 PM

S12

Page 6: Deleted User 3/13/2019 2:53:00 PM

Page 6: Deleted User 3/23/2019 10:58:00 AM

extracted from

Page 6: Inserted User 3/23/2019 10:58:00 AM

added to

Page 6: Inserted User 3/14/2019 4:56:00 PM

Eq.

Page 6: Deleted User 3/13/2019 3:57:00 PM

A

Page 6: Inserted User 3/21/2019 5:01:00 PM

The VCD_{GC2} patterns for the whole GOME period are shown in Fig. 1c.

$$CF2(x, y) = \frac{1}{n} \left(\sum_{t=t_1}^{t_2} (VCD_{SC}(x, y, t)) - \sum_{t=t_1}^{t_2} (VCD_{GC1}(x, y, t)) \right)$$

(4)

where t is the time in one month steps for the common GOME-SCIAMACHY period (t_1 : 8/2002 to t_2 : 6/2003) of $n=11$ months.

$$VCD_{GC2}(x, y, t) = VCD_{GC1}(x, y, t) + CF2(x, y)$$

(5)

Page 6: Formatted User 3/23/2019 10:57:00 AM

Lowered by 18 pt

Page 6: Formatted User 3/23/2019 10:59:00 AM

Lowered by 6 pt

Page 6: Deleted User 3/13/2019 3:13:00 PM

Page 6: Inserted User 3/13/2019 4:40:00 PM

to the long-term average

Page 6: Deleted User 3/13/2019 4:41:00 PM

extracted from

Page 6: Inserted User 3/13/2019 4:41:00 PM

divided by

Page 6: Inserted User 3/13/2019 4:41:00 PM

of the SCIAMACHY data (VCD_{sc})

Page 6: Inserted User 3/13/2019 4:41:00 PM

to the long-term average of the twice corrected GOME data (VCD_{GC2})

Page 6: Formatted User 3/13/2019 4:42:00 PM

Not Superscript/ Subscript

Page 6: Inserted User 3/13/2019 4:42:00 PM

Page 6: Deleted User 3/13/2019 4:42:00 PM

Page 6: Inserted User 3/22/2019 6:03:00 PM

and is unitless

Page 6: Inserted User 3/13/2019 4:43:00 PM

Eq.

Page 6: Deleted User 3/13/2019 4:29:00 PM

A

Page 6: Inserted User 3/22/2019 12:39:00 AM

Like in the case of CF1, to avoid having unreasonably large values due to very low tropospheric NO_2 levels, CF3 was set equal to 1 for grid cells with VCD_{sc} or VCD_{GC2} levels lower than 0.1×10^{15} molecules cm^{-2} .

Page 6: Formatted User 3/22/2019 12:43:00 AM

Not Superscript/ Subscript

Page 6: Formatted User 3/22/2019 12:55:00 AM

Not Superscript/ Subscript

Page 6: Inserted User 3/22/2019 5:11:00 PM

total and the monthly mean

Page 6: Deleted User 3/21/2019 5:03:00 PM

annual mean

Page 6: Inserted User 3/22/2019 5:18:00 PM

south-eastern Asia

Page 6: Deleted User 3/22/2019 5:18:00 PM

China

Page 6: Inserted **User** **3/21/2019 5:03:00 PM**

s

Page 6: Inserted **User** **3/21/2019 5:03:00 PM**

1

Page 6: Deleted **User** **3/21/2019 5:03:00 PM**

9, S10, S11 and S12

Page 6: Inserted **User** **3/21/2019 5:03:00 PM**

3-S20

Page 6: Deleted **User** **3/23/2019 11:28:00 AM**

, respectively

Page 6: Inserted **User** **3/22/2019 5:53:00 PM**

The CF3 patterns are pretty patchy and cannot be connected to areas with low or high tropospheric NO₂ like in the case of CF1 and CF2.

Page 6: Formatted **User** **3/22/2019 4:50:00 PM**

Subscript

Page 6: Deleted **User** **3/22/2019 4:53:00 PM**

then

Page 6: Deleted **User** **3/13/2019 4:45:00 PM**

A

Page 6: Inserted **User** **3/21/2019 5:02:00 PM**

The VCD_{GC3} patterns for the whole GOME period are shown in Fig. 1d.

Page 6: Inserted **User** **3/13/2019 5:09:00 PM**

The GOME-2A and GOME-2B data were assumed to be of equal quality and resolution in the averaging process.

Page 6: Inserted **User** **3/7/2019 1:19:00 PM**

$$CF3(x, y, m) = \left[\frac{VCD_{SC}(x, y, m)}{n_{SC}} \left(\sum_{t=t_{SC1}}^{t_{SC2}} (VCD_{SC}(x, y, t)) \right) \right] / \left[\frac{VCD_{GC2}(x, y, m)}{n_G} \left(\sum_{t=t_{G1}}^{t_{G2}} (VCD_{GC2}(x, y, t)) \right) \right]$$

(6)

where t is the time in one month steps for the whole SCIAMACHY period (t_{SC1} : 8/2002 to t_{SC2} : 3/2012) of $n_{SC}=116$ months and for the whole GOME period (t_{G1} : 4/1996 to t_{G2} : 6/2003) of $n_G=87$ months.

$$VCD_{GC3}(x, y, t) = VCD_{GC2}(x, y, t) \times CF3(x, y, m)$$

(7)

Page 7: Inserted **User** **3/14/2019 2:24:00 PM**
 (see Eq. 8 and 9)

Page 7: Deleted **User** **3/14/2019 2:27:00 PM**
 a detailed description of the method is given in Appendix B

Page 7: Inserted **User** **3/14/2019 2:27:00 PM**
 Eq. 10

Page 7: Inserted **User** **3/14/2019 2:23:00 PM**
 the

Page 7: Deleted **User** **3/21/2019 5:09:00 PM**
 below

Page 7: Inserted **User** **3/14/2019 2:24:00 PM**

$$Y_t = A + BX_t + \sum_{n=1}^6 [a_n \sin(\frac{2\pi}{T}nX_t) + b_n \cos(\frac{2\pi}{T}nX_t)] + N_t$$

(8)

where Y_t is the monthly mean value for month t , X_t is the number of the month after the first month of the timeseries, A is the monthly mean of the first month of the timeseries and B is the trend. The seasonal component contains the amplitudes a_n and b_n , T is the period and N_t is the difference between the modeled and the measured value, termed usually as remainder.

$$N_t = \varphi N_{t-1} + \varepsilon_t$$

(9)

where φ is the autocorrelation in the remainder and ε_t is the white noise. Autocorrelation φ affects the precision of the trend σ_B which is given as a function of φ , the length of the data set in years m and the variance σ_N of the remainder for small autocorrelations:

$$\sigma_B \approx \left[\frac{\sigma_N}{m^{3/2}} \sqrt{\frac{1+\varphi}{1-\varphi}} \right]$$

(10)

The calculated trend B is considered to be statistically significant at the 95% confidence level if $|B/\sigma_B| > 2$.

Page 7: Formatted **User** **3/14/2019 2:30:00 PM**
 Subscript

Page 7: Formatted **User** **3/14/2019 2:30:00 PM**
 Subscript

Page 7: Deleted **User** **3/14/2019 2:26:00 PM**

Page 7: Formatted **User** **3/14/2019 2:24:00 PM**

English (U.S.)

Page 7: Inserted **User** **3/21/2019 5:09:00 PM**

the

Page 8: Deleted **User** **3/14/2019 4:13:00 PM**

It has to be highlighted that our study, in line with Cermak et al. (2010), focuses on detecting only one major trend reversal and hence minor reversals that may appear in the timeseries are not reported. The method is based on the minimization of a value S which is calculated on an annual basis (a detailed description is given in Appendix C). In this study, a trend reversal is reported only when the trend for the period before or the trend for the period after the reversal year (including the reversal year) is statistically significant at the 95% confidence level.

Page 8: Inserted **User** **3/14/2019 2:32:00 PM**

The trend reversal method is based on the minimization of a value $S(t)$ which is calculated for each year t of the period $[t_1=2000, t_n=2012]$:

$$S(t) = \frac{\min(p(B_l), p(B_r))}{\text{abs}(B_l - B_r) \times \sigma_{B_{l+r}}}$$

(11)

where $p(B_l)$ and $p(B_r)$ express the probability that the trends B_l and B_r for the short periods on the left $[t-4, t]$ and on the right $[t, t+4]$ of the year t are statistically insignificant (1-significance level of the trend) and $\sigma_{B_{l+r}}$ is the standard error of the trend for the combined sub-periods $[t-4, t+4]$. We use a time window of 4 in our calculations so that each trend is calculated for at least five years and hence we can search for a trend reversal only within the period 2000-2012. The year t_r when S takes its lower value and there is a switch from a positive trend to a negative one or from a negative trend to a positive one is considered to be a potential trend reversal year. The trends with the corresponding significance levels and probabilities are calculated here using least-squares linear regression (TREND function in IDL). In this study, only when the trend B_b for the whole period before t_r (including t_r) $[t_1-4, t_r]$ or the trend B_a for the whole period after t_r (including t_r) $[t_r, t_n+4]$ is statistically significant at the 95% confidence level, a trend reversal is reported. Specifically, for the four extended regions of interest, the country and the megacities and large urban agglomeration analyses performed in this paper, the B_b and B_a trends are calculated from the monthly timeseries using the method presented in the previous paragraph (Eq. 8, 9 and 10) in order to be consistent with the trends for the whole time period (4/1996 - 9/2017) which are reported in the paper.

Page 8: Formatted **User** **3/14/2019 3:08:00 PM**

Not Superscript/ Subscript

Page 8: Formatted **User** **3/14/2019 3:17:00 PM**

Not Superscript/ Subscript

Page 8: Deleted User 3/14/2019 3:02:00 PM

Page 8: Formatted User 3/14/2019 2:32:00 PM

English (U.S.)

Page 8: Inserted User 3/18/2019 12:31:00 PM

multi-year average

Page 8: Inserted User 3/18/2019 12:32:00 PM

Page 8: Deleted User 3/14/2019 5:08:00 PM

1

Page 8: Inserted User 3/14/2019 5:08:00 PM

2

Page 8: Inserted User 3/18/2019 12:41:00 PM

see

Page 8: Inserted User 3/18/2019 12:49:00 PM

; Krotkov et al., 2016; de Foy et al., 2016

Page 8: Inserted User 3/18/2019 12:58:00 PM

(see also in van der A, 2008; Schneider et al., 2015; Krotkov et al., 2016 and references therein)

Page 9: Inserted User 3/18/2019 1:21:00 PM

socioeconomic

Page 9: Deleted User 3/14/2019 5:08:00 PM

2

Page 9: Inserted User 3/14/2019 5:08:00 PM

3

Page 9: Deleted User 3/14/2019 5:08:00 PM

2a

Page 9: Inserted User 3/14/2019 5:08:00 PM

3a

Page 9: Inserted User 3/14/2019 5:08:00 PM

3

Page 9: Deleted User 3/14/2019 5:08:00 PM

2

Page 9: Inserted User 3/18/2019 5:48:00 PM

The trend values over these areas are higher than 0.05×10^{15} molecules $\text{cm}^{-2} \text{yr}^{-1}$, with a maximum value of 2.18×10^{15} molecules $\text{cm}^{-2} \text{yr}^{-1}$ appearing within the BTH urban cluster in eastern China.

Page 9: Inserted **User** **3/18/2019 5:51:00 PM**

The absolute trend values over these areas are higher than 0.05×10^{15} molecules $\text{cm}^{-2} \text{yr}^{-1}$, with a maximum trend of -1.40×10^{15} molecules $\text{cm}^{-2} \text{yr}^{-1}$ appearing close to Los Angeles city in the eastern U.S.

Page 9: Inserted **User** **3/18/2019 6:46:00 PM**

here

Page 9: Deleted **User** **3/18/2019 6:45:00 PM**

are similar

Page 9: Inserted **User** **3/18/2019 6:45:00 PM**

resemble

Page 9: Deleted **User** **3/18/2019 6:45:00 PM**

to

Page 9: Deleted **User** **3/18/2019 5:09:00 PM**

on average

Page 9: Inserted **User** **3/18/2019 5:05:00 PM**

during the whole period of interest

Page 9: Deleted **User** **3/18/2019 4:59:00 PM**

yr^{-1}

Page 10: Inserted **User** **3/14/2019 5:07:00 PM**

4

Page 10: Deleted **User** **3/14/2019 5:07:00 PM**

3

Page 10: Inserted **User** **3/14/2019 5:07:00 PM**

4

Page 10: Deleted **User** **3/14/2019 5:07:00 PM**

3

Page 10: Inserted **User** **3/14/2019 5:07:00 PM**

4

Page 10: Deleted **User** **3/14/2019 5:07:00 PM**

3

Page 10: Deleted **User** **3/14/2019 5:07:00 PM**

3a

Page 10: Inserted **User** **3/14/2019 5:07:00 PM**

4a

Page 10: Inserted **User** **3/14/2019 5:08:00 PM**

3

Page 10: Deleted	User	3/14/2019 5:08:00 PM
-------------------------	-------------	-----------------------------

2

Page 10: Inserted	User	3/19/2019 10:25:00 AM
--------------------------	-------------	------------------------------

(2011)

Page 10: Deleted	User	3/19/2019 10:25:00 AM
-------------------------	-------------	------------------------------

during the period 2011-2015

Page 10: Inserted	User	3/19/2019 10:25:00 AM
--------------------------	-------------	------------------------------

(2015)

Page 10: Inserted	User	3/14/2019 5:07:00 PM
--------------------------	-------------	-----------------------------

4

Page 10: Deleted	User	3/14/2019 5:07:00 PM
-------------------------	-------------	-----------------------------

3

Page 10: Inserted	User	3/19/2019 10:33:00 AM
--------------------------	-------------	------------------------------

The maximum allowed amount of

Page 10: Inserted	User	3/19/2019 10:32:00 AM
--------------------------	-------------	------------------------------

NO_x emissions was reduced by 50%.

Page 10: Formatted	User	3/19/2019 10:33:00 AM
---------------------------	-------------	------------------------------

Subscript

Page 10: Inserted	User	3/19/2019 10:38:00 AM
--------------------------	-------------	------------------------------

a ban on older polluting cars in

Page 10: Inserted	User	3/19/2019 10:43:00 AM
--------------------------	-------------	------------------------------

(see

Page 10: Deleted	User	3/19/2019 10:43:00 AM
-------------------------	-------------	------------------------------

in

Page 10: Inserted	User	3/14/2019 5:07:00 PM
--------------------------	-------------	-----------------------------

4

Page 10: Deleted	User	3/14/2019 5:07:00 PM
-------------------------	-------------	-----------------------------

3

Page 10: Inserted	User	3/19/2019 10:43:00 AM
--------------------------	-------------	------------------------------

)

Page 10: Deleted	User	3/19/2019 10:43:00 AM
-------------------------	-------------	------------------------------

"

Page 10: Deleted	User	3/19/2019 10:43:00 AM
-------------------------	-------------	------------------------------

"

Page 10: Inserted User 3/14/2019 5:07:00 PM

4

Page 10: Deleted User 3/14/2019 5:07:00 PM

3

Page 11: Inserted User 3/19/2019 10:45:00 AM

,

Page 11: Inserted User 3/19/2019 4:08:00 PM

On the contrary, areas in central-southern India experienced a reversal from negative to positive trends at some point in the period 2000-2006. India experienced a population growth of ~37% (relative to 1996) during the period 1996-2017, mostly in urban areas, which was accompanied by a gross domestic product (GDP) increase of ~29% (World Bank, 2019). NO_x emissions generally increased as a result of large-scale urbanization (rural population decreased from ~73% of the total population in 1996 to ~66% in 2017), industrialization and economic growth, energy production, industry and transportation being the main contributors to the emissions (Ghude et al., 2013 and references therein). The Indian economy started developing at much higher rates after 2002 (World Bank, 2019) which might explain the observed negative to positive trend reversals appearing in the years 2000-2006 over specific regions (e.g. increase of tropospheric NO₂ in the greater Ballari region due to the rapid growth of the steel industry, especially after 2006). India's economic growth experienced a slow-down after 2011 (GDP still increased but at a lower rate) which might explain part of the observed positive to negative trend reversals over specific areas. Hilboll et al. (2017) also observed a stagnation of tropospheric NO₂ over India, attributing it to a combination of a slow-down in Indian economic development, the implementation of cleaner technology (e.g. Bansal and Bandivadekar, 2013), meteorological factors (see Voulgarakis et al., 2010) and changes in tropospheric chemistry. However, it has to be noted that the way all these parameters may influence the tropospheric NO₂ levels and trends over India is pretty complicated and should be studied in more detail in the future.

Page 11: Deleted User 3/19/2019 3:43:00 PM

and largest

Page 11: Inserted User 3/19/2019 3:49:00 PM

Page 11: Formatted User 3/19/2019 4:09:00 PM

English (U.S.)

Page 11: Inserted User 3/14/2019 5:08:00 PM

4

Page 11: Deleted User 3/14/2019 5:08:00 PM

3

Page 11: Deleted User 3/20/2019 1:15:00 PM

Sea

Page 11: Inserted User 3/20/2019 1:15:00 PM

Basin

Page 11: Deleted User 3/19/2019 6:48:00 PM

(Cuevas et al., 2014)

Page 11: Inserted User 3/19/2019 6:47:00 PM

More specifically, in Cuevas et al. (2014) a continuous drop of surface NO₂ is seen after 1999-2000 over the two cities.

Page 11: Formatted User 3/19/2019 6:50:00 PM

Subscript

Page 11: Inserted User 3/20/2019 3:17:00 PM

(EEA-APFS-Spain., 2014). Following the European Union directives,

Page 11: Deleted User 3/20/2019 2:12:00 PM

Page 11: Inserted User 3/20/2019 2:09:00 PM

Spain introduced its First National Emission Reduction Program in 2003 setting stringent combustion emission standards (IEA, 2017). This was afterwards updated and revised leading to the Second National Emission Reduction Program in 2008.

Page 11: Inserted User 3/20/2019 2:09:00 PM

T

Page 11: Inserted User 3/21/2019 1:50:00 PM

the

Page 11: Inserted User 3/20/2019 3:03:00 PM

(EEA-APFS-Portugal., 2014)

Page 11: Inserted User 3/20/2019 3:32:00 PM

as

Page 11: Inserted User 3/21/2019 1:50:00 PM

the

Page 11: Deleted User 3/20/2019 2:54:00 PM

2010s

Page 11: Inserted User 3/20/2019 2:54:00 PM

2000s

Page 11: Inserted User 3/20/2019 2:58:00 PM

, probably due to the 2008 financial recession

Page 11: Inserted User 3/20/2019 2:42:00 PM

of

Page 12: Inserted **User** **3/14/2019 5:08:00 PM**

4

Page 12: Deleted **User** **3/14/2019 5:08:00 PM**

3

Page 12: Deleted **User** **3/21/2019 12:48:00 PM**

a direct (less

Page 12: Inserted **User** **3/21/2019 12:49:00 PM**

a decrease of

Page 12: Inserted **User** **3/21/2019 12:49:00 PM**

Page 12: Deleted **User** **3/21/2019 12:48:00 PM**

) or indirect (political and financial involvement of Iran) effect of

Page 12: Inserted **User** **3/21/2019 12:48:00 PM**

due to

Page 12: Deleted **User** **3/21/2019 12:49:00 PM**

on the observed trend reversal

Page 12: Inserted **User** **3/21/2019 1:51:00 PM**

the

Page 12: Deleted **User** **3/21/2019 2:31:00 PM**

and

Page 12: Inserted **User** **3/21/2019 2:31:00 PM**

,

Page 12: Inserted **User** **3/21/2019 2:34:00 PM**

and

Page 12: Inserted **User** **3/21/2019 2:31:00 PM**

and the Nile River in Egypt

Page 12: Inserted **User** **3/21/2019 1:50:00 PM**

the

Page 12: Deleted **User** **3/21/2019 2:31:00 PM**

.

Page 12: Deleted **User** **3/21/2019 2:31:00 PM**

A similar trend reversal is observed over the region of Nile River in Egypt

Page 12: Inserted **User** **3/14/2019 5:08:00 PM**

4

Page 12: Deleted User 3/14/2019 5:08:00 PM

3

Page 12: Inserted User 3/14/2019 5:08:00 PM

4

Page 12: Deleted User 3/14/2019 5:08:00 PM

3

Page 12: Inserted User 3/21/2019 1:50:00 PM

the

Page 12: Deleted User 3/14/2019 5:08:00 PM

3b

Page 12: Inserted User 3/14/2019 5:08:00 PM

4b

Page 12: Deleted User 3/19/2019 12:36:00 PM

gross domestic product (

Page 12: Deleted User 3/19/2019 12:36:00 PM

)

Page 12: Deleted User 3/19/2019 11:59:00 AM

2018

Page 12: Inserted User 3/19/2019 11:59:00 AM

2019

Page 12: Deleted User 3/19/2019 11:59:00 AM

2018

Page 12: Inserted User 3/19/2019 11:59:00 AM

2019

Page 12: Inserted User 3/14/2019 5:06:00 PM

5

Page 12: Deleted User 3/14/2019 5:06:00 PM

4

Page 12: Deleted User 3/14/2019 5:06:00 PM

4

Page 12: Inserted User 3/14/2019 5:06:00 PM

5

Page 12: Deleted User 3/14/2019 5:06:00 PM

4

Page 12: Inserted User 3/14/2019 5:06:00 PM

5

Page 12: Deleted **User** **3/14/2019 5:06:00 PM**

4

Page 12: Inserted **User** **3/14/2019 5:06:00 PM**

5

Page 12: Inserted **User** **3/14/2019 5:06:00 PM**

5

Page 12: Deleted **User** **3/14/2019 5:06:00 PM**

4

Page 12: Inserted **User** **3/14/2019 5:07:00 PM**

5

Page 12: Deleted **User** **3/14/2019 5:07:00 PM**

4

Page 13: Inserted **User** **3/14/2019 5:07:00 PM**

5

Page 13: Deleted **User** **3/14/2019 5:07:00 PM**

4

Page 13: Inserted **User** **3/14/2019 5:07:00 PM**

5

Page 13: Deleted **User** **3/14/2019 5:07:00 PM**

4

Page 13: Inserted **User** **3/14/2019 5:07:00 PM**

5

Page 13: Deleted **User** **3/14/2019 5:07:00 PM**

4

Page 13: Inserted **User** **3/14/2019 5:06:00 PM**

6

Page 13: Deleted **User** **3/14/2019 5:06:00 PM**

5

Page 13: Inserted **User** **3/14/2019 5:06:00 PM**

6

Page 13: Deleted **User** **3/14/2019 5:06:00 PM**

5

Page 13: Deleted **User** **3/14/2019 5:08:00 PM**

2

Page 13: Inserted User 3/14/2019 5:08:00 PM

3

Page 13: Inserted User 3/14/2019 5:06:00 PM

6

Page 13: Deleted User 3/14/2019 5:06:00 PM

5

Page 13: Inserted User 3/14/2019 5:06:00 PM

6

Page 13: Deleted User 3/14/2019 5:06:00 PM

5

Page 14: Deleted User 3/20/2019 6:21:00 PM

In order to save space,

Page 14: Inserted User 3/20/2019 6:29:00 PM

,

Page 14: Deleted User 3/20/2019 6:28:00 PM

one may also find

Page 14: Inserted User 3/20/2019 6:29:00 PM

are shown

Page 14: Inserted User 3/14/2019 5:05:00 PM

7

Page 14: Deleted User 3/14/2019 5:05:00 PM

6

Page 14: Inserted User 3/14/2019 5:06:00 PM

7

Page 14: Deleted User 3/14/2019 5:06:00 PM

6

Page 14: Deleted User 3/14/2019 5:05:00 PM

7

Page 14: Inserted User 3/14/2019 5:05:00 PM

8

Page 14: Inserted User 3/14/2019 5:05:00 PM

8

Page 14: Deleted User 3/14/2019 5:05:00 PM

7

Page 14: Inserted User 3/14/2019 5:05:00 PM

8

Page 14: Deleted	User	3/14/2019 5:05:00 PM
-------------------------	-------------	-----------------------------

7

Page 14: Deleted	User	3/14/2019 5:05:00 PM
-------------------------	-------------	-----------------------------

7c

Page 14: Inserted	User	3/14/2019 5:05:00 PM
--------------------------	-------------	-----------------------------

8c

Page 14: Inserted	User	3/21/2019 11:00:00 AM
--------------------------	-------------	------------------------------

(by ~18% relative to 2008)

Page 14: Deleted	User	3/19/2019 11:59:00 AM
-------------------------	-------------	------------------------------

2018

Page 14: Inserted	User	3/19/2019 11:59:00 AM
--------------------------	-------------	------------------------------

2019

Page 14: Inserted	User	3/21/2019 11:01:00 AM
--------------------------	-------------	------------------------------

mean

Page 14: Deleted	User	3/21/2019 11:02:00 AM
-------------------------	-------------	------------------------------

VCDs

Page 14: Inserted	User	3/21/2019 11:02:00 AM
--------------------------	-------------	------------------------------

levels

Page 15: Inserted	User	3/14/2019 5:05:00 PM
--------------------------	-------------	-----------------------------

8

Page 15: Deleted	User	3/14/2019 5:05:00 PM
-------------------------	-------------	-----------------------------

7

Page 15: Deleted	User	3/19/2019 11:59:00 AM
-------------------------	-------------	------------------------------

2018

Page 15: Inserted	User	3/19/2019 11:59:00 AM
--------------------------	-------------	------------------------------

2019

Page 15: Inserted	User	3/14/2019 5:05:00 PM
--------------------------	-------------	-----------------------------

8

Page 15: Deleted	User	3/14/2019 5:05:00 PM
-------------------------	-------------	-----------------------------

7

Page 15: Inserted	User	3/21/2019 11:14:00 AM
--------------------------	-------------	------------------------------

s

Page 15: Deleted	User	3/21/2019 11:14:00 AM
-------------------------	-------------	------------------------------

both

Page 15: Inserted User 3/21/2019 11:14:00 AM

two

Page 15: Deleted User 3/14/2019 5:04:00 PM

8

Page 15: Inserted User 3/14/2019 5:04:00 PM

9

Page 15: Deleted User 3/14/2019 5:04:00 PM

8

Page 15: Inserted User 3/14/2019 5:04:00 PM

9

Page 15: Inserted User 3/14/2019 5:05:00 PM

9

Page 15: Deleted User 3/14/2019 5:05:00 PM

8

Page 16: Inserted User 3/14/2019 5:04:00 PM

10

Page 16: Deleted User 3/14/2019 5:04:00 PM

9

Page 16: Inserted User 3/14/2019 5:04:00 PM

10

Page 16: Deleted User 3/14/2019 5:04:00 PM

9

Page 16: Inserted User 3/14/2019 5:04:00 PM

1

Page 16: Deleted User 3/14/2019 5:04:00 PM

0

Page 16: Inserted User 3/21/2019 1:50:00 PM

the

Page 17: Deleted User 3/21/2019 11:44:00 AM

,

Page 17: Inserted User 3/21/2019 11:44:00 AM

,

Page 17: Deleted User 3/21/2019 11:41:00 AM

, in order to reproduce what SCIAMACHY would measure if being in orbit for the whole period of interest.

Page 17: Inserted User 3/21/2019 11:44:00 AM

and

Page 17: Deleted	User	3/21/2019 11:44:00 AM
-------------------------	-------------	------------------------------

The

Page 17: Inserted	User	3/21/2019 11:44:00 AM
--------------------------	-------------	------------------------------

the multi-satellite

Page 17: Deleted	User	3/18/2019 5:08:00 PM
-------------------------	-------------	-----------------------------

on average

Page 17: Inserted	User	3/18/2019 5:10:00 PM
--------------------------	-------------	-----------------------------

during the whole period of interest (

Page 17: Inserted	User	3/18/2019 5:10:00 PM
--------------------------	-------------	-----------------------------

)

Page 17: Inserted	User	3/21/2019 11:46:00 AM
--------------------------	-------------	------------------------------

the

Page 17: Inserted	User	3/21/2019 11:45:00 AM
--------------------------	-------------	------------------------------

the

Page 17: Inserted	User	3/21/2019 11:46:00 AM
--------------------------	-------------	------------------------------

the

Page 17: Inserted	User	3/21/2019 11:46:00 AM
--------------------------	-------------	------------------------------

the

Page 18: Deleted	User	3/21/2019 11:47:00 AM
-------------------------	-------------	------------------------------

could

Page 18: Inserted	User	3/21/2019 11:47:00 AM
--------------------------	-------------	------------------------------

can

Page 18: Inserted	User	3/21/2019 12:01:00 PM
--------------------------	-------------	------------------------------

be

Page 18: Inserted	User	3/21/2019 12:01:00 PM
--------------------------	-------------	------------------------------

during

Page 18: Inserted	User	3/21/2019 12:01:00 PM
--------------------------	-------------	------------------------------

year

Page 19: Inserted	User	3/21/2019 1:50:00 PM
--------------------------	-------------	-----------------------------

the

Page 19: Deleted	User	3/13/2019 4:08:00 PM
-------------------------	-------------	-----------------------------

Appendix A: Merging GOME, SCIAMACHY and GOME-2 observations

Step 1: VCD_{SCsm} is calculated from VCD_{SC} using a boxcar algorithm with an averaging window of $13 \times 0.25^\circ$ (3.25°)

$$VCD_{SCsm}(x, y, t) = \frac{1}{13} \left(\sum_{w=-6}^6 (VCD_{SC}(x + w \times 0.25, y, t)) \right) \quad (A1)$$

where x and y are the central longitude and latitude of a grid cell in degrees and t is the time in one month steps (from 1/2003 to 12/2011), ..., while $w=-6, -5, \dots, 0, 5, 6$ (a total of 13 values).

$$CF1(x, y, m) = VCD_{SC}(x, y, m) / VCD_{SCsm}(x, y, m) \quad (A2)$$

where $m=1, 2, \dots, 12$ is the month for which the climatological monthly values $VCD_{SC}(x,y,m)$ and $VCD_{SCsm}(x,y,m)$ are calculated.

$$VCD_{GC1}(x, y, t) = VCD_G(x, y, t) \times CF1(x, y, m) \quad (A3)$$

$$\text{Step 2: } CF2(x, y) = \frac{1}{n} \left(\sum_{t=t_1}^{t_2} (VCD_{GC1}(x, y, t)) - \sum_{t=t_1}^{t_2} (VCD_{SC}(x, y, t)) \right) \quad (A4)$$

where t is the time in one month steps for the common GOME-SCIAMACHY period (t_1 : 8/2002 to t_2 : 6/2003) of $n=11$ months.

$$VCD_{GC2}(x, y, t) = VCD_{GC1}(x, y, t) - CF2(x, y) \quad (A5)$$

$$\text{Step 3: } CF3(x, y, m) = \left[\frac{VCD_{SC}(x, y, m)}{n_{SC}} \left(\sum_{t=t_{SC1}}^{t_{SC2}} (VCD_{SC}(x, y, t)) \right) \right] / \left[\frac{VCD_{GC2}(x, y, m)}{n_G} \left(\sum_{t=t_{G1}}^{t_{G2}} (VCD_{GC2}(x, y, t)) \right) \right] \quad (A6)$$

where t is the time in one month steps for the whole SCIAMACHY period (t_{SC1} : 8/2002 to t_{SC2} : 3/2012) of $n_{SC}=116$ months and for the whole GOME period (t_{G1} : 4/1996 to t_{G2} : 6/2003) of $n_G=87$ months.

$$VCD_{GC3}(x, y, t) = VCD_{GC2}(x, y, t) \times CF3(x, y, m) \quad (A7)$$

Appendix B: Trend analysis

The timeseries are fitted by using a model with a linear trend and a Fourier-based seasonal component:

$$Y_t = A + BX_t + \sum_{n=1}^6 [a_n \sin(\frac{2\pi}{T}nX_t) + b_n \cos(\frac{2\pi}{T}nX_t)] + N_t \quad (B1)$$

where Y_t is the monthly mean value for month t , X_t is the number of the month after the first month of the timeseries, A is the monthly mean of the first month of the timeseries and B is the trend. The seasonal component contains the amplitudes a_n and b_n , T is the period and N_t is the difference between the modeled and the measured value termed, usually as remainder.

$$N_t = \varphi N_{t-1} + \varepsilon_t \quad (B2)$$

where φ is the autocorrelation in the remainder and ε_t is the white noise. Autocorrelation φ affects the precision of the trend σ_B which is given as a function of φ , the length of the data set in months m and the variance σ_N of the remainder for small autocorrelations:

$$\sigma_B \approx \left[\frac{\sigma_N}{m^{3/2}} \sqrt{\frac{1+\varphi}{1-\varphi}} \right] \quad (B3)$$

The calculated trend B is considered to be statistically significant at the 95% confidence level if $|B/\sigma_B| > 2$.

Appendix C: Trend reversal detection

The trend reversal method is based on the minimization of a value $S(t)$ which is calculated for each year t of the period $[t_1=2000, t_n=2012]$:

$$S(t) = \frac{\min(p(B_l), p(B_r))}{\text{abs}(B_l - B_r) \times \sigma_{B_{l+r}}} \quad (C1)$$

where $p(B_l)$ and $p(B_r)$ express the possibility that the trends B_l and B_r for the short periods on the left $[t-4, t]$ and on the right $[t, t+4]$ of the year t are statistically insignificant and $\sigma_{B_{l+r}}$ is the standard error of the trend

for the combined sub-periods $[t-4, t+4]$. The year t_r when S takes its lower value and there is a switch from a positive trend to a negative one or from a negative trend to a positive one is considered to be a potential trend reversal year. The trends are calculated using ordinary least-squares linear regression with 95% confidence intervals. In this study, only when the trend B_b for the whole period before t_r (including t_r) $[t_1, t_r]$ or the trend B_a for the whole period after t_r (including t_r) $[t_r, t_n]$ is statistically significant at the 95% confidence level, a trend reversal is reported. Specifically, for the four extended regions of interest, the country and the megacities and large urban agglomeration analyses performed in this paper, the B_b and B_a trends are calculated from the monthly timeseries using the method presented in Appendix B in order to be consistent with the trends for the whole time period (4/1996 - 9/2017) which are reported in the paper.

Page 19: Inserted **User** **3/19/2019 5:38:00 PM**

Bansal, G. and Bandivadekar, G.: Overview of India's vehicle emissions control program, Tech. rep., The International Council on Clean Transportation, Washington, D.C., available at: http://www.theicct.org/sites/default/files/publications/ICCT_IndiaRetrospective_2013.pdf (last access: 19 March 2018), 2013.

Page 20: Deleted **User** **2/1/2019 12:26:00 PM**

Callies, J., Corpaccioli, E., Eisinger, M., Hahne, A., and Lefebvre, A.: GOME-2 - Metop's second-generation sensor for operational ozone monitoring, *ESA Bull.-Eur. Space*, 102, 28-36, 2000.

Page 20: Deleted **User** **3/19/2019 12:01:00 PM**

15

Page 20: Inserted **User** **3/19/2019 12:01:00 PM**

19

Page 20: Deleted **User** **3/19/2019 12:01:00 PM**

September

Page 20: Inserted **User** **3/19/2019 12:01:00 PM**

March

Page 20: Deleted **User** **3/19/2019 12:01:00 PM**

2018

Page 20: Inserted **User** **3/19/2019 12:01:00 PM**

2019

Page 20: Inserted **User** **3/20/2019 3:18:00 PM**

EEA-APFS-Portugal: European Environment Agency - Air pollution fact sheet - Portugal, available at: https://www.eea.europa.eu/themes/air/air-pollution-country-fact-sheets-2014/portugal-air-pollutant-emissions-country-fact-sheet/at_download/file (last access: 19 March 2019), 2014.

EEA-APFS-Spain: European Environment Agency - Air pollution fact sheet - Spain, available at: https://www.eea.europa.eu/themes/air/air-pollution-country-fact-sheets-2014/spain-air-pollutant-emissions-country-factsheet/at_download/file (last access: 19 March 2019), 2014.

Page 21: Formatted	User	3/20/2019 3:20:00 PM
---------------------------	-------------	-----------------------------

Font: Not Italic

Page 21: Deleted	User	3/20/2019 3:18:00 PM
-------------------------	-------------	-----------------------------

Page 21: Deleted	User	3/19/2019 12:01:00 PM
-------------------------	-------------	------------------------------

15

Page 21: Inserted	User	3/19/2019 12:01:00 PM
--------------------------	-------------	------------------------------

19

Page 21: Deleted	User	3/19/2019 12:01:00 PM
-------------------------	-------------	------------------------------

September

Page 21: Inserted	User	3/19/2019 12:01:00 PM
--------------------------	-------------	------------------------------

March

Page 21: Deleted	User	3/19/2019 5:41:00 PM
-------------------------	-------------	-----------------------------

201

Page 21: Inserted	User	3/19/2019 5:41:00 PM
--------------------------	-------------	-----------------------------

2019

Page 21: Deleted	User	3/19/2019 5:41:00 PM
-------------------------	-------------	-----------------------------

8

Page 21: Inserted	User	3/19/2019 5:31:00 PM
--------------------------	-------------	-----------------------------

Ghude, S. D., Pfister, G. G., Jena, C., van der A, R., Emmons, L. K., and Kumar, R.: Satellite constraints of nitrogen oxide (NO_x) emissions from India based on OMI observations and WRF-Chem simulations, Geophys. Res. Lett., 40, 423-428, doi:10.1002/grl.50065, 2013.

Page 21: Deleted	User	3/19/2019 12:02:00 PM
-------------------------	-------------	------------------------------

15

Page 21: Inserted	User	3/19/2019 12:02:00 PM
--------------------------	-------------	------------------------------

19

Page 21: Deleted	User	3/19/2019 12:02:00 PM
-------------------------	-------------	------------------------------

September

Page 21: Inserted	User	3/19/2019 12:02:00 PM
--------------------------	-------------	------------------------------

March

Page 21: Deleted	User	3/19/2019 12:02:00 PM
-------------------------	-------------	------------------------------

2018

Page 21: Inserted **User** **3/19/2019 12:02:00 PM**

2019

Page 21: Inserted **User** **3/20/2019 2:33:00 PM**

IEA - Clean Coal Center report, available at: <https://www.iea-coal.org/wp-content/uploads/2017/12/spain-1>
(last access: 19 March 2019), 2017.

Page 22: Inserted **User** **2/1/2019 12:44:00 PM**

Levelt, P. F., Joiner, J., Tamminen, J., Veefkind, J. P., Bhartia, P. K., Stein Zweers, D. C., Duncan, B. N., Streets, D. G., Eskes, H., van der A, R., McLinden, C., Fioletov, V., Carn, S., de Laat, J., DeLand, M., Marchenko, S., McPeters, R., Ziemke, J., Fu, D., Liu, X., Pickering, K., Apituley, A., González Abad, G., Arola, A., Boersma, F., Chan Miller, C., Chance, K., de Graaf, M., Hakkarainen, J., Hassinen, S., Ialongo, I., Kleipool, Q., Krotkov, N., Li, C., Lamsal, L., Newman, P., Nowlan, C., Suleiman, R., Tilstra, L. G., Torres, O., Wang, H., and Wargan, K.: The Ozone Monitoring Instrument: overview of 14 years in space, *Atmos. Chem. Phys.*, 18, 5699-5745, doi:10.5194/acp-18-5699-2018, 2018.

Page 22: Deleted **User** **2/1/2019 12:44:00 PM**

Levelt, P. F., van den Oord, G. H. J., Dobber, M. R., Mälkki, A., Visser, H., de Vries, J., Stammes, P., Lundell, J., and Saari, H.: The Ozone Monitoring Instrument, *IEEE T. Geosci. Remote*, 44, 1093-1101, doi:10.1109/TGRS.2006.872333, 2006.

Page 22: Inserted **User** **2/1/2019 12:27:00 PM**

Munro, R., Lang, R., Klaes, D., Poli, G., Retscher, C., Lindstrot, R., Huckle, R., Lacan, A., Grzegorski, M., Holdak, A., Kokhanovsky, A., Livschitz, J., and Eisinger, M.: The GOME-2 instrument on the Metop series of satellites: instrument design, calibration, and level 1 data processing - an overview, *Atmos. Meas. Tech.*, 9, 1279-1301, doi:10.5194/amt-9-1279-2016, 2016.

Page 24: Inserted **User** **3/19/2019 5:35:00 PM**

Voulgarakis, A., Savage, N. H., Wild, O., Braesicke, P., Young, P. J., Carver, G. D., and Pyle, J. A.: Interannual variability of tropospheric composition: the influence of changes in emissions, meteorology and clouds, *Atmos. Chem. Phys.*, 10, 2491-2506, doi:10.5194/acp-10-2491-2010, 2010.

Page 24: Deleted **User** **2/1/2019 12:32:00 PM**

Wang, Y., Beirle, S., Lampel, J., Koukouli, M., De Smedt, I., Theys, N., Li, A., Wu, D., Xie, P., Liu, C., Van Roozendael, M., Stavrakou, T., Müller, J.-F., and Wagner, T.: Validation of OMI, GOME-2A and GOME-2B tropospheric NO₂, SO₂ and HCHO products using MAX-DOAS observations from 2011 to 2014 in Wuxi, China: investigation of the effects of priori profiles and aerosols on the satellite products, *Atmos. Chem. Phys.*, 17, 5007-5033, doi:10.5194/acp-17-5007-2017, 2017.

Page 24: Deleted User 3/19/2019 12:02:00 PM

15

Page 24: Inserted User 3/19/2019 12:02:00 PM

19

Page 24: Deleted User 3/19/2019 12:02:00 PM

September

Page 24: Inserted User 3/19/2019 12:02:00 PM

March

Page 24: Deleted User 3/19/2019 12:02:00 PM

2018

Page 24: Inserted User 3/19/2019 12:02:00 PM

2019

Page 24: Deleted User 3/19/2019 12:00:00 PM

15

Page 24: Inserted User 3/19/2019 12:00:00 PM

19

Page 24: Deleted User 3/19/2019 12:00:00 PM

September

Page 24: Inserted User 3/19/2019 12:00:00 PM

March

Page 24: Deleted User 3/19/2019 12:00:00 PM

2018

Page 24: Inserted User 3/19/2019 12:00:00 PM

2019

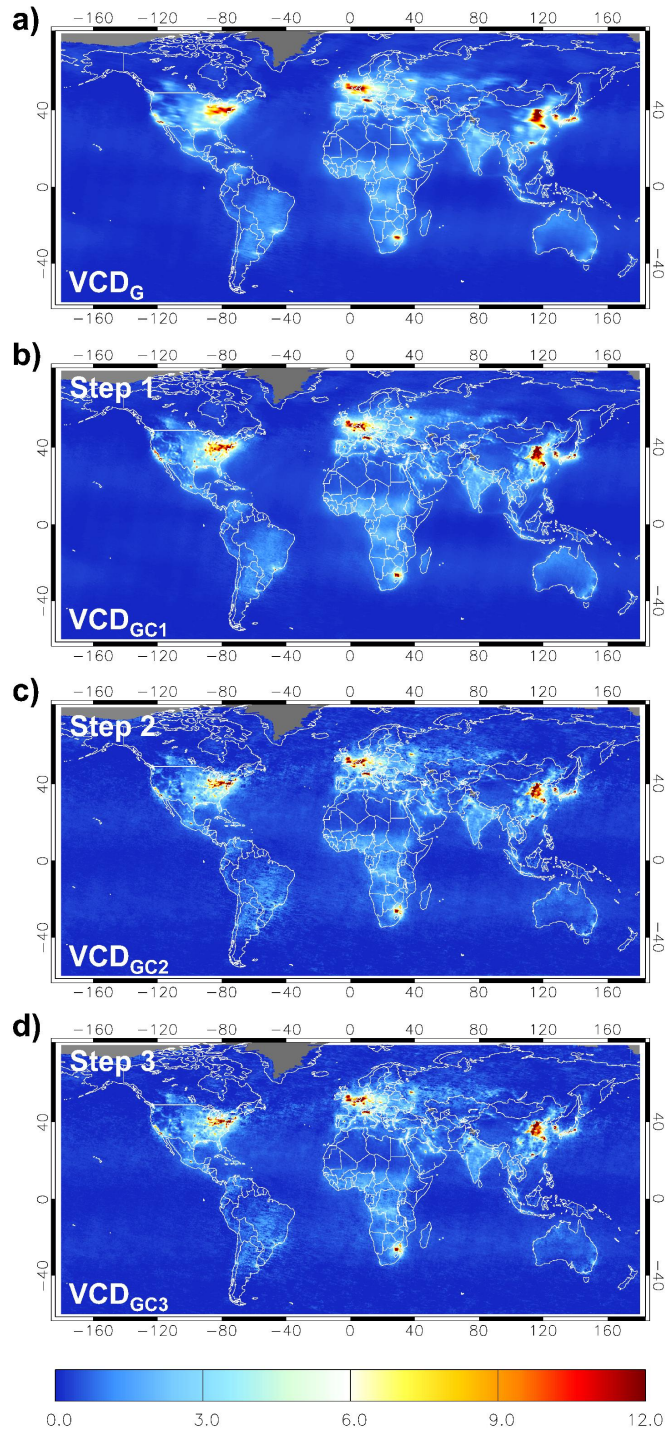
Page 24: Deleted User 3/19/2019 12:00:00 PM

2018

Page 24: Inserted User 3/19/2019 12:00:00 PM

2019

Page 30: Inserted User 3/23/2019 1:25:00 PM



Page 30: Formatted User 3/14/2019 5:37:00 PM
Centered

Page 30: Deleted User 3/14/2019 5:36:00 PM

Page 30: Inserted User 3/14/2019 5:36:00 PM

Figure 1: GOME tropospheric NO₂ VCD (in 10¹⁵ molecules cm⁻²) patterns for the whole GOME period from the original (VCD_G) data (a), from the corrected in step 1 (VCDG_{C1}) data (b), from the corrected in step 2 (VCDG_{C2}) data (c) and from the corrected in step 3 (VCDG_{C3}) data (d).

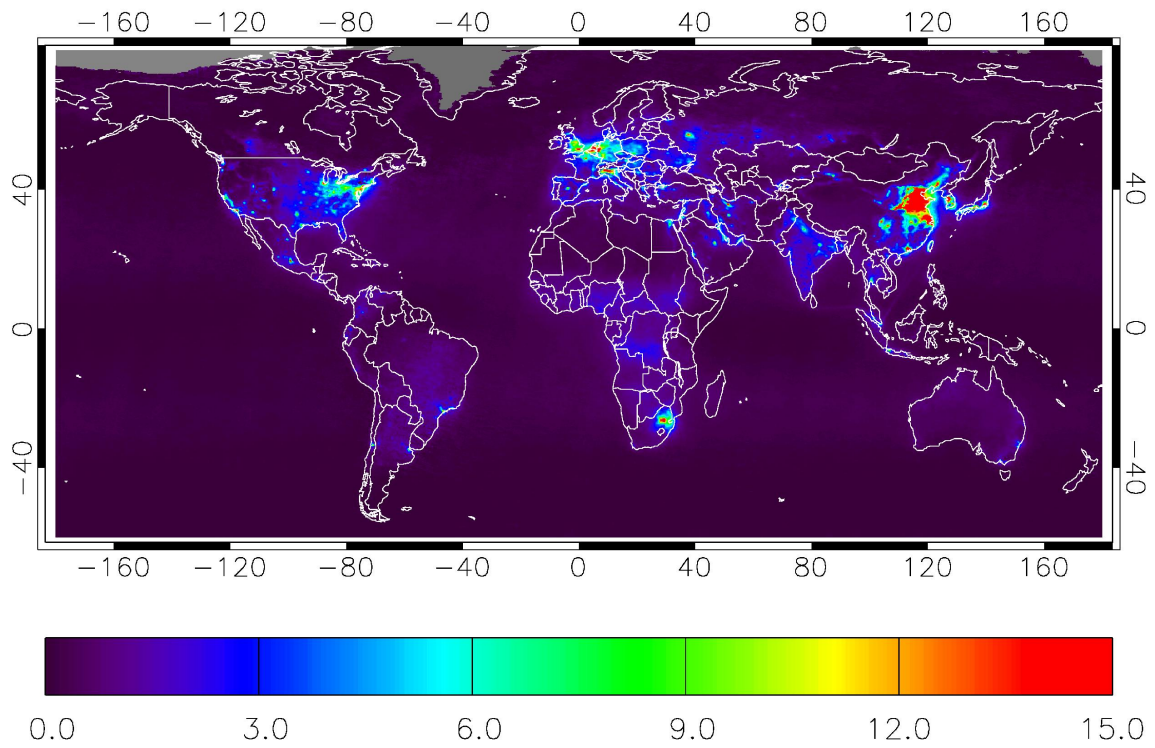
Page 30: Formatted **User** **3/14/2019 5:37:00 PM**

Subscript

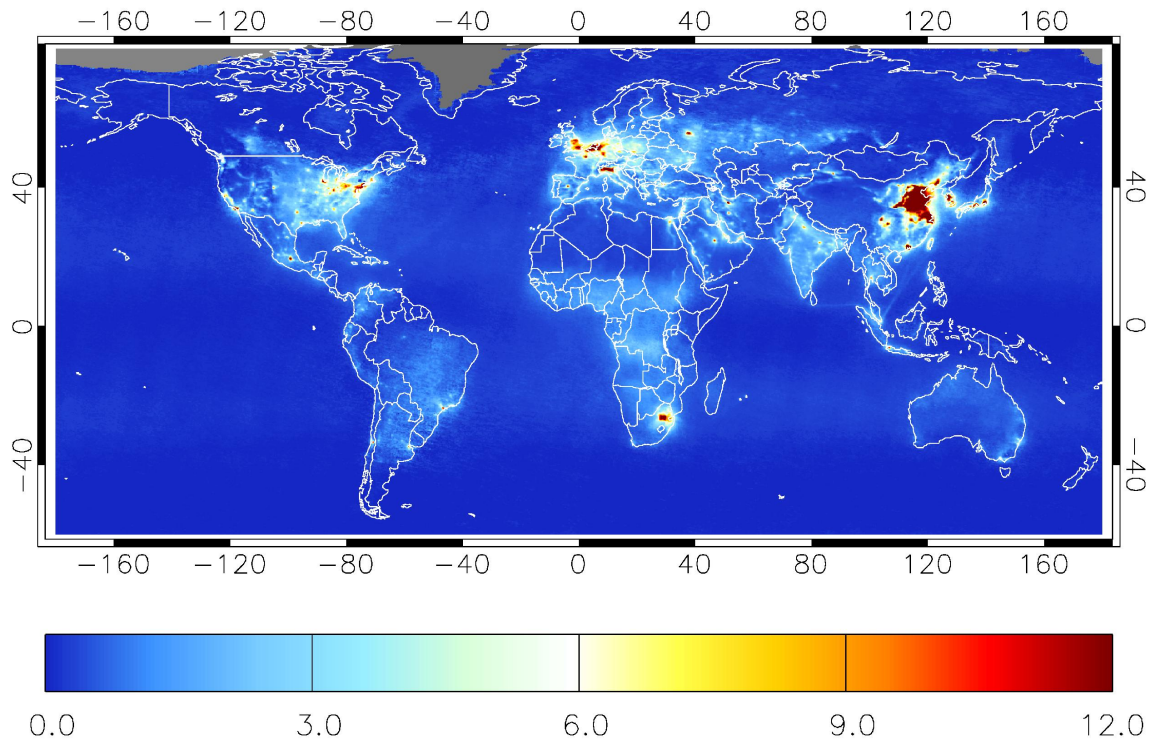
Page 30: Formatted **User** **3/14/2019 5:39:00 PM**

Subscript

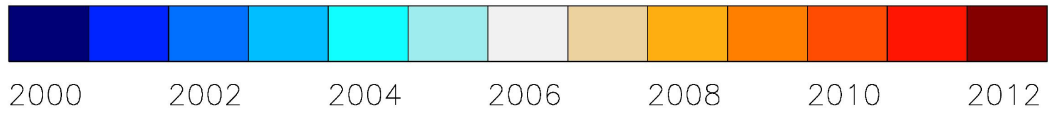
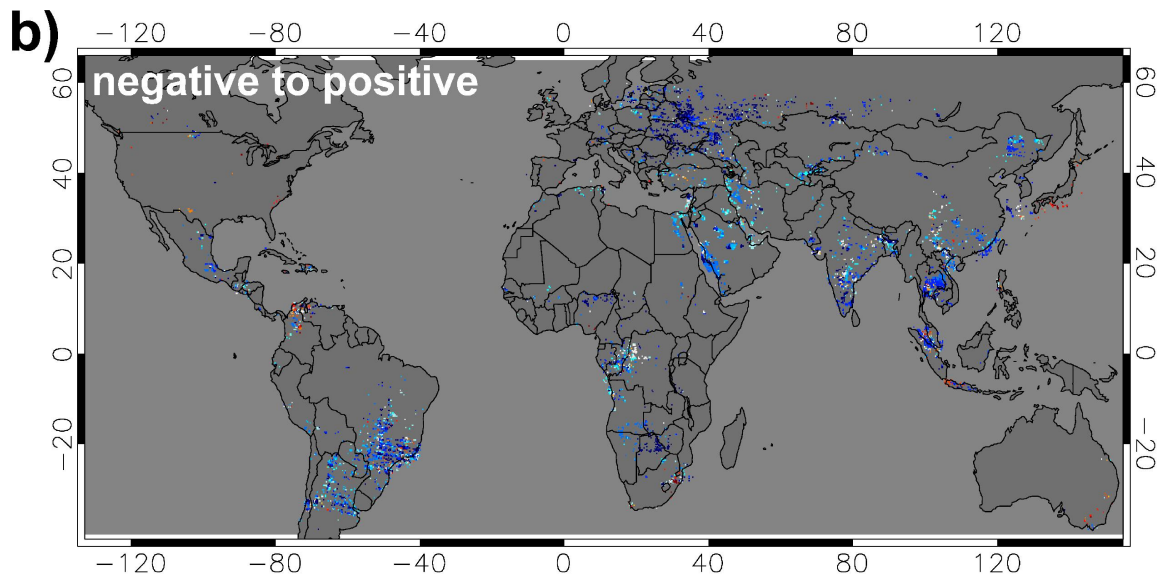
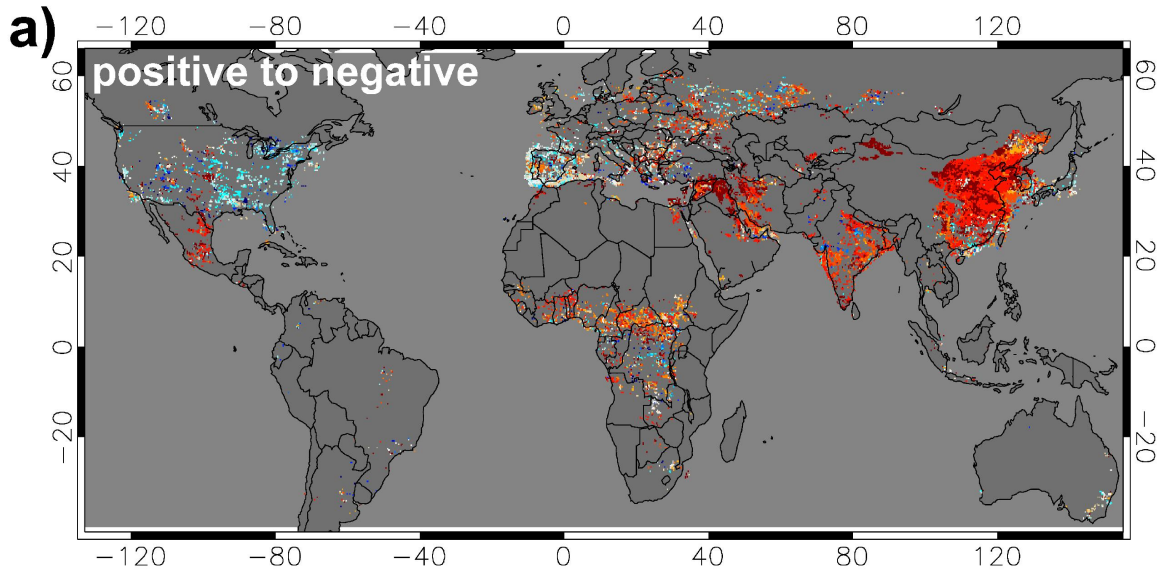
Page 31: Deleted **User** **3/14/2019 5:12:00 PM**

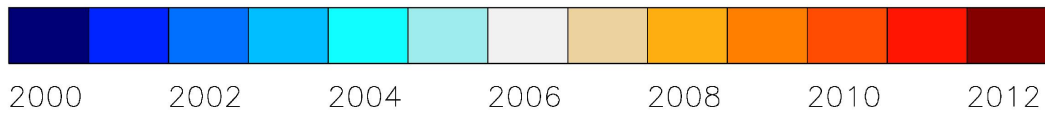
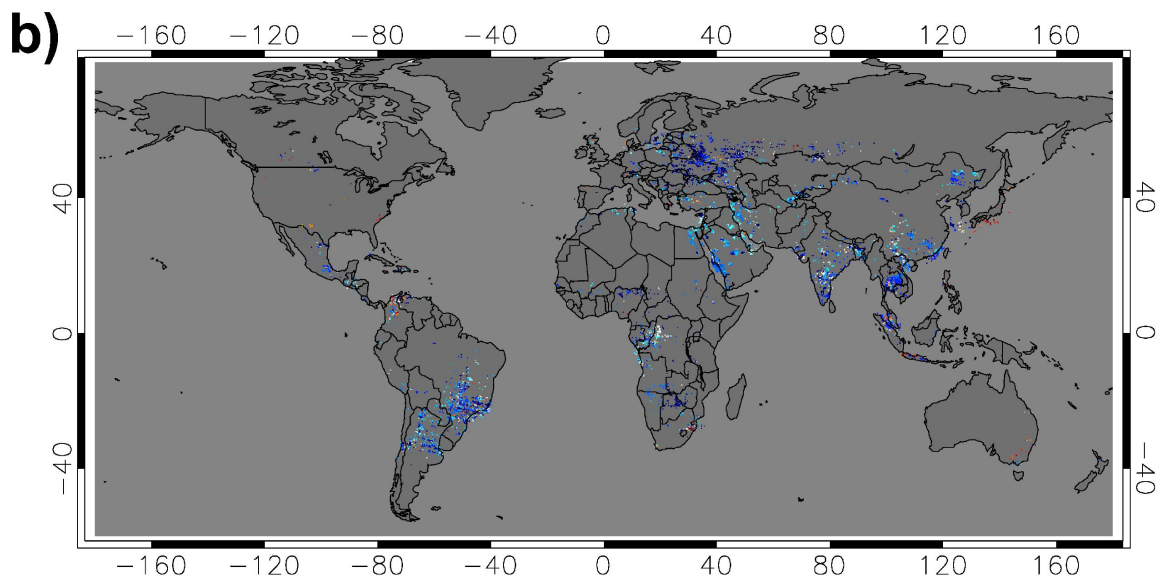
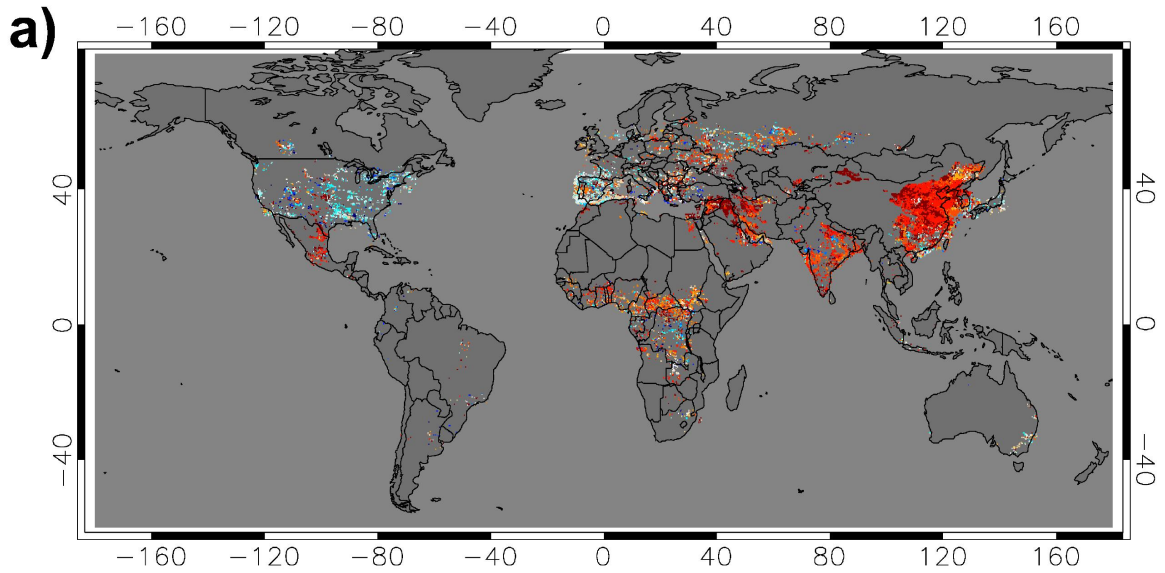


Page 31: Inserted **User** **3/14/2019 5:12:00 PM**



Page 31: Formatted	User	3/14/2019 5:12:00 PM
English (U.S.), Do not check spelling or grammar		
Page 31: Deleted	User	3/14/2019 5:09:00 PM
1		
Page 31: Inserted	User	3/14/2019 5:09:00 PM
2		
Page 32: Deleted	User	3/14/2019 5:09:00 PM
2		
Page 32: Inserted	User	3/14/2019 5:09:00 PM
3		
Page 33: Inserted	User	3/19/2019 10:13:00 AM





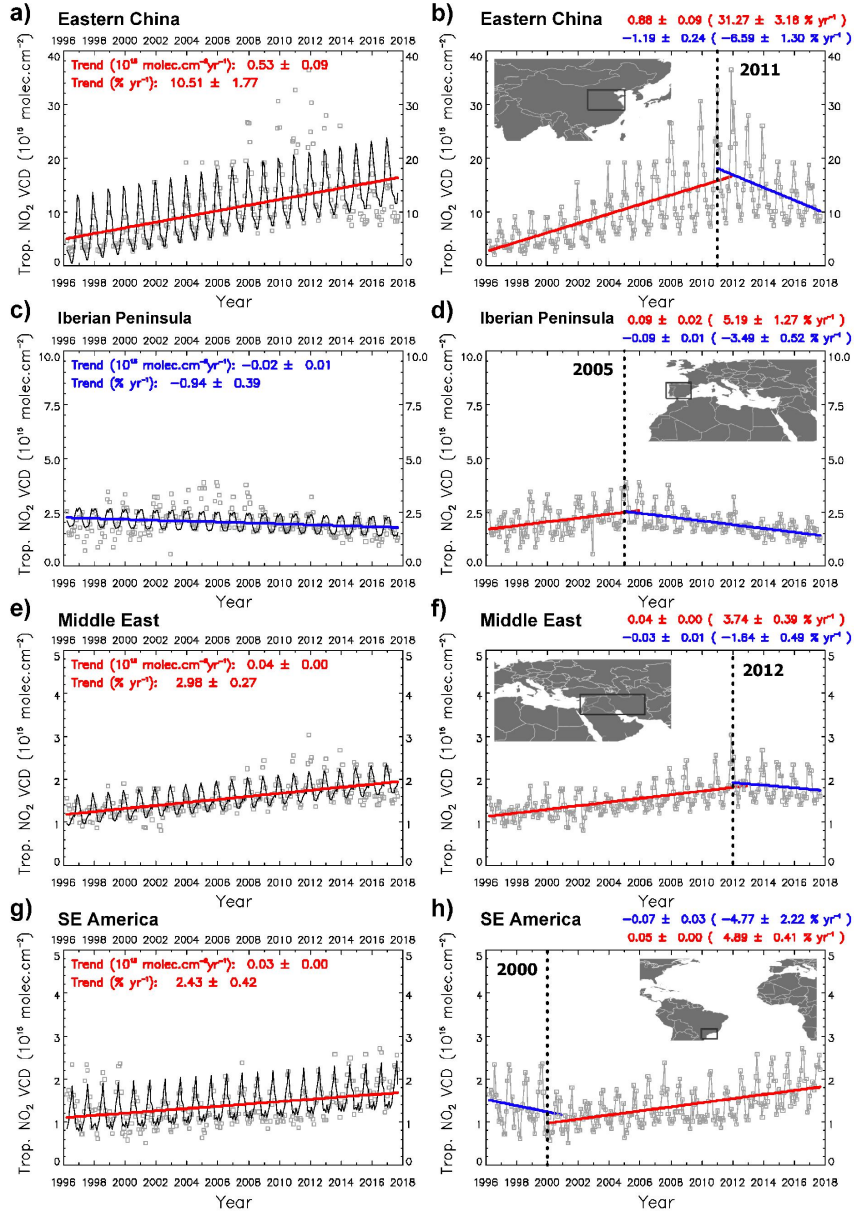
Page 33: Deleted **User** **3/14/2019 5:09:00 PM**

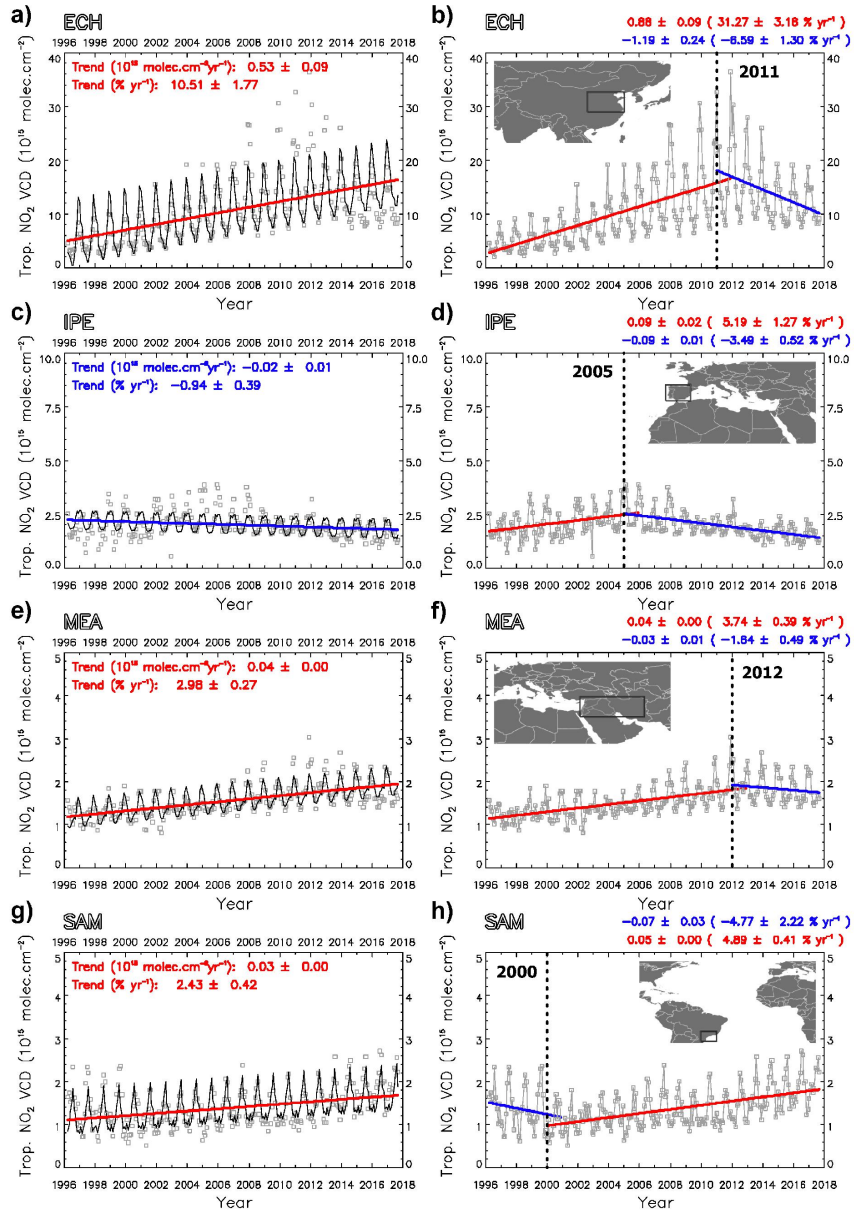
3

Page 33: Inserted **User** **3/14/2019 5:09:00 PM**

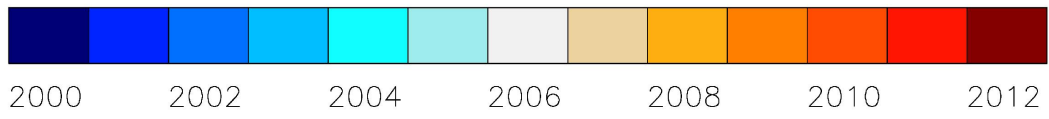
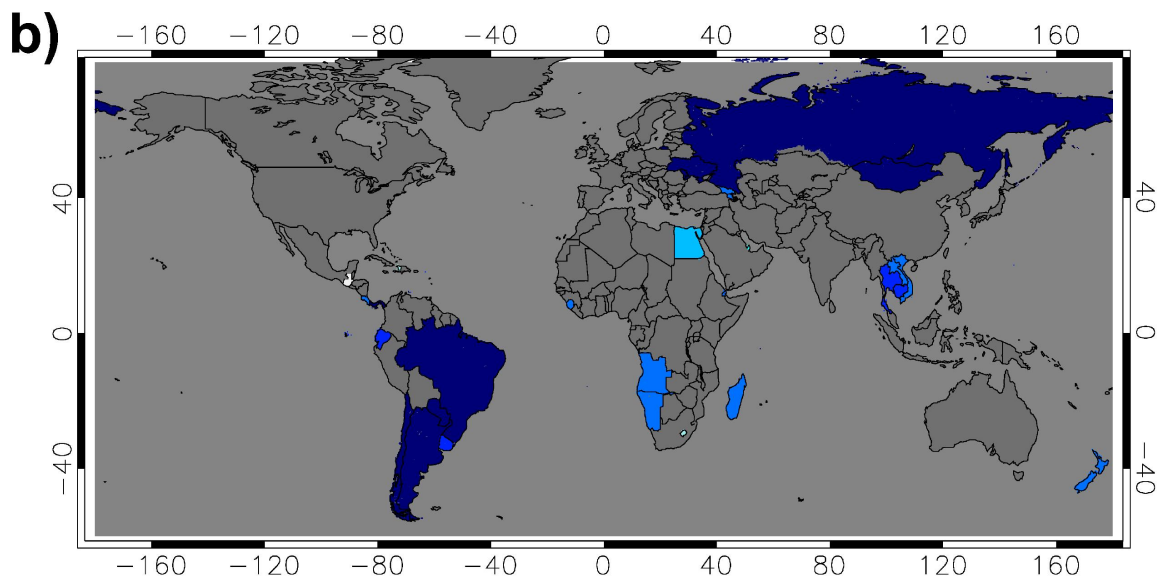
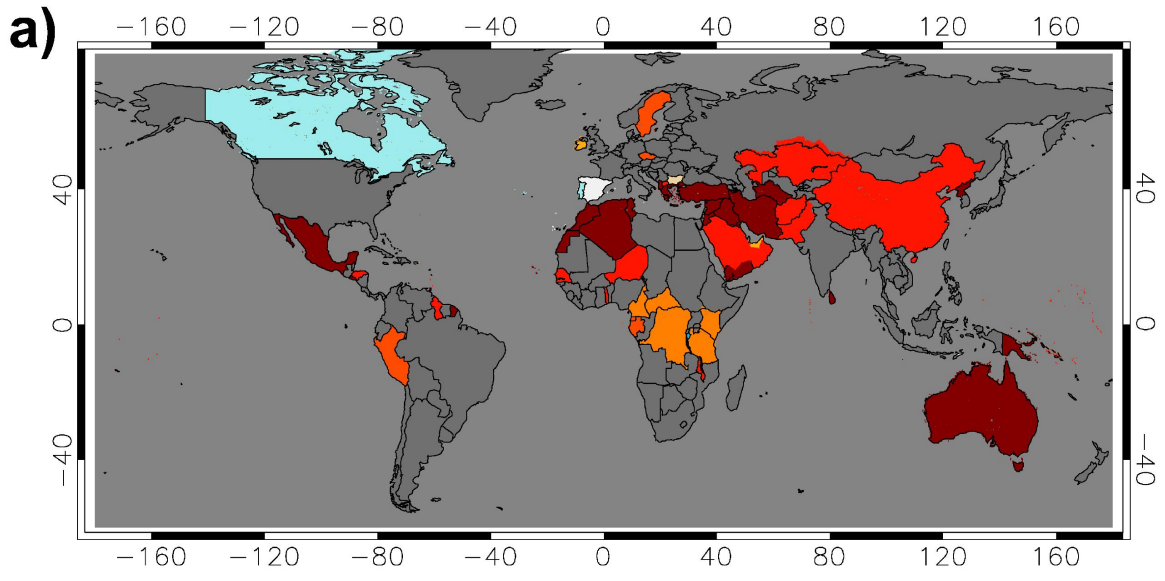
4

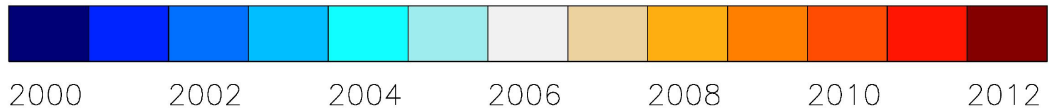
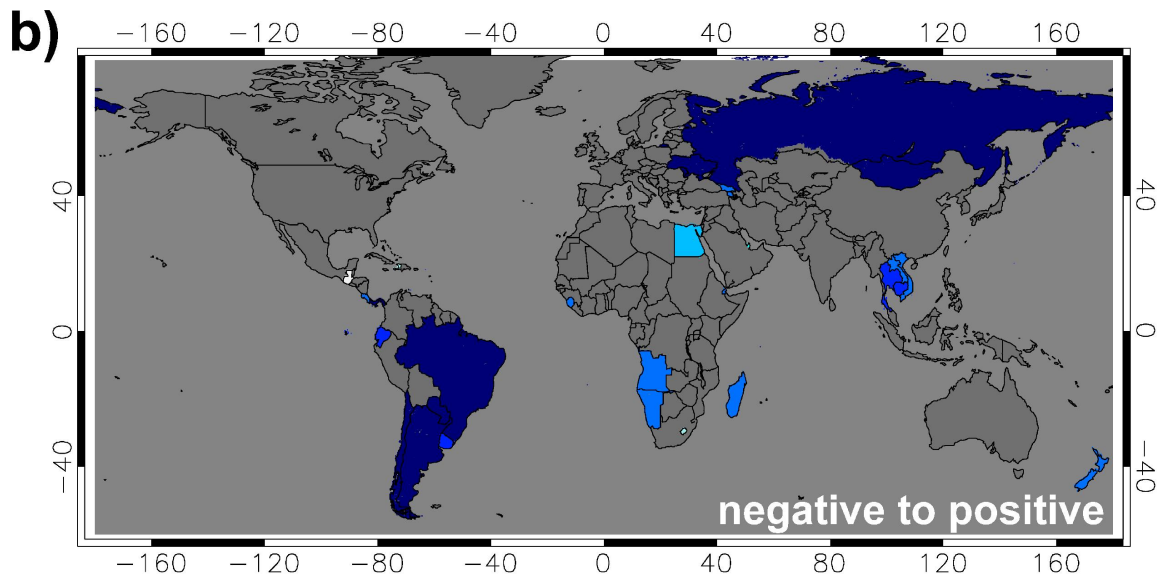
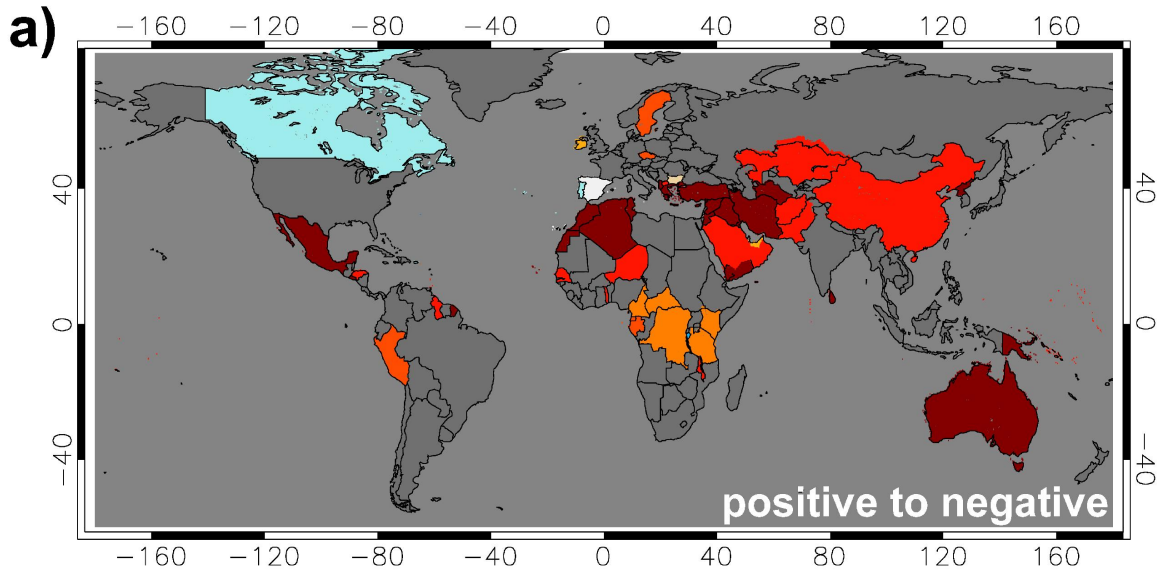
Page 34: Inserted **User** **3/20/2019 6:35:00 PM**





Page 34: Deleted	User	3/14/2019 5:10:00 PM
4		
Page 34: Inserted	User	3/14/2019 5:10:00 PM
5		
Page 35: Deleted	User	3/14/2019 5:10:00 PM
5		
Page 35: Inserted	User	3/14/2019 5:10:00 PM
6		
Page 36: Deleted	User	3/21/2019 7:27:00 PM





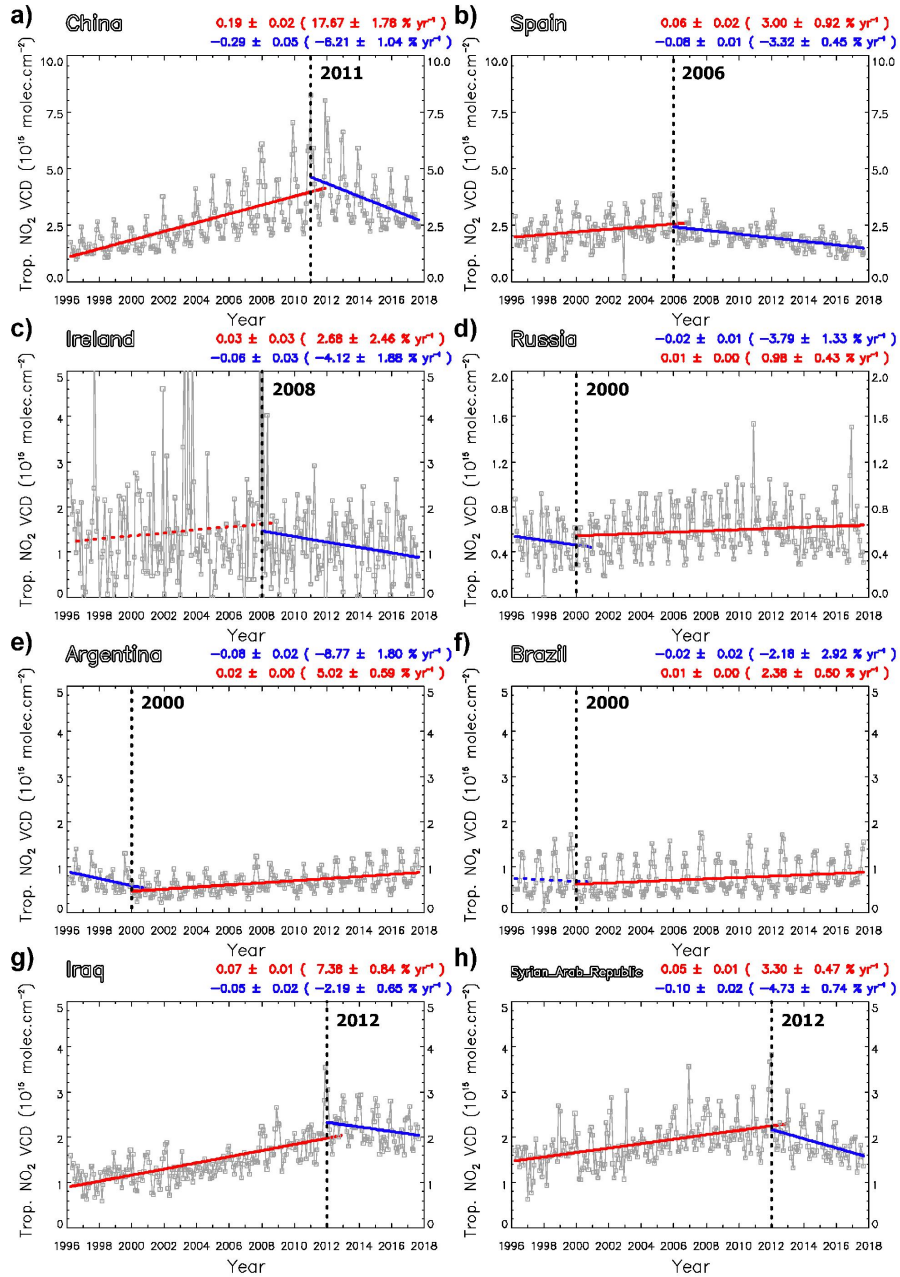
Page 36: Deleted User 3/14/2019 5:10:00 PM

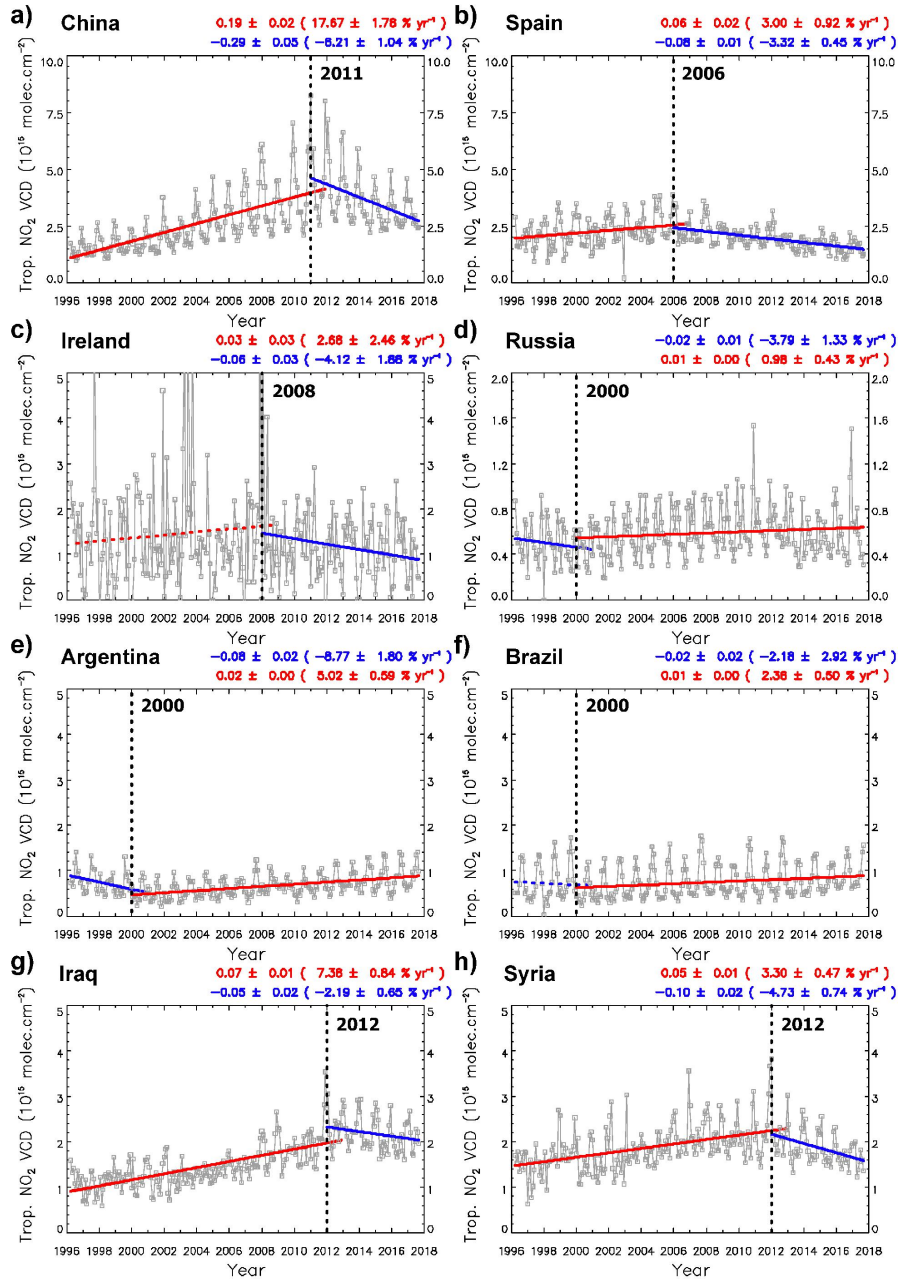
6

Page 36: Inserted User 3/14/2019 5:10:00 PM

7

Page 37: Deleted User 3/21/2019 10:35:00 AM





Page 37: Deleted User 3/14/2019 5:11:00 PM

7

Page 37: Inserted User 3/14/2019 5:11:00 PM

8

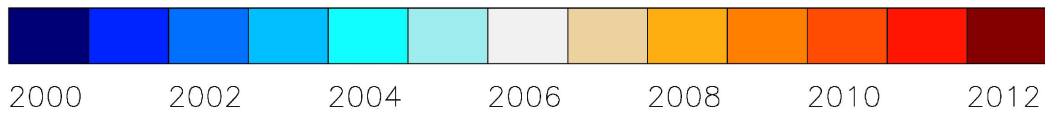
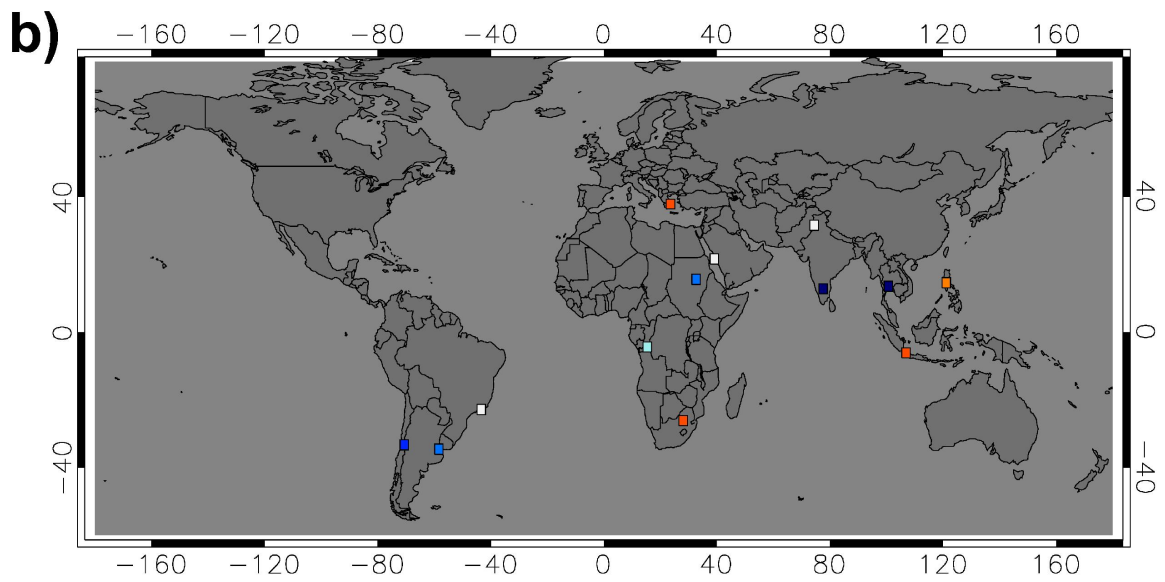
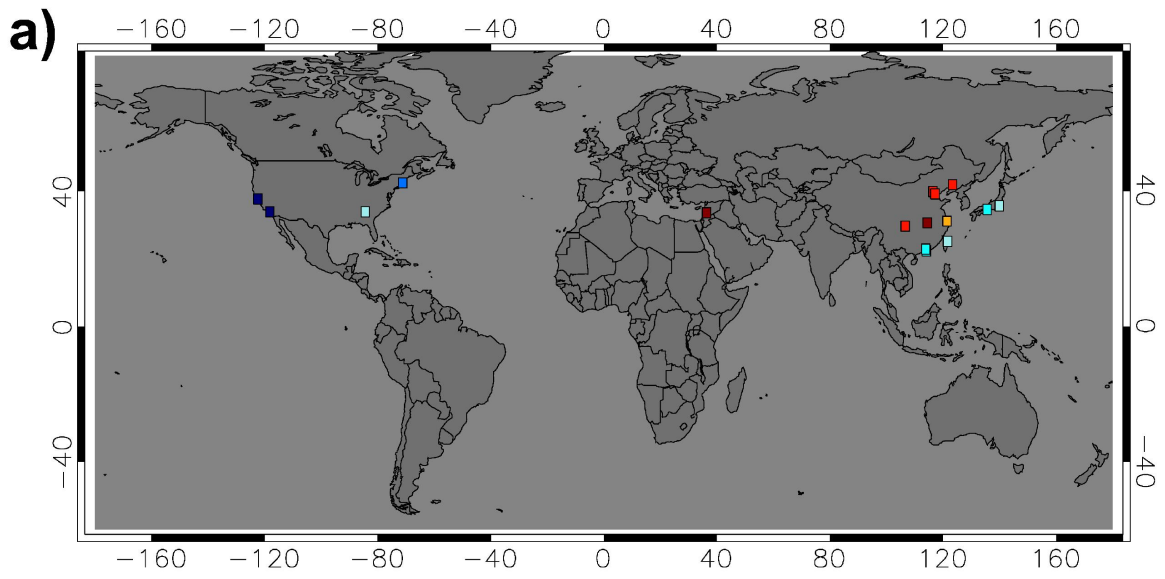
Page 38: Deleted User 3/14/2019 5:11:00 PM

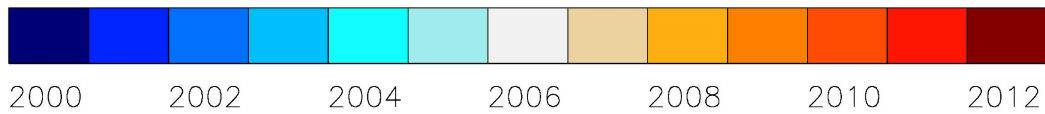
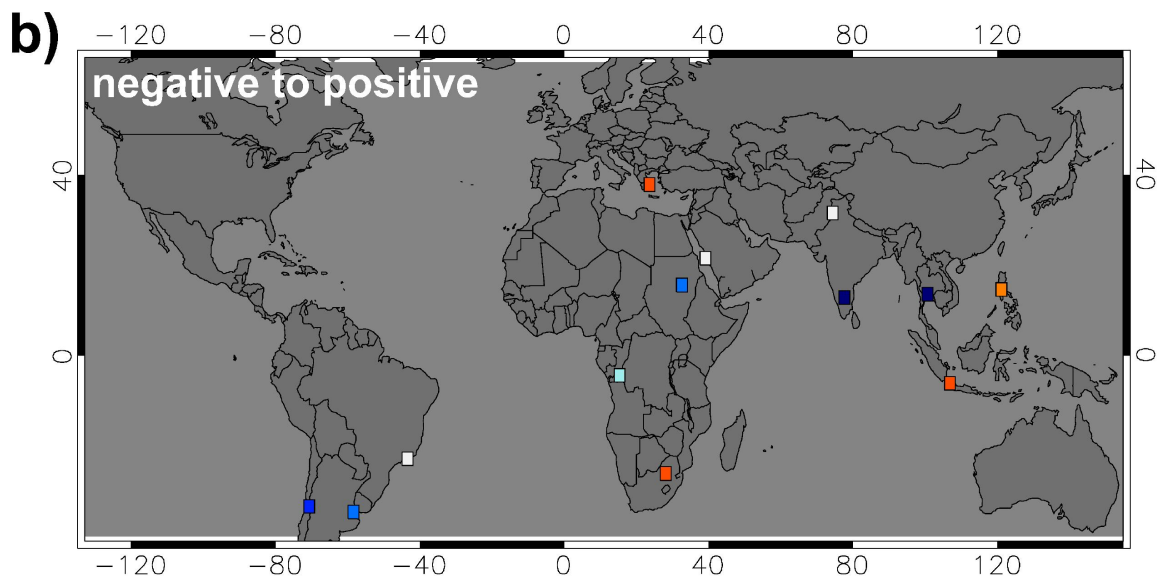
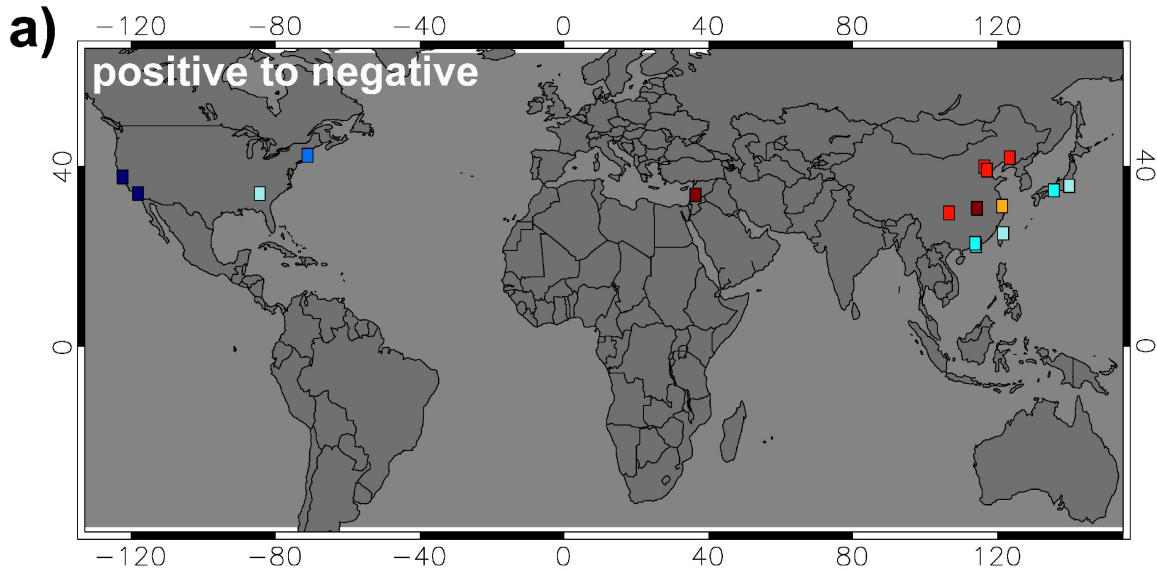
8

Page 38: Inserted User 3/14/2019 5:11:00 PM

9

Page 39: Deleted User 3/21/2019 7:19:00 PM





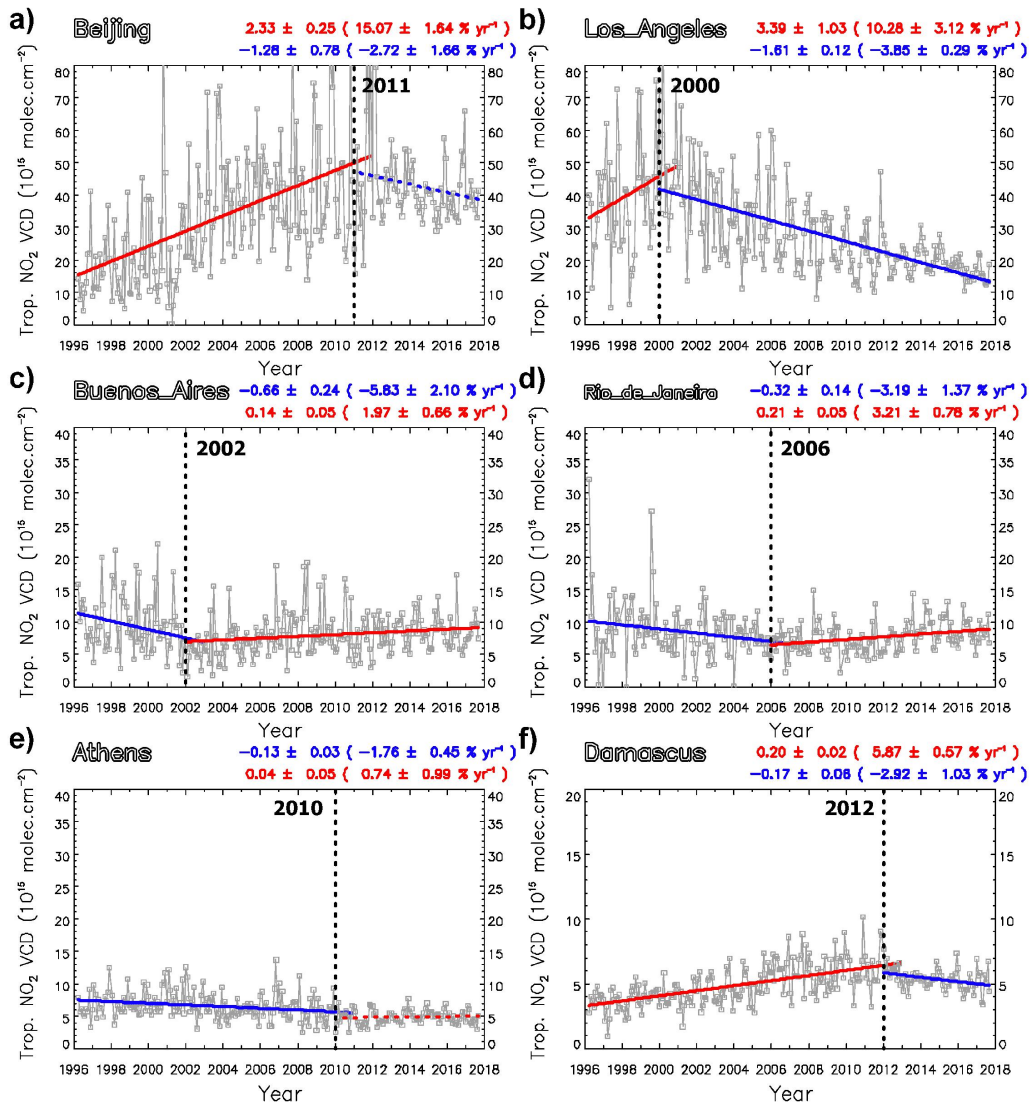
Page 39: Inserted **User** **3/14/2019 5:11:00 PM**

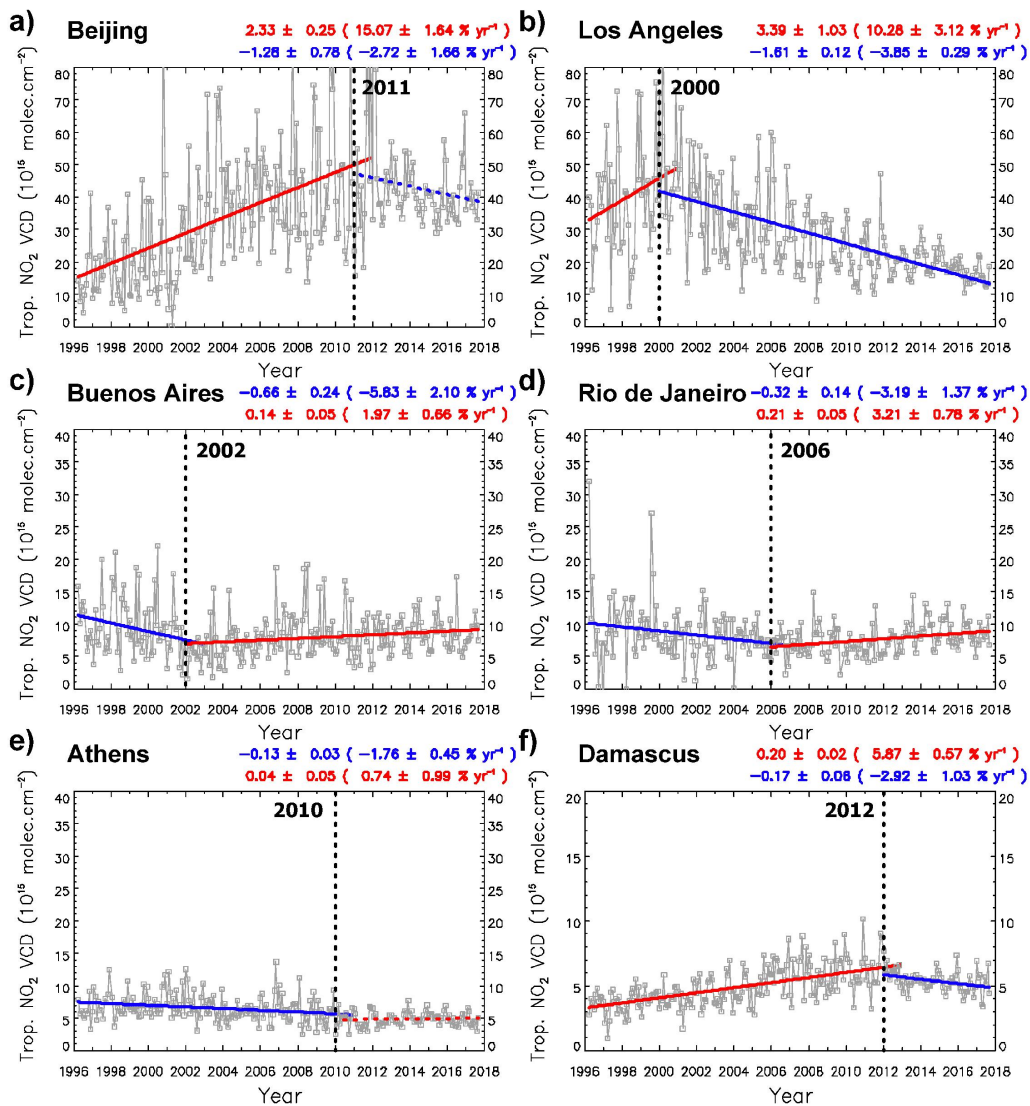
10

Page 39: Deleted **User** **3/14/2019 5:11:00 PM**

9

Page 40: Deleted **User** **3/21/2019 7:18:00 PM**





Page 40: Deleted User 3/14/2019 5:11:00 PM

10

Page 40: Inserted User 3/14/2019 5:11:00 PM

11

Page 40: Deleted User 3/14/2019 5:05:00 PM

7

Page 40: Inserted User 3/14/2019 5:05:00 PM

8

Header and footer changes

Text Box changes

Header and footer text box changes

Footnote changes

Endnote changes

Trends and trend reversal detection in two decades of tropospheric NO₂ satellite observations

Aristeidis K. Georgoulas^{1,a,b*}, Ronald J. van der A¹, Piet Stammes¹, K. Folkert Boersma^{1,2}, Henk J. Eskes¹

¹Royal Netherlands Meteorological Institute (KNMI), De Bilt, the Netherlands

²Wageningen University, Wageningen, the Netherlands

^acurrent address: Institute for Astronomy, Astrophysics, Space Application and Remote Sensing, National Observatory of Athens, Athens, Greece

^{ba}current address: Department of Meteorology and Climatology, School of Geology, Aristotle University of Thessaloniki, Thessaloniki, Greece

Correspondence to: Aristeidis K. Georgoulas (ageor@auth.gr)

Abstract. In this work, a ~21-years ~~self-consistent~~ global dataset from four different satellite sensors with a mid-morning overpass (GOME/ERS-2, SCIAMACHY/ENVISAT, GOME-2/Metop-A and GOME-2/Metop-B) is compiled to study the long-term tropospheric NO₂ patterns and trends. The GOME and GOME-2 data are "corrected" relative to the SCIAMACHY ~~data data in order to reproduce what SCIAMACHY would measure if it was in orbit for~~ to produce a self-consistent dataset that covers the period 4/1996-9/2017. The highest tropospheric NO₂ concentrations are seen over urban, industrialized and highly populated areas and over ship tracks in the oceans. Tropospheric NO₂ has generally decreased during the last two decades over the industrialized and highly populated regions of the Western World (~~e.g. average a total~~ decrease of the order of ~49% over the U.S., the Netherlands and the U.K., ~36% over Italy and Japan and ~32% over Germany and France) and increased over developing regions (~~e.g. averagea total~~ increase of ~160% over China and ~33% over India). It is suggested here that linear trends cannot be used efficiently worldwide for such long periods. Tropospheric NO₂ is very sensitive to socioeconomic changes (e.g. environmental protection policies, economic recession, warfare, etc.) which may cause either short term changes or even a reversal of the trends. The application of a method capable of detecting the year when a reversal of trends happened shows that tropospheric NO₂ concentrations switched from positive to negative trends and vice versa over several regions around the globe. A country-level analysis revealed clusters of countries that exhibit similar positive-to-negative or negative-to-positive reversals while 29 out of a total of 64 examined megacities and large urban agglomerations experienced a trend reversal at some point within the last two decades.

1 Introduction

Nitrogen dioxide (NO₂) constitutes one of the most important air pollutants in the atmosphere being responsible for the air quality degradation in many regions across the Earth. It plays a major role in a number of processes in the troposphere such as the photochemical production of ozone (O₃) and the formation of nitric acid (HNO₃) (Seinfeld and Pandis, 2016 and references therein), the formation of nitrate aerosols (Basset and Seinfeld, 1983), and modifies the radiative balance in the atmosphere either directly (by absorbing solar radiation) (Solomon et al., 1999) or indirectly (e.g. by the formation of ozone or the modification of greenhouses gas lifetime such as methane) (Isaksen et al., 2014). In addition, NO₂ has a diverse effect on human health, being toxic at high concentrations. Long exposure to NO₂ may lead to the development of asthma and increase susceptibility to respiratory infections (WHO, 2003).

As NO₂ is largely produced by anthropogenic activities (e.g. transportation, industry, domestic heating, power plants and smelters) it is mostly abundant in urban environments. A small part of the global NO₂ concentration is produced by natural sources such as biomass burning, lightning flashes and soil microbial activity (Hilboll et al. 2013 and references therein). Socioeconomic changes from the beginning of the industrial revolution until today had a critical impact on the NO₂ levels over various locations around the planet (Vestreng et al., 2009). At the same time, the continuous growth of the global population and its concentration into urban agglomerations (cities, megacities, conurbations) led to the development of major NO₂ hotspots which can be detected from space (Schneider et al., 2015).

It has been more than two decades now that a series of sensors onboard sun-synchronous orbit satellites continuously measure the tropospheric NO₂ vertical column density (VCD) at nearly the same time (equator crossing time in mid-morning) offering global coverage at timescales ranging from 6 up to 1 days. The first sensor to measure NO₂ VCDs was the Global Ozone Monitoring Experiment (GOME) (Burrows et al., 1999) onboard European Space Agency (ESA) satellite ERS-2. GOME flew on a sun-synchronous near polar orbit from mid 1995 delivering NO₂ measurements at a nominal spatial resolution of 320 x 40 km² (crossing equator time: 10:30 LT) until June 2003 when the ERS-2 tape recorder failed leading to a very low global coverage. Till June 2003, the daily coverage was achieved every three days. Except from the nominal GOME operation, narrow swath mode measurements were taken three days each month at a spatial resolution four times higher (80 x 40 km²) (Beirle et al., 2004). In this mode, global coverage was achieved using 12 days of data. Due to a saturation of the visible channels under certain circumstances during the first months of its operation, GOME had a smaller ground pixel (80 x 40 km²) (worse ground coverage) until March 1996 when the problem was solved.

GOME was succeeded by the SCanning Imaging Absortion spectroMeter for Atmospheric Cartography (SCIAMACHY) (Burrows et al., 1995; Bovensmann et al., 1999) onboard ESA's satellite ENVISAT. SCIAMACHY was on a sun-synchronous near polar orbit delivering NO₂ measurements at a spatial resolution of 60 x 30 km² (crossing equator time: 10:00 LT) from August 2002 until April 2012 when contact was lost. The sensor's global coverage time was six days.

SCIAMACHY was succeeded by two GOME-2 satellite instruments (Callies et al., 2000; Munro et al., 2016) onboard Metop-A (October 2006) and Metop-B (September 2012) with morning equator crossing times, which were

developed by ESA and are operated by the European Organization for the Exploitation of Meteorological Satellites (EUMETSAT). GOME-2A flies on a sun-synchronous near polar orbit with an equator crossing equator time of 09:30 LT. Originally, GOME-2A had a 1920 km swath and a 80 x 40 km² footprint covering the earth once every 1.5 days. In July 2013 GOME-2A swath was changed to 960 km and its footprint to 40 x 40 km². GOME-2B shares the same characteristics with GOME-2A before July 2013 (Munro et al., 2016; Wang et al., 2017). GOME-2A delivers NO₂ measurements from January 2007 and GOME-2B from January 2013 onwards.

The instruments mentioned above are different by means of their technical characteristics, calibration and their spatial resolution which makes the use of their observations as one single dataset very challenging. Several studies in the past made use of the tropospheric NO₂ data from the aforementioned sensors simultaneously; however, in most cases, the datasets were either used separately (e.g. van der A et al., 2006; Schneider et al., 2012; Valks et al., 2011) or they were downgraded to a low spatial resolution (e.g. van der A et al., 2008; Konovalov et al., 2010). Some studies have suggested a method that accounts for the spatial resolution difference between GOME and SCIAMACHY observations (e.g. Konovalov et al., 2006, 2008) in order to preserve the high spatial resolution. On top of this correction, Hilboll et al. (2013) suggested a method that accounts for all the other instrumental differences, including instrument-dependent offsets in a fitted trend function. They applied their method on GOME, SCIAMACHY, OMI (Ozone Monitoring Instrument) and GOME-2A data. Geddes et al. (2016) followed a similar approach by applying a spatial resolution and a shift correction on data from GOME, SCIAMACHY and GOME-2A sensors.

Here, we proceed ~~for the first time~~ to the compilation of a ~21-years self-consistent dataset, using morning data from GOME/ERS-2, SCIAMACHY/ENVISAT, GOME-2/Metop-A and GOME-2/Metop-B, by following a three-step procedure. It has to be noted that OMI (Levelt et al., 2006; 2018) onboard EOS Aura (2004-today) has also been measuring tropospheric NO₂ since October 2004; however, its equator crossing time is in the afternoon. Taking into account that tropospheric NO₂ is characterized by a significant diurnal variability (Boersma et al., 2008), the use of mixed morning and afternoon measurements might insert large uncertainties and hence we decided to focus on morning measurements only.

Details about the datasets which are merged along with a description of the methodology followed are given in Sect. 2 ~~and Appendix A. All the methods used in this work are described comprehensively in the Appendix in order to make it easier for the reader to focus on the results and the discussion.~~ The joint dataset is used for a detailed global trend analysis (see Sect. 2 ~~and Appendix B for details about the trend calculations~~). The long-term tropospheric NO₂ global patterns and trends are presented in Sect. 3.1. A method that detects trend reversals was developed (see Sect. 2 ~~and Appendix C for details~~) in order to show that a single linear trend cannot be used efficiently worldwide for such long periods. The method is applied on a global scale, on a country basis and for a number of megacities/large urban agglomerations around the world and the year of the reversal along with the trends for the period before and after the reversals are reported (Sect. 3.2, 3.3 and 3.4). The coincidence of the trend reversals with different socioeconomic changes is also examined. At the end of the paper the main findings and conclusions of this research are summarized.

2 Data and methods

2.1 Satellite data

In this work, we use tropospheric NO₂ VCD data from the GOME (4/1996-6/2003), SCIAMACHY (8/2002-3/2012), GOME-2A (1/2007-9/2017) and GOME-2B (1/2013-9/2017) TM4NO2A v.2.3 datasets which are available from the Royal Netherlands Meteorological Institute (KNMI). The retrieval scheme consists of three steps. First, the NO₂ slant column density (SCD) is retrieved applying the differential optical absorption spectroscopy (DOAS) method (Platt, 1994), then the stratospheric and tropospheric contribution to the NO₂ SCD is calculated with a data assimilation approach (Dirksen et al., 2011), and finally the tropospheric SCD is converted into tropospheric VCD using a calculated air mass factor (AMF) (Boersma et al., 2004). With DOAS, the reflectance spectrum in the wavelength range from 425-450 nm measured by the sensors is fitted by a model that takes into account absorption cross sections for NO₂, O₃, O₂-O₂, and H₂O and the Ring effect while a low-order polynomial accounts for the scattering from aerosols and clouds and for the Rayleigh scattering (Vandaele et al., 2005). The separation between stratospheric and tropospheric SCD is achieved by assimilating the total SCD retrieved with the DOAS into the TM4 chemistry transport model (Dirksen et al., 2011). The AMFs which are used in step 3 for the conversion of the tropospheric SCDs from step 2 into tropospheric VCDs are pre-calculated using the Doubling-Adding KNMI (DAK) radiative transfer model (Stammes, 2001). The retrieval scheme uses satellite-based surface albedo climatological data (Boersma et al., 2004) while cloud fraction and cloud top height is retrieved using the FRESCO algorithm (Koelemeijer et al., 2001). Specifically, the version TM4NO2A v.2.3 dataset used here is the result of a major update that was implemented during the switch from TM4NO2A v.1.1 to TM4NO2A v.2.0 (new altitude-dependent AMF look-up table, a more realistic surface albedo dataset from MERIS sensor onboard ENVISAT satellite, an improved terrain height dataset, and better sampling of TM4 profiles) and the correction of minor retrieval errors thereafter (details in Boersma et al., 2011 and on TEMIS website: www.temis.nl, last access: ~~15-19 September-March 2018~~2019). Single pixel GOME, SCIAMACHY, GOME-2A and GOME-2B retrievals were attributed to a standard grid of 0.25° x 0.25° and the observations were averaged on a monthly basis. When averaging, each observation is weighted by its fractional area (%) within the grid cell. For each valid observation, the cloud radiance fraction has to be less than 50% (cloud fraction less than about 20%) and the surface albedo not higher than 0.3, while observations with a solar zenith angle higher than 80° are filtered-out. In addition, there is no limitation in the number of observations used, negative columns are taken into account, and the observational error is ignored in the averaging process (e.g. Schneider et al., 2015).

2.2 Methodology

In order to produce a self-consistent tropospheric NO₂ VCD monthly gridded dataset from GOME, SCIAMACHY, GOME-2A and GOME-2B (~~from~~for the period 4/1996 to 9/2017, we followed a three-step methodology based on the methods of Hilboll et al. (2013) and Geddes et al. (2016). A basic difference with Hilboll et al. (2013) is that we first produced a self-

Formatted: Superscript

consistent dataset applying all the necessary corrections and then we proceeded to a trend analysis instead of fitting part of the corrections during the trend analysis. In addition, the trend analysis is applied on monthly data instead of annual data ~~like~~ ~~in~~ ~~contrary~~ ~~to~~ Geddes et al. (2016). The SCIAMACHY dataset was used as a reference as SCIAMACHY shared common periods of measurements with both GOME and GOME-2A. ~~This way, we managed to reproduce what SCIAMACHY would measure if the sensor was in orbit for ~21 years (from 4/1996 to 9/2017).~~

The GOME data were first corrected for the low horizontal resolution they exhibit relative to SCIAMACHY (320 x 40 km² vs 60 x 30 km²) (step 1) (see also Hilboll et al., 2013). ~~Of course the grid cell size is the same (0.25° x 0.25°) for the GOME and SCIAMACHY monthly datasets; however, this does not impact the fact that the information included in a larger swath corresponds to a larger area. Hence, the gridded data which are produced from larger pixels (320 x 40 km² for GOME) will be of "lower resolution" than the ones produced from smaller pixels (60 x 30 km² for SCIAMACHY) and the resulting maps will be much smoother. As the GOME nominal resolution is nearly 3 times lower than that of SCIAMACHY at the horizontal dimension, following the reasoning of Geddes et al. (2016), we may assume that each grid cell of the GOME gridded dataset will correspond to an area nearly 3 times larger. Hence, ~~in step 1~~ ~~to~~ ~~so~~ the SCIAMACHY monthly gridded VCD data (VCD_{SC}) were first smoothed in the horizontal dimension in order to match GOME's horizontal resolution. This was achieved by using a boxcar algorithm with an averaging window of 13 x 0.25° (3.25°) in longitudinal direction (Eq. A1) similarly to Geddes et al. (2016). ~~The correction is applied in the horizontal dimension only as the along track dimensions are close in the two datasets (40 km vs 30 km) and also close to the latitudinal dimension of the gridded dataset (0.25°).~~ Then climatological monthly values for the full 9-years period (1/2003-12/2011) were calculated from the original and the smoothed SCIAMACHY (VCD_{SCsm}) dataset on a grid cell basis (Eq. A2). The ratio of the original and the smoothed climatological values is termed as spatial resolution climatological correction factor (CF1: 1 value for each month of the year, a total of 12 values for each grid cell) (see also Hilboll et al., 2013). ~~To avoid having unreasonably large CF1 values due to very low tropospheric NO₂ levels, CF1 was set equal to 1, in cases of VCD_{SCsm} lower than 0.1 x 10¹⁵ molecules cm⁻² which corresponds to SCIAMACHY's precision.~~ The total and the monthly mean ~~annual mean~~ CF1 values for the whole globe as well as for North America, Europe and ~~China-south-eastern Asia~~ can be seen in Figs. S1, S2, S3 and S4S8, ~~respectively.~~ ~~CF1 is unitless and exhibits characteristic spatial patterns with values greater than and lower than 1 over and adjacent to pollution hotspots, respectively. The CF1 patterns are pretty persistent throughout the year.~~ The original GOME gridded data (VCD_G) were multiplied with the corresponding CF1 values to produce a GOME dataset (VCD_{GCI}) with apparently higher spatial resolution (see Eq. A3). This method, generally assumes that the relative spatial structure of the central dataset (SCIAMACHY) persists during the GOME ~~and GOME-2~~ periods. ~~The VCD_G and VCD_{GCI} patterns for the whole GOME period are shown in Fig. 1a and Fig. 1b, respectively.~~~~

$$\text{VCD}_{\text{SCsm}}(x, y, t) = \frac{1}{13} \left(\sum_{w=-6}^6 (\text{VCD}_{\text{SC}}(x + w \times 0.25, y, t)) \right) \quad (1)$$

Formatted: English (U.K.)

Formatted: Subscript

Formatted: Subscript

Formatted: Left

where x and y are the central longitude and latitude of a grid cell in degrees and t is the time in one month steps (from 1/2003 to 12/2011), ..., while $w = -6, -5, \dots, 0, \dots, 5, 6$ (a total of 13 values).

$$CF1(x, y, m) = VCD_{SC}(x, y, m) / VCD_{SCsm}(x, y, m) \quad (2)$$

where $m = 1, 2, \dots, 12$ is the month for which the climatological monthly values $VCD_{SC}(x, y, m)$ and $VCD_{SCsm}(x, y, m)$ are calculated.

$$VCD_{GC1}(x, y, t) = VCD_G(x, y, t) \times CF1(x, y, m) \quad (3)$$

The different spatial resolution leads to different spatial and temporal sampling by the two instruments which affects the observed NO_2 levels, the seasonal variability and its amplitude. The spatial resolution correction is expected to correct only part of those biases and hence further corrections ~~had to~~ be applied. Following (Hilboll et al., (2016)2013) who used a trend model that explicitly accounts for a level shift between the two instruments and for a change in the amplitude of the seasonal variation, we applied a shift correction (step 2) and a seasonal amplitude correction (step 3) successively, on top of the spatial resolution correction (step 1). More specifically, ~~The~~ the corrected GOME data (VCD_{GC1}) for the 11-month GOME-SCIAMACHY common period 8/2002-6/2003 were compared against SCIAMACHY data (VCD_{SC}) for the same period and a shift correction was further applied to account for the instrumental bias between the two sensors (step 2). The shift correction factor ($CF2$: 1 value for each grid cell) is equal to the difference between the two datasets for the common period and was calculated on a grid cell basis (Eq. A4) similarly to Geddes et al. (2016). $CF2$ (in 10^{15} molecules cm^{-2}) takes higher positive and negative values over several pollution hot spots (absolute values higher than 0.5) showing that further corrections should be applied on the data. The global $CF2$ patterns as well as the corresponding $CF2$ values for North America, Europe and south-eastern AsiaChina are shown in Fig. S5S9, S6S10, S7-S11 and S8S12, respectively. $-CF2$ was ~~extracted from~~ added to the spatial resolution corrected GOME data to produce a further corrected GOME dataset (VCD_{GC2}) (Eq. A5). The VCD_{GC2} patterns for the whole GOME period are shown in Fig. 1c.

$$CF2(x, y) = \frac{1}{n} \left(\sum_{t=t_1}^{t_2} (VCD_{SC}(x, y, t)) - \sum_{t=t_1}^{t_2} (VCD_{GC1}(x, y, t)) \right) \quad (4)$$

where t is the time in one month steps for the common GOME-SCIAMACHY period (t_1 : 8/2002 to t_2 : 6/2003) of $n=11$ months.

$$VCD_{GC2}(x, y, t) = VCD_{GC1}(x, y, t) + CF2(x, y) \quad (5)$$

Finally, the GOME data were brought closer to the SCIAMACHY data by applying a correction for the different seasonal amplitudes that may still exist after the first two corrections (step 3). The normalized to the long-term average seasonal variability (climatological monthly values were ~~extracted from~~ divided by the long-term average) of the

Formatted: Left

Formatted: Superscript

Formatted: Superscript

Formatted: Lowered by 18 pt

Formatted: Lowered by 6 pt

SCIAMACHY data (VCD_{sc}) for the whole SCIAMACHY period is divided by the normalized seasonal variability to the long-term average of the twice corrected GOME data (VCD_{GC2}) for the whole GOME period. The seasonal amplitude correction factor (CF3: 1 value for each month of the year, a total of 12 values for each grid cell) is equal to the ratio of the SCIAMACHY and GOME-normalized seasonal variability and is unitless (Eq. A6). Like in the case of CF1, to avoid having unreasonably large values due to very low tropospheric NO_2 levels, CF3 was set equal to 1 for grid cells with VCD_{sc} or VCD_{GC2} levels lower than 0.1×10^{15} molecules cm^{-2} . The total and the monthly mean annual mean CF3 values for the whole globe as well as for North America, Europe and south-eastern AsiaChina can be seen in Figs. S19, S10, S11 and S123-S20, respectively. The CF3 patterns are pretty patchy and cannot be connected to areas with low or high tropospheric NO_2 , like in the case of CF1 and CF2. The already twice-corrected GOME data (VCD_{GC2}) were then multiplied with the CF3 on a monthly basis to produce the final GOME dataset (VCD_{GC3}) (see Eq. A7). The VCD_{GC3} patterns for the whole GOME period are shown in Fig. 1d. As SCIAMACHY and GOME-2 have a comparable spatial resolution, in the case of GOME-2 data, step 1 was omitted. The GOME-2A and 2B data were averaged on a monthly basis to produce a common GOME-2 dataset which is then corrected following steps 2 and 3. The GOME-2A and GOME-2B data were assumed to be of equal quality and resolution in the averaging process.

$$CF3(x, y, m) = \frac{\left[VCD_{sc}(x, y, m) / \frac{1}{n_{sc}} \left(\sum_{t=t_{sc1}}^{t_{sc2}} (VCD_{sc}(x, y, t)) \right) \right]}{\left[VCD_{GC2}(x, y, m) / \frac{1}{n_G} \left(\sum_{t=t_{G1}}^{t_{G2}} (VCD_{GC2}(x, y, t)) \right) \right]} \quad (6)$$

where t is the time in one month steps for the whole SCIAMACHY period (t_{sc1} : 8/2002 to t_{sc2} : 3/2012) of $n_{sc}=116$ months and for the whole GOME period (t_{G1} : 4/1996 to t_{G2} : 6/2003) of $n_G=87$ months.

$$VCD_{GC3}(x, y, t) = VCD_{GC2}(x, y, t) \times CF3(x, y, m) \quad (7)$$

The self-consistent GOME-SCIAMACHY-GOME-2 timeseries were fitted by using a model with a linear trend and a Fourier-based seasonal component (see Eq. 8 and 9). The method is based on Weatherhead et al. (1998) and has been frequently used in previous studies to calculate the trends of trace gases, aerosols, surface solar radiation, etc. (e.g. van der A et al., 2008; De Smedt et al., 2010; de Meij et al., 2012; Pozzer et al., 2015; Georgoulis et al., 2016; Alexandri et al., 2017) and check whether they are statistically significant at the 95% confidence level (a detailed description of the method is given in Appendix B Eq. 10). Due to the systematic lack of valid tropospheric NO_2 retrievals (due to clouds, snow/ice cover, etc.), especially over areas at high latitudes, only trends calculated for timeseries with at least 8 months per year are considered reliable and hence are shown below (see also Pozzer et al., 2015).

$$Y_t = A + BX_t + \sum_{n=1}^6 \left[a_n \sin\left(\frac{2\pi}{T} nX_t\right) + b_n \cos\left(\frac{2\pi}{T} nX_t\right) \right] + N_t \quad (8)$$

Formatted: Not Superscript/ Subscript

Formatted: Not Superscript/ Subscript

Formatted: Not Superscript/ Subscript

Formatted: Subscript

where Y_t is the monthly mean value for month t , X_t is the number of the month after the first month of the timeseries, A is the monthly mean of the first month of the timeseries and B is the trend. The seasonal component contains the amplitudes a_n and b_n . T is the period and N_t is the difference between the modeled and the measured value, termed usually as remainder.

$$N_t = \varphi N_{t-1} + \varepsilon_t \quad (9)$$

where φ is the autocorrelation in the remainder and ε_t is the white noise. Autocorrelation φ affects the precision of the trend σ_B which is given as a function of φ , the length of the data set in years m and the variance σ_N of the remainder for small autocorrelations:

$$\sigma_B \approx \left[\frac{\sigma_N}{m^{3/2}} \sqrt{\frac{1+\varphi}{1-\varphi}} \right] \quad (10)$$

The calculated trend B is considered to be statistically significant at the 95% confidence level if $|B/\sigma_B| > 2$.

In order to detect trend reversals in the self-consistent GOME-SCIAMACHY-GOME-2 timeseries, a method similar to the one that was originally suggested in a solar dimming/brightening study was used (Cermak et al., 2010). The method is capable of finding the year when a reversal from positive to negative trends or from negative to positive trends appeared with a very limited error of 0.5-1%. It has to be highlighted that our study, in line with Cermak et al. (2010), focuses on detecting only one major trend reversal and hence minor reversals that may appear in the timeseries are not reported. The method is based on the minimization of a value S which is calculated on an annual basis (a detailed description is given in Appendix C). In this study, a trend reversal is reported only when the trend for the period before or the trend for the period after the reversal year (including the reversal year) is statistically significant at the 95% confidence level. The trend reversal method is based on the minimization of a value $S(t)$ which is calculated for each year t of the period $[t_1=2000, t_r=2012]$:

$$S(t) = \frac{\min(p(B_l), p(B_r))}{\text{abs}(B_l - B_r) \times \sigma_{B_{l+r}}} \quad (11)$$

where $p(B_l)$ and $p(B_r)$ express the probability that the trends B_l and B_r for the short periods on the left $[t-4, t]$ and on the right $[t, t+4]$ of the year t are statistically insignificant (1-significance level of the trend) and $\sigma_{B_{l+r}}$ is the standard error of the trend for the combined sub-periods $[t-4, t+4]$. We use a time window of 4 in our calculations so that each trend is calculated for at least five years and hence we can search for a trend reversal only within the period 2000-2012. The year t_r when S takes its lower value and there is a switch from a positive trend to a negative one or from a negative trend to a positive one is considered to be a potential trend reversal year. The trends with the corresponding significance levels and probabilities are calculated here using least-squares linear regression (TREND function in IDL). In this study, only when the trend B_b for the whole period before t_r (including t_r) $[t_1-4, t_r]$ or the trend B_a for the whole period after t_r (including t_r) $[t_r, t_r+4]$ is statistically significant at the 95% confidence level, a trend reversal is reported. Specifically, for the four extended regions of interest, the

Formatted: Subscript

Formatted: Subscript

Formatted: English (U.S.)

Formatted: Not Superscript/ Subscript

Formatted: Not Superscript/ Subscript

country and the megacities and large urban agglomeration analyses performed in this paper, the B_y and B_a trends are calculated from the monthly timeseries using the method presented in the previous paragraph (Eq. 8, 9 and 10) in order to be consistent with the trends for the whole time period (4/1996 - 9/2017) which are reported in the paper.

Formatted: English (U.S.)

5 **3 Results and Discussion**

3.1 Long term NO₂ patterns and linear trends

The [multi-year average](#) tropospheric NO₂ VCD patterns from the combined GOME-SCIAMACHY-GOME-2 dataset for the period 4/1996-9/2017 are shown in Fig. 42. It is obvious that the highest NO₂ concentrations are confined over urban, industrialized and highly populated areas. A careful look over oceanic regions reveals local maxima over ship tracks (e.g. Indian Ocean, Mediterranean Sea, Red Sea) highlighting the contribution of ship emissions on the global NO₂ burden. The highest tropospheric NO₂ VCDs appear over an extended area located in eastern China. This area encloses the Beijing-Tianjin-Hebei (BTH) and the Yangtze River Delta (YRD) urban clusters which have experienced an unprecedented population growth and a rapid industrial development over the last two decades ([see Kourtidis et al., 2015; Krotkov et al., 2016; de Foy et al., 2016](#)). Some very striking NO₂ hotspots that can be seen on the map (red color) are the Pearl River Delta (PRD) in southern China, Seoul in South Korea, Tokyo in Japan, Tehran in Iran, Moscow in Russia, the Highveld in South Africa, the Po Valley in northern Italy, the area covering the triangle Netherlands-Belgium-Germany, Paris/France, London/U.K., New York/U.S., and other ([see also in van der A, 2008; Schneider et al., 2015; Krotkov et al., 2016 and references therein](#)). Despite the fact that NO₂ is transported from one region to another and there is transboundary transport, due to the short NO₂ lifetime (from a few hours up to a day) its concentrations are generally representative of the local NO₂ emission strength.

During the last two decades various [socioeconomic](#) changes, that impacted the local NO₂ concentrations, have taken place over different areas around the globe. In Fig. 23, the linear trends of the tropospheric NO₂ VCD are shown in 10¹⁵ molecules cm⁻² yr⁻¹. More specifically, in Fig. 2a3a, all the grid cells are shown, while in Fig. 32b, only grid cells with statistically significant trends at the 95% confidence level and a long term tropospheric NO₂ VCD mean of at least 1 x 10¹⁵ molecules cm⁻² are shown as in Schneider et al. (2012). To exclude the existence of a large systematic bias in the trends a remote region located in the south of the Pacific Ocean [40° S-50° S, 130° W-150° W] with near zero mean tropospheric NO₂ levels ($-0.02 \pm 0.07 \times 10^{15}$ molecules cm⁻² for the period of interest) was examined. Indeed, a very low negative trend of -0.0037×10^{15} molecules cm⁻² yr⁻¹ was found, which is well below SCIAMACHY's precision of 0.1×10^{15} molecules cm⁻² (Hilboll et al., 2013) and can be considered negligible. Taking into account this and following previous studies, the trend values given in the manuscript are rounded to two decimal places except for Table 2 and 3 for intercomparison reasons between the various countries and megacities (see Sect. 3.3 and 3.4).

Strong statistically significant positive trends appear over extended regions in south-eastern Asia (e.g. eastern China, India, Thailand and Indonesia), the Middle East (e.g. Iraq, Iran, Persian Gulf, east coast of Red Sea), eastern Europe (e.g. northern Balkans, Black Sea and the continental areas around it), northern Africa (e.g. regions around the Nile, Morocco and northern Algeria), South Africa (the eastern part of the Highveld Plateau), South America (e.g. the region around Rio in Brazil, central Argentina, the region around Santiago/Chile, northern Colombia and Venezuela), central America (the region of Mexico city). The trend values over these areas are higher than 0.05×10^{15} molecules $\text{cm}^{-2} \text{yr}^{-1}$, with a maximum value of 2.18×10^{15} molecules $\text{cm}^{-2} \text{yr}^{-1}$ appearing within the BTH urban cluster in eastern China. On the contrary, strong statistically significant negative trends appear over the largest part of the U.S. (especially the eastern U.S. and the state of California), western and central Europe, Japan and Taiwan in south-eastern Asia and the region around the Johannesburg-Pretoria conurbation in South Africa. The absolute trend values over these areas are higher than 0.05×10^{15} molecules $\text{cm}^{-2} \text{yr}^{-1}$, with a maximum trend of -1.40×10^{15} molecules $\text{cm}^{-2} \text{yr}^{-1}$ appearing close to Los Angeles city in the eastern U.S.

_____ In general, the trend patterns ~~here are similar~~ resemble to the ones appearing in previous satellite-based studies for shorter periods (e.g. van der A et al., 2008; Schneider et al., 2012; Hilboll et al., 2013; Krotkov et al., 2016). Concluding, our results confirm that tropospheric NO_2 concentrations have generally decreased during the last ~21 years over the industrialized and highly populated regions of the so-called "Western World" and increased over developing regions. Indicatively, according to the calculated trends, the tropospheric NO_2 levels have decreased ~~on average~~ by ~49% during the whole period of interest (relative to the fitted mean of the first year) over the U.S., the Netherlands and the U.K., by ~36% over Italy and Japan and by ~32 % yr^{-1} over Germany and France during this period and increased over regions like China (an average increase of ~160% with an increase of 200-300% over specific regions of eastern China) or India (~33%).

3.2 Trend reversals

As shown in the previous paragraph, the tropospheric NO_2 linear trends during the last two decades appear to be strong and statistically robust over different regions around the world. However, it has been reported in previous studies that the implementation of environmental protection policies (e.g. van der A et al., 2017 for eastern China), economic recession (e.g. Castellanos and Boersma, 2012 for Europe, Vrekoussis et al., 2013 for Greece and Cuevas et al., 2014 for Spain), warfare (e.g. Lelieveld et al., 2015 for the Middle East) and other events (e.g. Mijling et al., 2009 for the Beijing Olympic Games) may have led to temporal or persistent changes to trace gases (e.g. SO_2 and NO_2) concentrations. This study mostly focuses on persistent changes which have led to a significant trend reversal of tropospheric NO_2 at some point during the last ~ 21 years. As shown in Fig. 43, trend reversals may indeed be detected over several regions around the globe. Fig. 43a shows the year when a reversal from positive to negative trends started and Fig. 43b shows the year when a reversal from negative to positive trends started. Only grid cells with a statistically significant trend at the 95% confidence level for the period before or after the year of the reversal and a long term tropospheric NO_2 VCD mean of at least 1×10^{15} molecules cm^{-2} are shown.

Extended areas over eastern China exhibit a clear reversal from positive to negative trends mostly in 2011 (see Fig. [3a4a](#)) while the same areas are characterized by strong statistically significant positive trends in Fig. [3b](#). It becomes more than obvious that by using a linear trend model for the whole period of interest one cannot depict the change in tropospheric NO₂. A smaller area with a persistent trend reversal from positive to negative in 2012 appears in north-western China. These striking features are in accordance to recent studies focusing on eastern Asia. van der A et al. (2017) showed that NO_x emissions in eastern China reached a peak in 2012 and slowly decreased thereafter while the economy kept growing. Similar results were recently shown for aerosols (Sogacheva et al., 2018). This situation is attributed to the installation of NO_x filtering systems at power plants and heavy industry. With the 12th five-year plan (ChinaFAQs project, 2012) China set the target to reduce NO_x emissions by 10% during the period 2010-2015 and seems to have achieved it (de Foy et al., 2016). Selective catalytic reduction (SCR) systems were installed in this period growing from a penetration of about 18% (2011) to 86% during the period 2011-2015 (2015) (Liu et al., 2016). The use of SCR technologies in power plants is expected to cause a reduction of the emissions by at least 70% (ICAC, 2009). This is the most significant measure taken by the Chinese State and largely coincides with the reversal years appearing in Fig. [43a](#). In the meantime, China also introduced several new national emission standards for cars switching from China 3 to China 4 standard in 2011 (Wu et al., 2017). The maximum allowed amount of on-road vehicle NO_x emissions was reduced by 50%. Stricter regulations were implemented on a city level for on-road vehicles (e.g. a ban on older polluting cars in Beijing). The approval of the 1st national environmental standard for limiting the concentrations of fine particles in the atmosphere by China's State Council accelerated the implementation of various measures after 2012 particularly over the urban clusters of BTH, YRD and PRD (Zhao et al., 2013) which generally exhibit a trend reversal in 2011 (see ~~in~~ Fig. [43a](#)). The stricter and faster implementation of environmental policies in the capital city of Beijing and other "key regions" might explain the 1-year lag observed in the trend reversal over eastern China (2011) and north-western China (2012) (see Fig. [43a](#)).

Similarly to eastern China, large parts of India experienced a reversal from positive to negative trends mostly in 2011. On the contrary, areas in central-southern India experienced a reversal from negative to positive trends at some point in the period 2000-2006. India experienced a population growth of ~37% (relative to 1996) during the period 1996-2017, mostly in urban areas, which was accompanied by a gross domestic product (GDP) increase of ~29% (World Bank, 2019). NO_x emissions generally increased as a result of large-scale urbanization (rural population decreased from ~73% of the total population in 1996 to ~66% in 2017), industrialization and economic growth, energy production, industry and transportation being the main contributors to the emissions (Ghude et al., 2013 and references therein). The Indian economy started developing at much higher rates after 2002 (World Bank, 2019) which might explain the observed negative to positive trend reversals appearing in the years 2000-2006 over specific regions (e.g. increase of tropospheric NO₂ in the greater Ballari region due to the rapid growth of the steel industry, especially after 2006). India's economic growth experienced a slow-down after 2011 (GDP still increased but at a lower rate) which might explain part of the observed positive to negative trend reversals over specific areas. Hilboll et al. (2017) also observed a stagnation of tropospheric NO₂ over India, attributing it to a combination of a slow-down in Indian economic development, the implementation of cleaner technology (e.g. Bansal and

Formatted: Subscript

[Bandivadekar, 2013](#)), meteorological factors (see [Voulgarakis et al., 2010](#)) and changes in tropospheric chemistry. However, it has to be noted that the way all these parameters may influence the tropospheric NO₂ levels and trends over India is pretty complicated and should be studied in more detail in the future. and largest

Formatted: English (U.S.)

Another region with widely-spread positive-to-negative trend reversals is the Iberian Peninsula (see Fig. [43a](#)). Not only the continental areas but also the coastal areas around the Iberian Peninsula (outside and inside the Mediterranean [SeaBasin](#)) experienced this trend reversal mostly during the period 2003-2007. We observe an early trend reversal over the Madrid and Valencia areas in Spain in the period 2000-2002 which is in accordance to NO₂ ground concentration measurements ([Cuevas et al., 2014](#)). More specifically, in Cuevas et al. (2014) a continuous drop of surface NO₂ is seen after 1999-2000 over the two cities. A reversal with a time lag of few years (2009-2011) is observed over areas in the communities of Extremadura and Catalonia. The observed differences are probably connected to the different economic and political characteristics of each area and the fact that the NO₂ changes are driven by different reasons. The decline of the tropospheric NO₂ levels in the first half of the 2000s when the economy was rising might be attributed to the implementation of environmental measures and the optimization in combustion processes ([EEA-APFS-Spain., 2014](#)). Following the European Union directives, Spain introduced its First National Emission Reduction Program in 2003 setting stringent combustion emission standards (IEA, 2017). This was afterwards updated and revised leading to the Second National Emission Reduction Program in 2008. The decline in NO₂ in the late 2000s - early 2010s might be due to the financial recession that started in 2008 ([Cuevas et al., 2014](#)). Similar differences are observed over areas in Portugal. For example, the areas around Santarém, on the northeast of Lisbon, exhibit a trend reversal in 2004-2005 ([EEA-APFS-Portugal., 2014](#)) while areas around other important cities, such as Evora and Coimbra, exhibit a trend reversal in the late 2010s-2000s - early 2010s, probably due to the 2008 financial recession.

Formatted: Subscript

The Middle East is another region with a persistent positive-to-negative trend reversal. Almost the whole of Syria (officially: the Syrian Arab Republic) along with large parts of Iraq experienced a trend reversal during the period 2011-2012 (Fig. [43a](#)) as a consequence of the Syrian civil war which broke out in 2011. Large parts of Iran experienced a similar trend reversal mostly in 2011. This is mostly a result of the extension in 2010 of sanctions which were first imposed by the Nations Security Council in 2006 ([Lelieveld et al., 2015](#)), while a direct (lessa decrease of transboundary transport of NO₂ from neighbouring countries) or indirect (political and financial involvement of Iran) effect of due to the warfare on the observed trend reversal cannot be ruled out. Similarly, oceanic and continental areas around the Persian Gulf experienced a trend reversal in 2011 or earlier. [Lelieveld et al. \(2015\)](#) attributed this to air quality control in the Persian Gulf States from the mid-late 2000s onwards. Within the Middle East there are also sporadic areas (e.g. in Iran, in Iraq, areas around the Persian Gulf and, and areas around the east coast of the Red Sea in Saudi Arabia and the Nile River in Egypt) with a trend reversal from negative to positive in the early 2000s (2000-2003) probably due to changes in power generation, industrial, transport and shipping emissions ([Krotkov et al., 2016](#)). A similar trend reversal is observed over the region of Nile River in Egypt (Fig. [43b](#)).

Extended areas with a persistent positive-to-negative trend reversal are also located in central Africa and Mexico (late 2000s) and in the U.S. (early 2000s) (Fig. 43a). On the contrary, areas with a persistent negative-to-positive trend reversal in the early 2000s can be seen in South America (highly populated, industrialized areas in Brazil and Argentina) (Fig. 3b4b). The reversal points coincide with socioeconomic changes that took place in these two countries. Specifically, Argentina experienced a great economic depression during the period 1998-2002. The country's gross domestic product (GDP) declined by ~11% and the industrial production by ~22% in 2002 relative to 2001 (Cline, 2013) while the economy started reviving afterwards. Similarly, Brazil's GDP declined from 1997 to 2002, increased by a factor of ~5 by 2011 and then declined again reaching values close to the 2009 ones in 2016 (World Bank, 20182019). However, it has to be highlighted that in 2009 Brazil, and specifically Rio de Janeiro (also known as Rio), won the bid to host the 2016 Olympic Games. This, despite the country's GDP decline, is expected to have given a boost to construction activities in Rio and the other host cities (Sao Paulo, Belo Horizonte, Salvador, Brasília and Manaus) and hence to NO_x emissions. Indicative is the almost uninterrupted increase of CO₂ emissions from 2002 onwards (World Bank, 20182019).

To demonstrate the need for a different approach when looking into long-term linear trends of tropospheric NO₂, in Fig. 54 we present the timeseries and the trend for the whole period of measurements (4/1996 - 9/2017) and for the period before and after the trend reversal for four different regions of interest around the globe, i.e., eastern China (ECH) [30° N-40° N, 107° E-122° E], Iberian Peninsula (IPE) [36° N-44° N, 10° W-0° W], the Middle East (MEA) [28° N-38° N, 34° E-60° E] and south-eastern America (SAM) [29° S-19° S, 52° W-42° W] (see also embedded maps in Fig. 45). The four regions were selected because they represent areas that experienced a trend reversal in different periods and for different reasons (see Fig. 4-5 and discussion above). The absolute (in 10¹⁵ molecules cm⁻² yr⁻¹) and relative trends (relative to the fitted mean of the period/sub-period first year, in % yr⁻¹) for each region are given in Fig. 4-5 and Table 1.

While ECH exhibits a statistically significant positive trend for the whole period of interest, a clear trend reversal is observed in 2011, with a statistically significant positive trend during the period (4/1996 - 12/2011) and a statistically significant negative trend during the period (1/2011-9/2017) (Fig. 54a, b). Following the discussion above, the observed trend reversal in ECH may be attributed to the implementation of environmental protection policies. In addition, while IPE exhibits a statistically significant negative trend for the whole period (Fig. 54c), a clear trend reversal is observed in 2005 with a statistically significant positive trend during the period (4/1996 - 12/2005) and a statistically significant negative trend during the period (1/2005-9/2017) (Fig. 54d). The 2005 trend reversal in IPE might be attributed to a combination of environmental measures and optimization in combustion processes. Similarly to ECH, MEA exhibits a statistically significant positive trend for the whole period of interest with a clear trend reversal in 2012 (Fig. 54e). A statistically significant positive trend is observed during the period (4/1996 - 12/2012) and a statistically significant negative trend during the period (1/2012-9/2017) (Fig. 54f) which is attributed to the war that takes place in the area since 2011. Finally, SAM exhibits a statistically significant positive trend for the whole period of interest. A clear trend reversal is observed in 2000 with a statistically significant negative trend during the period (4/1996 - 12/2000) and a statistically positive negative trend

during the period (1/2000-9/2017). The trend reversal in SAM might be attributed to a revival of the economy after ~2000 in combination with the preparations of the Rio Olympic Games (see discussion above).

3.3 Countries

The same analysis was repeated on a country level basis which allows for safer interpretations of the observed trend reversals as the environmental policies, the socioeconomic changes and consequently NO_x emission changes are unique within each country. As country-level averages are used here there is no discrimination between national hot spots and background areas while transboundary transport cannot be excluded as well. In Fig. 65a, the linear trend of the tropospheric NO₂ VCD (in 10¹⁵ molecules cm⁻² yr⁻¹) for the period 4/1996 - 9/2017 is shown for each country. In Fig. 65b, only countries with a statistically significant trend at the 95% confidence level are shown. In line with Fig. 23, the U.S. and Canada in North America, countries in central and western Europe (the U.K., Spain, France, Switzerland, Belgium, the Netherlands, Germany, Denmark, Poland, the Czech Republic, Slovakia, Hungary, Romania, Italy, Slovenia, Croatia), Japan and Taiwan in south-eastern Asia and several countries in Africa (Libya, Chad, Sudan, Ethiopia, Mali, Guinea, Liberia, Ivory Coast, Ghana, the Democratic Republic of the Congo, Angola, Namibia, Botswana, Zimbabwe, Mozambique, South Africa) exhibit a statistically significant negative trend. On the contrary, statistically significant positive trends can be seen over countries in eastern Europe and the Middle East and over almost the whole Asia and South America.

The countries with the highest statistically significant negative trends (deep blue color in Fig. 65: absolute values higher than 0.1 x 10¹⁵ molecules cm⁻² yr⁻¹) in the world are the Netherlands (-0.30±0.02 x 10¹⁵ molecules cm⁻² yr⁻¹ / -2.33±0.18 % yr⁻¹), Belgium (-0.25±0.03 x 10¹⁵ molecules cm⁻² yr⁻¹ / -1.99±0.21 % yr⁻¹), the U.K. (-0.14±0.01 x 10¹⁵ molecules cm⁻² yr⁻¹ / -2.31±0.24 % yr⁻¹), Taiwan (-0.12±0.01 x 10¹⁵ molecules cm⁻² yr⁻¹ / -1.80±0.19 % yr⁻¹) and Germany (-0.11±0.01 x 10¹⁵ molecules cm⁻² yr⁻¹ / -1.58±0.21 % yr⁻¹) while the countries with the highest statistically significant positive trends (deep red color in Fig. 65: values higher than 0.1 x 10¹⁵ molecules cm⁻² yr⁻¹) in the world are Swaziland, a sovereign state in southern Africa (0.18±0.04 x 10¹⁵ molecules cm⁻² yr⁻¹ / 2.88±0.64 % yr⁻¹), Lebanon (0.17±0.02 x 10¹⁵ molecules cm⁻² yr⁻¹ / 5.05±0.48 % yr⁻¹), China (0.12±0.02 x 10¹⁵ molecules cm⁻² yr⁻¹ / 7.55±1.24 % yr⁻¹), Bahrain (0.10±0.02 x 10¹⁵ molecules cm⁻² yr⁻¹ / 1.66±0.25 % yr⁻¹), Korea (0.10±0.02 x 10¹⁵ molecules cm⁻² yr⁻¹ / 1.36±0.30 % yr⁻¹) and Kuwait (0.11±0.01 x 10¹⁵ molecules cm⁻² yr⁻¹ / 3.78±0.27 % yr⁻¹). These values along with the absolute (in 10¹⁵ molecules cm⁻² yr⁻¹) and relative trends (relative to the fitted mean of the first year, in % yr⁻¹) for all the world countries are given in Table S1 of the paper's Supplement.

~~In order to save space,~~ Table 2 includes the absolute and relative trends only for countries that experienced a trend reversal. In the same Table, ~~one may also find~~ the year of trend reversal along with the absolute and relative trends for the period before the trend reversal (including the reversal year) and after the trend reversal (including the reversal year) [are shown](#). In addition, Fig. 76a shows the year when a reversal from positive to negative trends was observed and Fig. 76b

shows the year when a reversal from negative to positive trends started on a country basis. Only countries with a statistically significant trend at the 95% confidence level for the period before or after the year of the reversal are shown.

In several regions around the world we can see clusters of countries that exhibit a reversal from positive to negative NO₂ trends in the years 2011-2012. For example Kazakhstan, China, North Korea in central-eastern Asia, Australia and Papua New Guinea in Oceania, Pakistan, Afghanistan, Turkmenistan in central Asia, Iran, Iraq, Syria, Jordan, Saudi Arabia, Yemen, Oman in the Middle East and the Arabian Peninsula, Greece, Cyprus, Turkey, Albania, FYROM in the eastern Mediterranean and the Balkan Peninsula, Morocco, Algeria, Tunisia in north-western Africa and Mexico, El Salvador, Honduras in central America. Another cluster of countries that exhibit similar trend reversals but for the years 2009-2010 is located in central Africa (Gabon, Equatorial Guinea, Cameroon, the Central African Republic, the Democratic Republic of the Congo, Tanzania, Malawi, Kenya). There are also other individual countries around the world that exhibit a reversal from positive to negative trends within the period 2009-2012 (e.g. Sweden in Europe, Peru in South America, Sri Lanka in South Asia, etc.) and also countries that exhibit such a trend reversal earlier than this (e.g. Canada and Portugal in 2005, Spain in 2006, Bulgaria in 2007, Ireland in 2008).

On the contrary, we can also see clusters of countries around the world that exhibit a reversal from negative to positive NO₂ trends in the years 2000-2002. For example Mongolia, Russia, Ukraine, Moldova, Georgia, Armenia in Eurasia, Chile, Argentina, Paraguay, Uruguay, Brazil in South America and Thailand, Cambodia, Laos, Vietnam in south-eastern Asia. As discussed in Sect. 3.2, despite the fact that trend reversals appear in the same year over different regions (here countries) the driving reasons may be completely different. Similarly to Fig.4, Fig. 7-8 presents the timeseries for the period before and after the trend reversal for eight countries of interest (China, Spain, Ireland, Russia, Argentina, Brazil, Iraq and Syria). These countries were selected according to the results from the global analysis so as to be representative of different driving reasons.

As discussed above the reversal from positive to negative trends over China in 2011 (Fig. 87a) is related to the extended implementation of environmental protection policies while the reversal from positive to negative trends over Spain in 2006 (Fig. 87b) is probably related to a combination of environmental measures and optimization in combustion processes (see Sect. 3.2 and references therein). The reversal from positive to negative trends in Ireland in 2008 (Fig. 7e8c) coincides with the global financial crisis which is also reflected to the sharp decline of Ireland's GDP ([by ~18% relative to 2008](#)) during the period 2008-2012 (World Bank, [20182019](#)). The annual [mean](#) tropospheric NO₂ [VCDs-levels](#) are almost stable after 2012 which is in line with Ireland's Environmental Protection Agency (EPA) report on air pollutant emissions (EPA, 2018). As shown in Fig. 87d, Russia exhibits a trend reversal from negative to positive in 2000. This is apparently connected to the economic boom of the Russian Federation after 1999 as the Russian GDP increased by a factor of 10 during the period 1999-2013 (World Bank, [20182019](#)). Similarly to Russia, Argentina and Brazil also exhibit a reversal from negative to positive tropospheric NO₂ trends in 2000 (Fig. 87e and f). As discussed in Sect. 3.2, this reversal point coincides with a revival from the economic recessions that ~~both~~ the [two](#) countries experienced the years around 2000. In the case of Brazil, the preparations for the 2016 Olympic Games may have affected the tropospheric NO₂ levels after 2009 and consequently

played a role in the positive trends observed after 2000 (see Sect. 3.2 and references therein). Finally, Iraq and Syria exhibit a trend reversal from positive to negative in 2012 as a consequence the Syrian civil war which broke out in 2011 (see also Sect. 3.2 and references therein) and affected largely the economic and industrial activities in those countries. Indicatively, for Syria, it has been estimated that during the period 2011-2016 the cumulative GDP loss was 226 billion U.S. dollars (four times the Syrian GDP in 2010) (World Bank Group, 2017).

3.4 Megacities and large urban agglomerations

The same analysis was repeated for a total of 64 megacities (population of more than 10 million inhabitants) and large urban agglomerations (population of more than ~5 million inhabitants). The list of megacities and large urban agglomerations (hereafter denoted also as population hot spots - PHSs) used here is taken from Schneider et al., (2015). Such areas are characterized by extensive human activities (transportation, industry, domestic heating, etc.). Hence, trace gas emissions are expected to be more sensitive to socioeconomic changes and trend reversals are expected to be sharper. In Fig. 8-9 the linear trend of the tropospheric NO₂ VCD (in 10¹⁵ molecules cm⁻² yr⁻¹) for the period 4/1996 - 9/2017 is shown for 64 PHSs out of a total of 66 PHSs appearing in Schneider et al. (2015) list as only trends calculated for timeseries with at least 8 months per year are reported. Statistically significant trends at the 95% confidence level are marked with a black outline.

As shown in Fig.8, the majority of the PHSs with the highest statistically significant negative trends are located in Europe and the U.S. while the PHSs with the highest statistically significant positive trends are mostly confined in south-eastern Asia (e.g. China, India), the Middle East - Arabian Peninsula and South America. More specifically, the PHSs with the highest statistically significant negative trends (deep blue color in Fig. 8: absolute values higher than 0.4 x 10¹⁵ molecules cm⁻² yr⁻¹) in the world are Los Angeles (-1.34±0.11 x 10¹⁵ molecules cm⁻² yr⁻¹ / -3.07±0.24 % yr⁻¹), New York (-0.70±0.09 x 10¹⁵ molecules cm⁻² yr⁻¹ / -2.28±0.29 % yr⁻¹), Boston (-0.60±0.07 x 10¹⁵ molecules cm⁻² yr⁻¹ / -3.50±0.43 % yr⁻¹), Po Valley (-0.54±0.07 x 10¹⁵ molecules cm⁻² yr⁻¹ / -2.23±0.30 % yr⁻¹), Chicago (-0.50±0.05 x 10¹⁵ molecules cm⁻² yr⁻¹ / -2.52±0.27 % yr⁻¹) and Philadelphia (-0.46±0.08 x 10¹⁵ molecules cm⁻² yr⁻¹ / -2.32±0.42 % yr⁻¹). On the contrary the PHSs with the highest statistically significant positive trends (deep red color in Fig. 9: values higher than 0.4 x 10¹⁵ molecules cm⁻² yr⁻¹) are Tianjin (1.78±0.17 x 10¹⁵ molecules cm⁻² yr⁻¹ / 14.88±1.42 % yr⁻¹), Beijing (1.36±0.18 x 10¹⁵ molecules cm⁻² yr⁻¹ / 6.38±0.86 % yr⁻¹), Shenyang (0.91±0.08 x 10¹⁵ molecules cm⁻² yr⁻¹ / 16.26±1.42 % yr⁻¹), Chongqing (0.86±0.14 x 10¹⁵ molecules cm⁻² yr⁻¹ / 28.11±4.66 % yr⁻¹), Tehran (0.81±0.06 x 10¹⁵ molecules cm⁻² yr⁻¹ / 8.58±0.58 % yr⁻¹), Chengdu (0.72±0.08 x 10¹⁵ molecules cm⁻² yr⁻¹ / 11.66±1.33 % yr⁻¹), Shanghai (0.59±0.09 x 10¹⁵ molecules cm⁻² yr⁻¹ / 2.74±0.42 % yr⁻¹), Wuhan (0.57±0.05 x 10¹⁵ molecules cm⁻² yr⁻¹ / 7.05±0.67 % yr⁻¹) and Baghdad (0.42±0.02 x 10¹⁵ molecules cm⁻² yr⁻¹ / 16.95±0.79 % yr⁻¹). These values along with the trends for all the PHSs examined in this work can be found in Table 3.

29 out of the 64 examined PHSs exhibit a trend reversal within the period of interest. Fig. 10a shows the year when a reversal from positive to negative trends started (Athens, Bangalore, Bangkok, Buenos Aires, Jakarta, Jeddah, Johannesburg, Khartoum, Kinshasa, Lahore, Manila, Rio de Janeiro, Santiago) and Fig. 10b shows the year when a reversal

from positive to negative trends started (Atlanta, Beijing, Boston, Chongqing, Damascus, Hong Kong, Los Angeles, Osaka, San Francisco, Shanghai, Shenyang, Shenzhen, Taipei, Tianjin, Tokyo, Wuhan). Only PHSs with a statistically significant trend at the 95% confidence level for the period before or after the year of the reversal are shown. The year of trend reversal along with the absolute and relative trends for the period before the trend reversal (including the reversal year) and after the trend reversal (including the reversal year) are given in Table 3.

On top of the discussions above, timeseries for the period before and after the trend reversal for six selected PHSs are presented in Fig. 110. Beijing, the capital of China, exhibits a sharp reversal from positive to negative (statistically insignificant) trends in 2011 as a result of emission control policies (see discussion in Sect. 3.2 and 3.3). Similarly, Los Angeles exhibits a sharp reversal from positive to negative trends in 2000 probably due the combined effect of efficient emission control measures in California, especially after the late 1990s - early 2000s, and economic activity slowdown following the 2008 global financial crisis (Russell et al., 2012; Hilboll et al., 2013; Lurmann et al., 2015). A reversal from negative to positive trends is observed in 2002 in Buenos Aires (capital city, financial, industrial and commercial center of Argentina) which coincides with the period that the country started recovering from the great economic depression of 1998-2002 (see also Sect. 3.2 and 3.3). Rio de Janeiro exhibits a sharp reversal from negative to positive trends in 2006, a bit later than the whole Brazil (trend reversal in 2000). The trend reversal coincides with the revival of Brazil's economy and with the preparations for the 2014 Football World Cup and the 2016 Olympic Games (see also Sect. 3.2 and 3.3). Athens, the capital city and financial center of Greece, where half the country's population lives, exhibits a reversal from negative to positive (statistically insignificant) trends in 2010. Vrekoussis et al. (2013) reported a 30-40% decrease of tropospheric NO₂ in Athens during the period 2008-2012 as a result of the unprecedented economic crisis that the country experienced from 2008 onwards. Our results suggest that there may be a stabilization of the tropospheric NO₂ levels after the rapid decline that was observed in the first years of the crisis. Finally, Damascus, the capital city and financial/industrial center of Syria, exhibits a sharp reversal from positive to negative trends in 2012 as a result of the Syrian civil war which broke out in 2011 (see Sect. 3.2 and 3.3 and references therein).

4. Conclusions

In this work, a self-consistent GOME, SCIAMACHY and GOME-2 tropospheric NO₂ VCD dataset is compiled for the period 4/1996-9/2017. The GOME and GOME-2A/GOME-2B data are "corrected" relative to the SCIAMACHY data following a three-step procedure, in order to reproduce what SCIAMACHY would measure if being in orbit for the whole period of interest. and The the multi-satellite dataset is then used to study the long-term global tropospheric NO₂ patterns and trends and search for possible trend reversals during this ~21-years period. The main findings of the present study are summarized in the following:

- The highest tropospheric NO₂ concentrations are seen over urban, industrialized and highly populated areas and over ship tracks in the oceans. Tropospheric NO₂ has generally decreased during the last two decades over the industrialized and highly populated regions of the Western World and increased over developing regions. Statistically significant negative trends appear over the largest part of the U.S., western and central Europe, Japan and Taiwan in south-eastern Asia and the region around the Johannesburg-Pretoria conurbation in South Africa. Strong statistically significant positive trends appear over regions in south-eastern Asia, the Middle East, eastern Europe, northern Africa, South Africa, and South and Central America. Indicatively, during the last ~21 years, the tropospheric NO₂ levels have decreased on average by ~49% during the whole period of interest (relative to the fitted mean of the first year) over the U.S., the Netherlands and the U.K., by ~36% over Italy and Japan and by ~32% over Germany and France, while, they increased over regions like China (an average increase of ~160% with an increase of 200-300% over the eastern part of the country) or India (~33%).

- The application of a trend reversal detection method on a global scale revealed that extended areas over eastern China exhibit a clear reversal from positive to negative trends, mostly in 2011, while a smaller area in north-western China exhibits a reversal from positive to negative trends in 2012. Similarly to eastern China, large parts of India experienced a reversal from positive to negative trends, mostly in 2011, while areas in central-southern India experienced a reversal from negative to positive trends during the first half of the 2000s. Other regions with widely-spread positive-to-negative trend reversals are the Iberian Peninsula (mostly during the first half of the 2000s) and the Middle East (2011-2012), despite the fact that within the Middle East there are sporadic areas with a trend reversal from negative to positive in the early 2000s. A similar negative-to-positive trend reversal is observed over the region of Nile River in Egypt. Extended areas with a persistent positive-to-negative trend reversal are also seen in central Africa and Mexico (late 2000s) and in the U.S. (early 2000s) while areas with a persistent negative-to-positive trend reversal in the early 2000s can be seen in South America, mostly in Brazil and Argentina.

- A country-level analysis showed clusters of countries that exhibit a reversal from positive to negative NO₂ trends in the years 2011-2012 in central-eastern Asia (Kazakhstan, China, North Korea), Oceania (Australia, Papua New Guinea), central Asia (Pakistan, Afghanistan and Turkmenistan), the Middle East and the Arabian Peninsula (Iran, Iraq, Syria, Jordan, Saudi Arabia, Yemen, Oman), the eastern Mediterranean and the Balkan Peninsula (Greece, Cyprus, Turkey, Albania, FYROM), north-western Africa (Morocco, Algeria, Tunisia) and central America (Mexico, El Salvador, Honduras). Another cluster of countries that exhibit similar trend reversals but for the years 2009-2010 is located in central Africa (Gabon, Equatorial Guinea, Cameroon, the Central African Republic, the Democratic Republic of the Congo, Tanzania, Malawi, Kenya). There are also individual countries around the world that exhibit a reversal from positive to negative trends within the period 2009-2012 (e.g. Sweden, Peru and Sri Lanka) and countries that exhibit such a trend reversal earlier than this (Canada and Portugal in 2005, Spain in 2006, Bulgaria in 2007, Ireland in 2008). On the contrary, we can see clusters of countries around the world that exhibit a reversal from negative to positive NO₂ trends in the years 2000-2002 in Eurasia (Mongolia, Russia,

Ukraine, Moldova, Georgia, Armenia), South America (Chile, Argentina, Paraguay, Uruguay, Brazil) and south-eastern Asia (Thailand, Cambodia, Laos, Vietnam).

5 - The application of the trend reversal detection method on 64 megacities and large urban agglomerations revealed that 29 of them exhibit a tropospheric NO₂ trend reversal. A reversal from negative to positive trends was observed for Athens/Greece, Bangalore/India, Bangkok/Thailand, Buenos Aires/Argentina, Jakarta/Indonesia, Jeddah/Saudi Arabia, Johannesburg/South Africa, Khartoum/Sudan, Kinshasa/Democratic Republic of the Congo, Lahore/Pakistan, Manila/Philippines, Rio de Janeiro/Brazil and Santiago/Chile, while a reversal from positive to negative trends was observed for Atlanta/U.S., Beijing/China, Boston/U.S., Chongqing/China, Damascus/Syria, Hong Kong, Los Angeles/U.S., Osaka/Japan, San Francisco/U.S., Shanghai/China, Shenyang/China, Shenzhen/China, Taipei/Taiwan, Tianjin/China, Tokyo/Japan and Wuhan/China.

15 - It is shown that the observed tropospheric NO₂ trend reversals over different areas, countries and megacities/large urban agglomerations ~~could~~can be associated with various socioeconomic changes (environmental policies, economic recession, warfare, etc.) that possibly had a direct impact on NO_x emissions. For example, the reversal from positive to negative trends in 2011-2012 over extended areas in China (including Beijing and other megacities) can be attributed to the efficient implementation of environmental protection policies. The reversal from positive to negative trends over Spain in 2006 might be attributed to a combination of environmental measures and optimization in combustion processes, while the reversal from positive to negative trends in Ireland in 2008 coincides with the bursting of the global financial crisis. Russia's reversal from negative to positive trends in 2000 might be connected to the economic boom of the country after 1999. Similarly, Argentina's and Brazil's reversal from negative to positive trends in 2000 coincides with a revival from the economic recession that both the countries experienced during the years around year 2000. The megacities Buenos Aires in Argentina and Rio de Janeiro in Brazil exhibit a similar trend reversal a bit later than the corresponding countries. In the case of Brazil, the preparations for the 2016 Olympic Games might have affected the tropospheric NO₂ levels after 2009 and consequently played a role in the positive trends observed after 2000. Iraq and Syria (including Damascus) exhibit a trend reversal from positive to negative in 2012 which is profoundly due to the Syrian civil war which broke out in 2011 and affected largely the economic and industrial activities. Athens/Greece exhibits a reversal from negative to positive (statistically insignificant) trends in 2010 pointing towards a stabilization of tropospheric NO₂ after the rapid decline that was observed during the first years of the Greek economic crisis. Finally, a positive-to-negative trend reversal is seen in Los Angeles/U.S. in 2000 which might be attributed to the combined effect of efficient emission control measures in California, especially after the late 1990s - early 2000s, and economic activity slowdown following the 2008 global financial crisis.

The next years, tropospheric NO₂ timeseries will be extended from new more sophisticated satellite sensors such as the recently launched Tropospheric Monitoring Instrument (TROPOMI) onboard ESA's Sentinel - 5 Precursor (S-5P) satellite

(Veeffkind et al., 2012). Hence, the need to develop similar methods in the future that will be able to incorporate both morning and afternoon measurements (e.g. from OMI and TROPOMI) and detect more than one trend reversal points in improved tropospheric NO₂ products (e.g. QA4ECV v.1.1.1, Zara et al., 2018 and references therein) is acknowledged.

Appendix A: Merging GOME, SCIAMACHY and GOME-2 observations

Step 1: VCD_{SCsm} is calculated from VCD_{SC} using a boxcar algorithm with an averaging window of $13 \times 0.25^\circ$ (3.25°)

$$VCD_{SCsm}(x, y, t) = \frac{1}{13} \left(\sum_{w=-6}^6 (VCD_{SC}(x + w \times 0.25, y, t)) \right) \quad (A1)$$

where x and y are the central longitude and latitude of a grid cell in degrees and t is the time in one month steps (from 1/2003 to 12/2011), ..., while $w = -6, -5, \dots, 0, 5, 6$ (a total of 13 values).

$$CF1(x, y, m) = VCD_{SC}(x, y, m) / VCD_{SCsm}(x, y, m) \quad (A2)$$

where $m = 1, 2, \dots, 12$ is the month for which the climatological monthly values $VCD_{SC}(x, y, m)$ and $VCD_{SCsm}(x, y, m)$ are calculated.

$$VCD_{GCl}(x, y, t) = VCD_G(x, y, t) \times CF1(x, y, m) \quad (A3)$$

$$\text{Step 2: } CF2(x, y) = \frac{1}{n} \left(\sum_{t=t_1}^{t_2} (VCD_{GCl}(x, y, t)) - \sum_{t=t_1}^{t_2} (VCD_{SC}(x, y, t)) \right) \quad (A4)$$

where t is the time in one month steps for the common GOME-SCIAMACHY period (t_1 : 8/2002 to t_2 : 6/2003) of $n=11$ months.

$$VCD_{GC2}(x, y, t) = VCD_{GCl}(x, y, t) - CF2(x, y) \quad (A5)$$

$$\text{CF3}(x, y, m) = \frac{\left[\text{VCD}_{\text{SC}}(x, y, m) / \frac{1}{n_{\text{SC}}} \left(\sum_{t=t_{\text{SC1}}}^{t_{\text{SC2}}} (\text{VCD}_{\text{SC}}(x, y, t)) \right) \right]}{\left[\text{VCD}_{\text{GC2}}(x, y, m) / \frac{1}{n_{\text{G}}} \left(\sum_{t=t_{\text{G1}}}^{t_{\text{G2}}} (\text{VCD}_{\text{GC2}}(x, y, t)) \right) \right]} \quad (\text{A6})$$

Step 3:

where t is the time in one month steps for the whole SCIAMACHY period (t_{SC1} : 8/2002 to t_{SC2} : 3/2012) of $n_{\text{SC}}=116$ months and for the whole GOME period (t_{G1} : 4/1996 to t_{G2} : 6/2003) of $n_{\text{G}}=87$ months.

$$\text{VCD}_{\text{GC3}}(x, y, t) = \text{VCD}_{\text{GC2}}(x, y, t) \times \text{CF3}(x, y, m) \quad (\text{A7})$$

Appendix B: Trend analysis

The timeseries are fitted by using a model with a linear trend and a Fourier based seasonal component:

$$Y_t = A + BX_t + \sum_{n=1}^6 \left[a_n \sin\left(\frac{2\pi}{T} n X_t\right) + b_n \cos\left(\frac{2\pi}{T} n X_t\right) \right] + N_t \quad (\text{B1})$$

where Y_t is the monthly mean value for month t , X_t is the number of the month after the first month of the timeseries, A is the monthly mean of the first month of the timeseries and B is the trend. The seasonal component contains the amplitudes a_n and b_n , T is the period and N_t is the difference between the modeled and the measured value termed, usually as remainder.

$$N_t = \phi N_{t-1} + \varepsilon_t \quad (\text{B2})$$

where ϕ is the autocorrelation in the remainder and ε_t is the white noise. Autocorrelation ϕ affects the precision of the trend σ_B , which is given as a function of ϕ , the length of the data set in months m and the variance σ_N of the remainder for small autocorrelations:

$$\sigma_B \approx \left[\frac{\sigma_N}{m^{3/2}} \sqrt{\frac{1+\phi}{1-\phi}} \right] \quad (\text{B3})$$

The calculated trend B is considered to be statistically significant at the 95% confidence level if $|B/\sigma_B| > 2$.

Appendix C: Trend reversal detection

The trend reversal method is based on the minimization of a value $S(t)$ which is calculated for each year t of the period $[t_i=2000, t_n=2012]$:

$$S(t) = \frac{\min(p(B_l), p(B_r))}{\text{abs}(B_l - B_r) \times \sigma_{B_{l+r}}} \quad (C1)$$

where $p(B_l)$ and $p(B_r)$ express the possibility that the trends B_l and B_r for the short periods on the left $[t-4, t]$ and on the right $[t, t+4]$ of the year t are statistically insignificant and $\sigma_{B_{l+r}}$ is the standard error of the trend for the combined sub-periods $[t-4, t+4]$. The year t_r when S takes its lower value and there is a switch from a positive trend to a negative one or from a negative trend to a positive one is considered to be a potential trend reversal year. The trends are calculated using ordinary least-squares linear regression with 95% confidence intervals. In this study, only when the trend B_b for the whole period before t_r (including t_r) $[t_i, t_r]$ or the trend B_a for the whole period after t_r (including t_r) $[t_r, t_n]$ is statistically significant at the 95% confidence level, a trend reversal is reported. Specifically, for the four extended regions of interest, the country and the megacities and large urban agglomeration analyses performed in this paper, the B_b and B_a trends are calculated from the monthly timeseries using the method presented in Appendix B in order to be consistent with the trends for the whole time period (4/1996–9/2017) which are reported in the paper.

Acknowledgements

This research has been implemented within the framework of the SCIAvisie project funded by the Netherlands Space Organization (NSO).

References

- Alexandri, G., Georgoulas, A. K., Meleti, C., Balis, D., Kourtidis, K. A., Sanchez-Lorenzo, A., Trentmann, J., and Zanis, P.: A high resolution satellite view of surface solar radiation over the climatically sensitive region of Eastern Mediterranean, *Atmos. Res.*, 188, 107-121, doi:10.1016/j.atmosres.2016.12.015, 2017.
- [Bansal, G. and Bandivadekar, G.: Overview of India's vehicle emissions control program. Tech. rep., The International Council on Clean Transportation, Washington, D.C., available at: \[http://www.theicct.org/sites/default/files/publications/ICCT_IndiaRetrospective_2013.pdf\]\(http://www.theicct.org/sites/default/files/publications/ICCT_IndiaRetrospective_2013.pdf\) \(last access: 19 March 2018\), 2013.](http://www.theicct.org/sites/default/files/publications/ICCT_IndiaRetrospective_2013.pdf)
- Basset, M. and Seinfeld, J. H.: Atmospheric Equilibrium Model of Sulfate and Nitrate Aerosols, *Atmos. Environ.*, 17, 2237-2252, 1983.

- Beirle, S., Platt, U., Wenig, M., and Wagner, T.: Highly resolved global distribution of tropospheric NO₂ using GOME narrow swath mode data, *Atmos. Chem. Phys.*, 4, 1913-1924, doi:10.5194/acp-4-1913-2004, 2004.
- Boersma, K. F., Eskes, H. J., and Brinksma, E. J.: Error analysis for tropospheric NO₂ retrieval from space, *J. Geophys. Res.*, 109, D04311, doi:10.1029/2003JD003962, 2004.
- 5 Boersma, K. F., Jacob, D. J., Eskes, H. J., Pinder, R. W., and Wang, J.: Intercomparison of SCIAMACHY and OMI tropospheric NO₂ columns: Observing the diurnal evolution of chemistry and emissions from space, *J. Geophys. Res.*, 113, D16S26, doi:10.1029/2007JD008816, 2008.
- Boersma, K. F., Eskes, H. J., Dirksen, R. J., van der A, R. J., Veeffkind, J. P., Stammes, P., Huijnen, V., Kleipool, Q. L., Sneep, M., Claas, J., Leitão, J., Richter, A., Zhou, Y., and Brunner, D.: An improved tropospheric NO₂ column retrieval
10 algorithm for the Ozone Monitoring Instrument, *Atmos. Meas. Tech.*, 4, 1905-1928, doi:10.5194/amt-4-1905-2011, 2011.
- Bovensmann, H., Burrows, J. P., Buchwitz, M., Frerick, F., Noël, S., and Rozanov, V. V.: SCIAMACHY: mission objectives and measurement modes, *J. Atmos. Sci.*, 56, 127-150, doi:10.1175/1520-0469(1999)056<0127:SMOAMM>2.0.CO;2, 1999.
- Burrows, J. P., Hölzle, E., Goede, A., Visser, H., and Fricke, W.: SCIAMACHY - scanning imaging absorption spectrometer
15 for atmospheric cartography, *Acta Astronaut.*, 35, 445-451, doi:10.1016/0094-5765(94)00278-T, 1995.
- Burrows, J. P., Weber, M., Buchwitz, M., Rozanov, V. V., Ladstätter-Weissenmayer, A., Richter, A., DeBeek, R., Hoogen, R., Bramstedt, K., Eichmann, K.-U., and Eisinger, M.: The Global Ozone Monitoring Experiment (GOME): mission concept and first scientific results, *J. Atmos. Sci.*, 56, 151-175, doi:10.1175/1520-0469(1999)056<0151:TGOMEG>2.0.CO;2, 1999.
- 20 ~~Callies, J., Corpaecioli, E., Eisinger, M., Hahne, A., and Lefebvre, A.: GOME 2 – Metop’s second generation sensor for operational ozone monitoring, *ESA Bull. Eur. Space*, 102, 28-36, 2000.~~
- Castellanos, P. and Boersma, K. F.: Reductions in nitrogen oxides over Europe driven by environmental policy and economic recession, *Sci. Rep.*, 2, 265, doi:10.1038/srep00265, 2012.
- Cermak, J., Wild, M., Knutti, R., Mishchenko, M. I., and Heidinger, A. K.: Consistency of global satellite-derived aerosol
25 and cloud data sets with recent brightening observations, *Geophys. Res. Lett.*, 37, L21704, doi:10.1029/2010GL044632, 2010.
- ChinaFAQs Project: China Adopts World-Class Pollutant Emissions Standards for Coal Power Plants, available at: <http://www.chinafaqs.org/library/chinafaqs-china-adopts-world-class-pollutant-emissions-standards-coal-power-plants> (last access: 15 September 2018), 2012.
- 30 Cline, W. R.: Restoring economic growth in Argentina (English), Working paper; no. 9 / 03, Washington, DC: World Bank, available at: <http://documents.worldbank.org/curated/en/805501468769277647/Restoring-economic-growth-in-Arentina> (last access: ~~15-19 September March 2018~~2019), 2003.
- Cuevas, C. A., Notario, A., Adame, J. A., Hilboll, A., Richter, A., Burrows, J. P., and Saiz-Lopez, A.: Evolution of NO₂ levels in Spain from 1996 to 2012, *Sci. Rep.*, 4, 5887, doi:10.1038/srep05887, 2014.

- de Foy, B., Lu, Z., and Streets, D. G.: Satellite NO₂ retrievals suggest China has exceeded its NO_x reduction goals from the twelfth Five-Year Plan, *Scientific Reports*, 6, 35912, doi:10.1038/srep35912, 2016.
- de Meij, A., Pozzer, A., and Lelieveld, J.: Trend analysis in aerosol optical depths and pollutant emission estimates between 2000 and 2009, *Atmos. Environ.*, 51, 75-85, doi:10.1016/j.atmosenv.2012.01.059, 2012.
- 5 De Smedt, I., Stavrou, T., Muller, J.-F., van der A, R. J., and Van Roozendael, M.: Trend detection in satellite observations of formaldehyde tropospheric columns, *Geophys. Res. Lett.*, 37, L18808, doi:10.1029/2010GL044245, 2010.
- Dirksen, R. J., Boersma, K. F., Eskes, H. J., Ionov, D. V., Bucsel, E. J., Levelt, P. F., and Kelder, H. M.: Evaluation of stratospheric NO₂ retrieved from the Ozone Monitoring Instrument: intercomparison, diurnal cycle and trending, *J. Geophys. Res.*, 116, D08305, doi:10.1029/2010JD014943, 2011.
- 10 [EEA-APFS-Portugal: European Environment Agency - Air pollution fact sheet - Portugal, available at: https://www.eea.europa.eu/themes/air/air-pollution-country-fact-sheets-2014/portugal-air-pollutant-emissions-country-fact-sheet/at_download/file \(last access: 19 March 2019\), 2014.](https://www.eea.europa.eu/themes/air/air-pollution-country-fact-sheets-2014/portugal-air-pollutant-emissions-country-fact-sheet/at_download/file)
- [EEA-APFS-Spain: European Environment Agency - Air pollution fact sheet - Spain, available at: https://www.eea.europa.eu/themes/air/air-pollution-country-fact-sheets-2014/spain-air-pollutant-emissions-country-factsheet/at_download/file \(last access: 19 March 2019\), 2014.](https://www.eea.europa.eu/themes/air/air-pollution-country-fact-sheets-2014/spain-air-pollutant-emissions-country-factsheet/at_download/file)
- 15 EPA: Ireland's Air Pollutant Emissions 2016, available at: <http://www.epa.ie/pubs/reports/air/airemissions/irelandsairpollutantemissions2016.html> (last access: ~~15-19 September-March 20120198~~), 2018.
- Geddes, J. A., Martin, R. V., Boys, B. L., and van Donkelaar, A.: Long-term trends worldwide in ambient NO₂ concentrations inferred from satellite observations, *Environ. Health Perspect.*, 124, 281-289, doi:10.1289/ehp.1409567, 2016.
- Georgoulias, A. K., Alexandri, G., Kourtidis, K. A., Lelieveld, J., Zanis, P., and Amiridis, V.: Differences between the MODIS Collection 6 and 5.1 aerosol datasets over the greater Mediterranean region, *Atmos. Environ.*, 147, 310-319, doi:10.1016/j.atmosenv.2016.10.014, 2016.
- 25 [Ghude, S. D., Pfister, G. G., Jena, C., van der A, R., Emmons, L. K., and Kumar, R.: Satellite constraints of nitrogen oxide \(NO_x\) emissions from India based on OMI observations and WRF-Chem simulations, *Geophys. Res. Lett.*, 40, 423-428, doi:10.1002/grl.50065, 2013.](https://doi.org/10.1002/grl.50065)
- Hilboll, A., Richter, A., and Burrows, J. P.: Long-term changes of tropospheric NO₂ over megacities derived from multiple satellite instruments, *Atmos. Chem. Phys.*, 13, 4145-4169, doi:10.5194/acp-13-4145-2013, 2013.
- 30 Hilboll, A., Richter, A., and Burrows, J. P.: NO₂ pollution over India observed from space - the impact of rapid economic growth, and a recent decline, *Atmos. Chem. Phys. Discuss.*, doi:10.5194/acp-2017-101, in review, 2017.
- ICAC: Institute of Clean Air Companies, Selective Catalytic Reduction (SCR) control of NO_x emissions from fossil fuel-fired electric power plants, available at: https://c.ymcdn.com/sites/icac.site-ym.com/resource/resmgr/Standards_WhitePapers/SCR_WhitePaper_final_2009.pdf (last access: ~~15-19 September-March 20182019~~), 2009.

Formatted: Font: Not Italic

- IEA - Clean Coal Center report, available at: <https://www.iea-coal.org/wp-content/uploads/2017/12/spain-1> (last access: 19 March 2019), 2017.
- 5 Isaksen, I. S. A., Berntsen, T. K., Dalsøren, S. B., Eleftheratos, K., Orsolini, Y., Rognerud, B., Stordal, F., Søvde, O. A., Zerefos, C., Holmes, C. D.: Atmospheric Ozone and Methane in a Changing Climate, *Atmosphere*, 5(3), 518-535, doi:10.3390/atmos5030518.
- Koelemeijer, R. B. A., Stammes, P., Hovenier, J. W., and de Haan, J. F.: A fast method for retrieval of cloud parameters using oxygen A band measurements from the Global Ozone Monitoring Experiment, *J. Geophys. Res.*, 106, 3475-3490, doi:10.1029/2000JD900657, 2001.
- Konovalov, I. B., Beekmann, M., Richter, A., and Burrows, J. P.: Inverse modelling of the spatial distribution of NO_x emissions on a continental scale using satellite data, *Atmos. Chem. Phys.*, 6, 1747-1770, doi:10.5194/acp-6-1747-2006, 2006.
- 10 Konovalov, I. B., Beekmann, M., Burrows, J. P., and Richter, A.: Satellite measurement based estimates of decadal changes in European nitrogen oxides emissions, *Atmos. Chem. Phys.*, 8, 2623-2641, doi:10.5194/acp-8-2623-2008, 2008.
- Konovalov, I. B., Beekmann, M., Richter, A., Burrows, J. P., and Hilboll, A.: Multi-annual changes of NO_x emissions in megacity regions: nonlinear trend analysis of satellite measurement based estimates, *Atmos. Chem. Phys.*, 10, 8481-8498, doi:10.5194/acp-10-8481-2010, 2010.
- 15 Kourtidis, K., Stathopoulos, S., Georgoulas, A. K., Alexandri, G., and Rapsomanikis, S.: A study of the impact of synoptic weather conditions and water vapor on aerosol-cloud relationships over major urban clusters of China, *Atmos. Chem. Phys.*, 15, 10955-10964, doi:10.5194/acp-15-10955-2015, 2015.
- 20 Krotkov, N. A., McLinden, C. A., Li, C., Lamsal, L. N., Celarier, E. A., Marchenko, S. V., Swartz, W. H., Bucsela, E. J., Joiner, J., Duncan, B. N., Boersma, K. F., Veefkind, J. P., Levelt, P. F., Fioletov, V. E., Dickerson, R. R., He, H., Lu, Z., and Streets, D. G.: Aura OMI observations of regional SO₂ and NO₂ pollution changes from 2005 to 2015, *Atmos. Chem. Phys.*, 16, 4605-4629, doi:10.5194/acp-16-4605-2016, 2016.
- Lelieveld, J., Beirle, S., Hörmann, C., Stenichikov, G., and Wagner, T.: Abrupt recent trend changes in atmospheric nitrogen dioxide over the Middle East, *Sci. Adv.*, 1, 2-6, doi:10.1126/sciadv.1500498, 2015.
- 25 [Levelt, P. F., Joiner, J., Tamminen, J., Veefkind, J. P., Bhartia, P. K., Stein Zweers, D. C., Duncan, B. N., Streets, D. G., Eskes, H., van der A, R., McLinden, C., Fioletov, V., Carn, S., de Laat, J., DeLand, M., Marchenko, S., McPeters, R., Ziemke, J., Fu, D., Liu, X., Pickering, K., Apituley, A., González Abad, G., Arola, A., Boersma, F., Chan Miller, C., Chance, K., de Graaf, M., Hakkarainen, J., Hassinen, S., Jalongo, I., Kleipool, Q., Krotkov, N., Li, C., Lamsal, L., Newman, P., Nowlan, C., Suleiman, R., Tilstra, L. G., Torres, O., Wang, H., and Wargan, K.: The Ozone Monitoring Instrument: overview of 14 years in space, *Atmos. Chem. Phys.*, 18, 5699-5745, doi:10.5194/acp-18-5699-2018, 2018.](#)
- [Levelt, P. F., van den Oord, G. H. J., Dobber, M. R., Mälikki, A., Visser, H., de Vries, J., Stammes, P., Lundell, J., and Saari, H.: The Ozone Monitoring Instrument, *IEEE T. Geosci. Remote*, 44, 1093-1101, doi:10.1109/TGRS.2006.872333, 2006.](#)

- Liu, F., Zhang, Q., Ronald, J. van der A., Zheng, B., Tong, D., Yan, L., Zheng, Y., and He, K.: Recent reduction in NO_x emissions over China: synthesis of satellite observations and emission inventories, *Environ. Res. Lett.*, 11, 114002, doi:10.1088/1748-9326/11/11/114002, 2016.
- Lurmann, F., Avol, E., and Gilliland, F.: Emissions reduction policies and recent trends in Southern California's ambient air quality, *J. Air Waste Manag. Assoc.*, 65(3), 324-335, doi:10.1080/10962247.2014.991856, 2015.
- Mijling, B., van der A, R. J., Boersma, K. F., Van Roozendael, M., De Smedt, I., and Kelder, H. M.: Reductions in NO₂ detected from space during the 2008 Beijing Olympic Games, *Geophys. Res. Lett.*, 36, L13801, doi:10.1029/2009GL038943, 2009.
- [Munro, R., Lang, R., Klaes, D., Poli, G., Retscher, C., Lindstrot, R., Huckle, R., Lacan, A., Grzegorski, M., Holdak, A., Kokhanovsky, A., Livschitz, J., and Eisinger, M.: The GOME-2 instrument on the Metop series of satellites: instrument design, calibration, and level 1 data processing - an overview, *Atmos. Meas. Tech.*, 9, 1279-1301, doi:10.5194/amt-9-1279-2016, 2016.](#)
- Platt, U.: Differential optical absorption spectroscopy (DOAS), in: *Air Monitoring by Spectroscopic Techniques*, edited by: Sigrist, M. W., Vol. 127, John Wiley & Sons, Hoboken, N.J., USA, 27-83, 1994.
- Pozzer, A., de Meij, A., Yoon, J., Tost, H., Georgoulias, A. K., and Astitha, M.: AOD trends during 2001–2010 from observations and model simulations, *Atmos. Chem. Phys.*, 15, 5521-5535, doi:10.5194/acp-15-5521-2015, 2015.
- Russell, A. R., Valin, L. C., and Cohen, R. C.: Trends in OMI NO₂ observations over the United States: effects of emission control technology and the economic recession, *Atmos. Chem. Phys.*, 12, 12197-12209, doi:10.5194/acp-12-12197-2012, 2012.
- Schneider, P. and van der A, R. J.: A global single-sensor analysis of 2002-2011 tropospheric nitrogen dioxide trends observed from space, *J. Geophys. Res.*, 117, 1-17, doi:10.1029/2012JD017571, 2012.
- Schneider, P., Laho, W. A., and van der A, R.: Recent satellite-based trends of tropospheric nitrogen dioxide over large urban agglomerations worldwide, *Atmos. Chem. Phys.*, 15, 1205-1220, doi:10.5194/acp-15-1205-2015, 2015.
- Seinfeld, J. H. and Pandis, S. N.: *Atmospheric chemistry and physics: from air pollution to climate change*, Wiley, New Jersey, USA, 2016.
- Sogacheva, L., Rodriguez, E., Kolmonen, P., Virtanen, T. H., Saponaro, G., de Leeuw, G., Georgoulias, A. K., Alexandri, G., Kourtidis, K., and van der A, R. J.: Spatial and seasonal variations of aerosols over China from two decades of multi-satellite observations - Part 2: AOD time series for 1995-2017 combined from ATSR ADV and MODIS C6.1 and AOD tendency estimations, *Atmos. Chem. Phys.*, 18, 16631-16652, doi:10.5194/acp-18-16631-2018, 2018.
- Solomon, S., Portmann, R. W., Sanders, R. W., and Daniels, J. S.: On the role of nitrogen dioxide in the absorption of solar radiation, *J. Geophys. Res.*, 104(D10), 12047-12058, doi:10.1029/1999JD900035, 1999.
- Stammes, P.: Spectral radiance modelling in the UV-Visible range, in: *IRS 2000: Current Problems in Atmospheric Radiation*, edited by: Smith, W. L. and Timofeyev, Y. M., A. Deepak Publ., Hampton, VA, 385-388, 2001.

- Valks, P., Pinardi, G., Richter, A., Lambert, J.-C., Hao, N., Loyola, D., Van Roozendael, M., and Emmadi, S.: Operational total and tropospheric NO₂ column retrieval for GOME-2, *Atmos. Meas. Tech.*, 4, 1491-1514, doi:10.5194/amt-4-1491-2011, 2011.
- van der A, R. J., Peters, D. H. M. U., Eskes, H., Boersma, K. F., Van Roozendael, M., De Smedt, I., and Kelder, H. M.:
5 Detection of the trend and seasonal variation in tropospheric NO₂ over China, *J. Geophys. Res.*, 111, 1-10, doi:10.1029/2005JD006594, 2006.
- van der A, R. J., Eskes, H. J., Boersma, K. F., van Noije, T. P. C., Van Roozendael, M., De Smedt, I., Peters, D. H. M. U., and Meijer, E.W.: Trends, seasonal variability and dominant NO_x source derived from a ten year record of NO₂ measured from space, *J. Geophys. Res.*, 113, 1-12, doi:10.1029/2007JD009021, 2008.
- 10 van der A, R. J., Mijling, B., Ding, J., Koukouli, M. E., Liu, F., Li, Q., Mao, H., and Theys, N.: Cleaning up the air: effectiveness of air quality policy for SO₂ and NO_x emissions in China, *Atmos. Chem. Phys.*, 17, 1775-1789, doi:10.5194/acp-17-1775-2017, 2017.
- Vandaele, A. C., Fayt, C., Hendrick, F., Hermans, C., Humbled, F., Van Roozendael, M., Gil, M., Navarro, M., Puentedura, O., Yela, M., Braathen, G., Stebel, K., Tørnkvist, K., Johnston, P., Kreher, K., Goutail, F., Mieville, A., Pommereau, J.-P.,
15 Khaikine, S., Richter, A., Oetjen, H., Wittrock, F., Bugarski, S., Friess, U., Pfeilsticker, K., Sinreich, R., Wagner, T., Corlett, G., and Leigh, R.: An intercomparison campaign of ground-based UV-visible measurements of NO₂, BrO, and OClO slant columns: Methods of analysis and results for NO₂, *J. Geophys. Res.*, 110, D08305, doi:10.1029/2004JD005423, 2005.
- Veefkind, J. P., Aben, I., McMullan, K., Forster, H., de Vries, J., Otter, G., Claas, J., Eskes, H. J., de Haan, J. F., Kleipool, Q., van Weele, M., Hasekamp, O., Hoogeveen, R., Landgraf, J., Snel, R., Tol, P., Ingmann, P., Voors, R., Kruizinga, B.,
20 Vink, R., Visser, H., and Levelt, P. F.: TROPOMI on the ESA Sentinel-5 Precursor: a GMES mission for global observations of the atmospheric composition for climate, air quality and ozone layer applications, *Remote Sens. Environ.*, 120, 70-83, doi:10.1016/j.rse.2011.09.027, 2012.
- Vestreng, V., Ntziachristos, L., Semb, A., Reis, S., Isaksen, I. S. A., and Tarrasón, L.: Evolution of NO_x emissions in Europe with focus on road transport control measures, *Atmos. Chem. Phys.*, 9, 1503-1520, doi:10.5194/acp-9-1503-2009, 2009.
- 25 Vrekoussis, M., Richter, A., Hilboll, A., Burrows, J. P., Gerasopoulos, E., Lelieveld, J., Barrie, L., Zerefos, C., and Mihalopoulos, N.: Economic Crisis Detected from Space: Air Quality observations over Athens/Greece, *Geophys. Res. Lett.*, 40, 458-463, doi:10.1002/grl.50118, 2013.
- [Voulgarakis, A., Savage, N. H., Wild, O., Braesicke, P., Young, P. J., Carver, G. D., and Pyle, J. A.: Interannual variability of tropospheric composition: the influence of changes in emissions, meteorology and clouds. *Atmos. Chem. Phys.*, 10, 2491-2506, doi:10.5194/acp-10-2491-2010, 2010.](#)
- 30 [Wang, Y., Beirle, S., Lampel, J., Koukouli, M., De Smedt, I., Theys, N., Li, A., Wu, D., Xie, P., Liu, C., Van Roozendael, M., Stavrou, T., Müller, J. F., and Wagner, T.: Validation of OMI, GOME-2A and GOME-2B tropospheric NO₂, SO₂ and HCHO products using MAX-DOAS observations from 2011 to 2014 in Wuxi, China: investigation of the effects of](#)

- priori profiles and aerosols on the satellite products, *Atmos. Chem. Phys.*, 17, 5007-5033, doi:10.5194/acp-17-5007-2017, 2017.
- 5 Weatherhead, E. C., Reinsel, G. C., Tiao, G. C., Meng, X.-L., Choi, D., Cheang, W.-K., Keller, T., DeLuisi, J., Wuebbles, D. J., Kerr, J. B., Miller, A. J., Oltmans, S. J. and Frederick, J. E.: Factors affecting the detection of trends: Statistical considerations and applications to environmental data, *J. Geophys. Res.*, 103(D14), 17149, doi:10.1029/98JD00995, 1998.
- WHO: Health Aspects of Air Pollution with Particulate Matter, Ozone and Nitrogen Dioxide, World Health Organization, Bonn, Germany, 2003.
- World Bank Group: The Toll of War: The Economic and Social Consequences of the Conflict in Syria, available at: <https://openknowledge.worldbank.org/bitstream/handle/10986/27541/The%20Toll%20of%20War.pdf> (last access: [15-19 September-March 20182019](#)), 2017.
- 10 World Bank: <https://data.worldbank.org> (last access: [15-19 September-March 20182019](#)), [20182019](#).
- Wu, Y., Zhang, S., Hao, J., Liu, H., Wu, X., Hu, J., Walsh, M. P., Wallington, T. J., and Zhang, K. M. S.: Stevanovic, On-road vehicle emissions and their control in China: A review and outlook, *Sci. Total Environ.*, 574, 332-349, doi:10.1016/j.scitotenv.2016.09.040, 2017.
- 15 Zara, M., Boersma, K. F., De Smedt, I., Richter, A., Peters, E., van Geffen, J. H. G. M., Beirle, S., Wagner, T., Van Roozendaal, M., Marchenko, S., Lamsal, L. N., and Eskes, H. J.: Improved slant column density retrieval of nitrogen dioxide and formaldehyde for OMI and GOME-2A from QA4ECV: intercomparison, uncertainty characterisation, and trends, *Atmos. Meas. Tech.*, 11, 4033-4058, doi:10.5194/amt-11-4033-2018, 2018.
- Zhao, B., Wang, S. X., Liu, H., Xu, J. Y., Fu, K., Klimont, Z., Hao, J. M., He, K. B., Cofala, J., and Amann, M.: NOx emissions in China: historical trends and future perspectives, *Atmos. Chem. Phys.*, 13, 9869-9897, doi:10.5194/acp-13-9869-2013, 2013.
- 20
- 25
- 30

Table 1: Absolute trends (in 10^{15} molecules $\text{cm}^{-2} \text{yr}^{-1}$) and trends relative to the fitted mean of the first year (in $\% \text{yr}^{-1}$) with the corresponding uncertainties ($\pm 1\sigma$) for the period 4/1996-9/2017 for four regions of interest: ECH (eastern China), IPE (Iberian Peninsula), MEA (the Middle East) and SAM (south-eastern America). The year when a trend reversal was detected and the absolute and relative

trend for the sub-period before and the sub-period after the detected trend reversal are also given. The year of reversal is included in both sub-periods while the relative trends are calculated relative to the fitted mean of each sub-period's first year. Bold characters are used to indicate the year of reversal and the statistically significant trends at the 95% confidence level.

Region	Whole period			Before the reversal		After the reversal	
	Abs. trend	Rel. trend	Reversal	Abs. trend	Rel. trend	Abs. trend	Rel. trend
ECH	0.53±0.09	10.51±1.77	2011	0.88±0.09	31.27±3.18	-1.19±0.24	-6.59±1.30
IPE	-0.02±0.01	-0.94±0.39	2005	0.09±0.02	5.19±1.27	-0.09±0.01	-3.49±0.52
MEA	0.04±0.00	2.98±0.27	2012	0.04±0.00	3.74±0.39	-0.03±0.01	-1.64±0.49
SAM	0.03±0.00	2.43±0.42	2000	-0.07±0.03	-4.77±2.22	0.05±0.00	4.89±0.41

5

Table 2: The same as Table 1 but for countries. In order to save space only countries that exhibit a trend reversal are shown here, while results for all the world countries are given in Table S1 of the Supplement.

Country	Whole period			Before the reversal		After the reversal	
	Abs. trend	Rel. trend	Reversal	Abs. trend	Rel. trend	Abs. trend	Rel. trend
Afghanistan	0.0029±0.0018	0.6114±0.3768	2011	0.0102±0.0024	2.3918±0.5525	-0.0338±0.0089	-5.3566±1.4061
Albania	0.0209±0.0055	2.7604±0.7302	2012	0.0448±0.0073	7.3462±1.2018	-0.0672±0.0267	-5.4265±2.1563
Algeria	0.0017±0.0015	0.3706±0.3100	2012	0.0045±0.0022	1.0024±0.4884	-0.0233±0.0066	-4.0611±1.1504
Angola	-0.0049±0.0019	-0.4141±0.1591	2002	-0.0290±0.0127	-2.2477±0.9822	0.0020±0.0023	0.1877±0.2147
Argentina	0.0104±0.0032	1.7992±0.5478	2000	-0.0775±0.0159	-8.7719±1.8040	0.0234±0.0027	5.0152±0.5857
Armenia	0.0250±0.0035	4.3776±0.6215	2002	-0.0290±0.0117	-3.8537±1.5580	0.0304±0.0061	4.5818±0.9141
Australia	-0.0018±0.0021	-0.2923±0.3375	2012	0.0036±0.0027	0.6205±0.4608	-0.0477±0.0148	-6.7697±2.1079
Bermuda	-0.0228±0.0034	-2.4517±0.3647	2002	0.0066±0.0213	0.7575±2.4317	-0.0200±0.0052	-2.5897±0.6755
Brazil	0.0094±0.0024	1.4344±0.3684	2000	-0.0164±0.0219	-2.1790±2.9159	0.0147±0.0031	2.3642±0.4951
Bulgaria	0.0220±0.0058	1.3198±0.3489	2007	0.0576±0.0142	3.8716±0.9559	-0.0211±0.0139	-0.9824±0.6472
Burundi	0.0012±0.0040	0.1153±0.3651	2003	0.0270±0.0237	2.7809±2.4419	-0.012±0.0050	-1.0016±0.4169
Cambodia	0.0203±0.0042	2.6936±0.5543	2001	-0.0483±0.0242	-5.2500±2.6257	0.0255±0.0060	3.1563±0.7381
Cameroon	-0.0039±0.0033	-0.2747±0.2341	2009	0.0078±0.0063	0.5757±0.4651	-0.0272±0.0107	-1.8324±0.7201
Canada	-0.0054±0.0015	-1.2625±0.3547	2005	0.0120±0.0036	3.4985±1.0472	-0.0175±0.0029	-3.69±0.6161
Cape Verde	-0.0046±0.0021	-1.1166±0.4999	2012	0.0037±0.0028	1.0087±0.7792	-0.0456±0.0079	-10.6582±1.8546
Central African Republic	-0.0005±0.0046	-0.0343±0.3148	2009	0.0207±0.0081	1.5706±0.6150	-0.0447±0.0118	-2.7184±0.7187
Chile	0.0093±0.0024	2.4781±0.6342	2000	-0.0469±0.0246	-8.3516±4.3721	0.0178±0.0022	5.6681±0.6909
China	0.1191±0.0196	7.5499±1.2398	2011	0.1939±0.0196	17.6742±1.7839	-0.2872±0.0480	-6.2108±1.0379
Congo Democratic Republic	-0.0056±0.0024	-0.3605±0.1565	2009	0.0019±0.0043	0.1245±0.2862	-0.0263±0.0089	-1.6575±0.5613
Costa Rica	-0.0020±0.0026	-0.3007±0.3880	2002	-0.0494±0.0209	-5.9015±2.4891	0.0061±0.0025	1.0466±0.4383
Cyprus	0.0052±0.0050	0.3552±0.3362	2012	0.0137±0.0071	0.9659±0.5015	-0.0947±0.0222	-5.1421±1.2077
Czech Republic	-0.0377±0.0171	-0.8947±0.4055	2010	0.0109±0.0340	0.2764±0.8620	-0.1432±0.0434	-3.5321±1.0702
Djibouti	-0.0032±0.0017	-0.4467±0.2427	2002	-0.0510±0.0094	-5.8558±1.0823	0.0035±0.0021	0.5575±0.3414
East Timor	-0.0037±0.0032	-0.9943±0.8493	2006	0.0151±0.0093	5.4103±3.3292	-0.0252±0.0062	-5.2562±1.2851
Ecuador	0.0294±0.0024	7.4325±0.6026	2001	-0.0246±0.0185	-4.6569±3.5030	0.0327±0.0037	6.5174±0.7347
Egypt	0.0017±0.0025	0.1842±0.2703	2003	-0.0284±0.0125	-2.7923±1.2302	0.006±0.0034	0.6797±0.3837
El Salvador	0.0200±0.0049	1.7220±0.4242	2012	0.0251±0.0067	2.2340±0.5990	-0.0494±0.0329	-2.952±1.9641
Equatorial Guinea	0.0088±0.0044	0.9342±0.4636	2010	0.0252±0.0086	2.9906±1.0231	-0.0202±0.0110	-1.7862±0.9737
Federated State of Micronesia	-0.0001±0.0023	-0.2939±4.9102	2011	0.0109±0.0029	45.4599±12.3399	-0.0407±0.0104	-26.455±6.7765
French Guiana	-0.0033±0.0016	-1.8853±0.8973	2012	0.0032±0.0020	2.3543±1.4845	-0.0409±0.0106	-19.466±5.0652
FYROM	0.0506±0.0087	4.7737±0.8199	2011	0.0921±0.0127	11.2700±1.5584	-0.0382±0.0284	-1.9504±1.4509

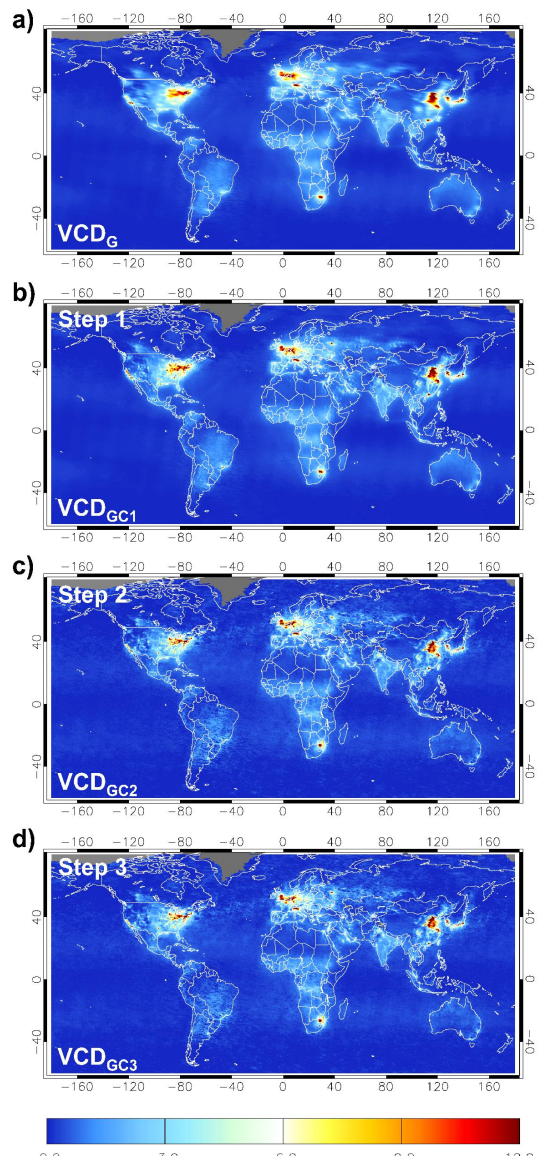
Gabon	0.0076±0.0025	0.7616±0.2480	2010	0.0168±0.0047	1.7778±0.4998	-0.0132±0.0066	-1.1266±0.5611
Georgia	0.0185±0.0030	3.3733±0.5425	2002	-0.0303±0.0167	-4.3192±2.3737	0.0231±0.0047	3.7750±0.7683
Greece	-0.0115±0.0050	-0.5762±0.2488	2012	0.0096±0.0065	0.5160±0.3497	-0.0804±0.02	-4.2204±1.0521
Guatemala	-0.0084±0.0030	-0.7180±0.2533	2006	-0.0305±0.0091	-2.4037±0.7162	0.0059±0.0049	0.5876±0.4919
Guyana	-0.0017±0.0016	-0.7935±0.7515	2011	0.0054±0.0023	3.1970±1.3736	-0.0273±0.0068	-10.6217±2.6354
Haiti	-0.0016±0.0025	-0.1687±0.2621	2005	-0.0278±0.0079	-2.5883±0.7390	0.0103±0.0044	1.200±0.5168
Honduras	0.0096±0.0027	1.3414±0.3820	2011	0.0132±0.0049	1.9054±0.7064	-0.0238±0.0103	-2.4065±1.0362
Hong Kong	-0.1302±0.0772	-0.7319±0.4341	2004	0.9438±0.3372	7.1514±2.5554	-0.5415±0.1310	-2.7016±0.6538
Iran	0.0320±0.0028	3.2601±0.2806	2012	0.0396±0.0039	4.2237±0.4127	-0.0193±0.0104	-1.2015±0.6469
Iraq	0.0638±0.0054	6.7853±0.5747	2010	0.0673±0.0077	7.3758±0.8428	-0.0509±0.0151	-2.1909±0.6517
Ireland	-0.0173±0.0117	-1.1594±0.7837	2008	0.0331±0.0304	2.6778±2.4644	-0.0604±0.0275	-4.1221±1.8770
Jordan	-0.0023±0.0030	-0.1431±0.1897	2012	0.0023±0.0041	0.1461±0.2623	-0.0786±0.0171	-4.4119±0.9570
Kazakhstan	0.0146±0.0017	2.8402±0.3358	2011	0.0214±0.0023	4.5142±0.4865	-0.0163±0.0088	-1.9778±1.0691
Kenya	0.0002±0.0030	0.0458±0.6632	2009	0.0132±0.0039	3.6187±1.0779	-0.0354±0.0101	-5.872±1.6733
Kiribati	-0.0047±0.0017	-4.8275±1.7292	2011	0.0030±0.0015	6.3332±3.1309	-0.0387±0.0085	-30.8337±6.7273
Korea Dem. Peoples Rep. of	0.0817±0.0146	10.7852±1.9232	2012	0.1409±0.0192	38.0448±5.1952	-0.2655±0.0958	-9.319±3.3648
Kuwait	0.1001±0.0071	3.7793±0.2697	2012	0.1027±0.0111	3.9036±0.4171	-0.0438±0.0420	-0.9225±0.8847
Laos Peoples Democratic Republic	0.0117±0.0037	1.4097±0.4467	2002	-0.0536±0.0177	-5.2885±1.7500	0.0156±0.0056	1.7881±0.6434
Lesotho	-0.008±0.0064	-0.5481±0.4428	2005	-0.0478±0.0220	-2.9513±1.3542	0.0074±0.0137	0.5805±1.0714
Madagascar	0.0000±0.0016	-0.0070±0.2623	2002	-0.0385±0.0096	-5.1708±1.2862	0.0055±0.0019	0.9849±0.3454
Malawi	-0.0014±0.0022	-0.1548±0.2420	2011	0.0042±0.0035	0.4749±0.3992	-0.0212±0.0071	-2.2921±0.7663
Maldives	-0.0043±0.0025	-1.9645±1.1350	2011	0.0116±0.0024	9.7829±2.0585	-0.0554±0.0079	-19.3643±2.7647
Malta	0.0177±0.0052	1.5767±0.4593	2006	0.0483±0.0142	5.1252±1.5113	-0.0349±0.0107	-2.1134±0.6484
Marshall Islands	-0.0035±0.0016	-3.0714±1.3829	2011	0.0034±0.0018	4.9668±2.6177	-0.0335±0.0062	-22.2594±4.0904
Mexico	0.0029±0.0022	0.2644±0.1982	2012	0.0094±0.0029	0.8960±0.2735	-0.0463±0.0126	-3.6619±0.9999
Mongolia	0.0001±0.0010	0.0302±0.5091	2000	-0.0251±0.0093	-9.2670±3.4436	0.0019±0.0012	1.1074±0.6748
Morocco (includes Western Sahara)	0.0046±0.0018	0.9063±0.3534	2012	0.0076±0.0027	1.5619±0.5433	-0.036±0.0072	-5.0847±1.0175
Namibia	-0.0096±0.0030	-1.0167±0.3168	2002	-0.0642±0.0196	-5.5977±1.7121	0.0004±0.0031	0.0461±0.3877
Netherland Antilles	0.0021±0.0025	0.3510±0.4331	2001	-0.0605±0.0147	-8.2963±2.0119	0.0015±0.0035	0.2542±0.5855
New Zealand	-0.0020±0.0015	-0.8321±0.6331	2002	-0.0275±0.0075	-8.7459±2.3723	0.0017±0.0024	0.9180±1.2578
Niger	-0.0019±0.0017	-0.3483±0.3195	2011	0.0018±0.0025	0.3571±0.4931	-0.0255±0.0085	-4.3612±1.4539
Northern Mariana Islands	0.0040±0.0021	3.2417±1.7180	2001	-0.0382±0.0101	-18.7322±4.9383	0.0038±0.0032	2.5953±2.1825
Occupied Palestinian Territory	-0.0290±0.0113	-0.4670±0.1826	2006	0.0314±0.0349	0.5336±0.5925	-0.0739±0.0238	-1.1904±0.3839
Oman	0.0014±0.0017	0.2335±0.2796	2011	0.0038±0.0029	0.6574±0.5016	-0.0191±0.0041	-2.7691±0.5890
Pakistan	0.0208±0.0030	2.3023±0.3363	2011	0.0335±0.0044	4.0560±0.5381	-0.0242±0.0088	-1.8079±0.6563
Palau	0.0004±0.0023	1.0487±6.5205	2011	0.0117±0.0034	35.1571±10.1795	-0.0263±0.0078	-28.3565±8.4076
Panama	0.0056±0.0021	0.9313±0.3520	2000	-0.0376±0.0245	-4.9519±3.2328	0.0112±0.0023	1.9829±0.4106
Papua New Guinea	-0.0011±0.0017	-0.4199±0.6719	2012	0.0045±0.0024	2.0089±1.0687	-0.0340±0.0077	-10.8245±2.4424
Paraguay	0.0184±0.0054	2.5541±0.7540	2000	-0.0602±0.0494	-5.7158±4.6892	0.0361±0.0060	6.2212±1.0286
Peru	0.0048±0.0023	1.0578±0.5008	2010	0.0139±0.0034	3.5134±0.8623	-0.0289±0.0077	-4.5065±1.195
Portugal	-0.008±0.0107	-0.4469±0.5982	2005	0.1169±0.0264	9.9875±2.2602	-0.0933±0.0158	-4.0221±0.6799
Puerto Rico	-0.0222±0.0035	-1.5354±0.2396	2005	0.0062±0.0121	0.4776±0.9298	-0.0490±0.0049	-3.375±0.3392
Qatar	0.0880±0.0086	2.8375±0.2772	2004	-0.0051±0.0286	-0.1483±0.8283	0.1094±0.0165	3.0132±0.4541
Republic of Moldova	0.0232±0.0078	1.3517±0.4519	2000	-0.1921±0.0619	-8.7806±2.8311	-0.0313±0.0105	1.8294±0.6159
Russia	0.0065±0.0018	1.2970±0.3503	2000	-0.0204±0.0072	-3.7857±1.3259	0.0053±0.0023	0.9787±0.4302
Saint Helena	0.002±0.0034	0.6229±1.0762	2000	-0.0944±0.0301	-16.3114±5.2061	0.0081±0.0041	3.2262±1.6367
Saint Vincent	-0.0024±0.0018	-0.6429±0.4857	2011	0.0054±0.0028	1.6802±0.8685	-0.0394±0.006	-8.7857±1.3412
Sao Tome and Principe	0.0043±0.0025	0.6455±0.3720	2010	0.0071±0.0048	1.1260±0.7615	-0.0182±0.008	-2.2260±0.9838
Saudi Arabia	0.0013±0.0020	0.1253±0.1958	2011	0.0007±0.0036	0.0715±0.3454	-0.0307±0.0049	-2.5586±0.4086
Senegal	-0.0013±0.0025	-0.1413±0.2828	2011	0.0057±0.0038	0.6671±0.4461	-0.0341±0.0122	-3.4912±1.2513
Seychelles	0.0100±0.0028	90.5183±25.5488	2000	-0.0344±0.0166	-98.5144±47.5564	0.0041±0.0035	3.5286±2.9576

Sierra Leone	-0.0019±0.0032	-0.1684±0.2927	2002	-0.0560±0.0244	-4.5381±1.9821	0.0001±0.0043	0.0064±0.3946
Solomon Islands	-0.0028±0.0017	-2.4917±1.5541	2011	0.0082±0.0015	19.3010±3.5311	-0.0456±0.0063	-24.4952±3.4029
Spain	-0.0291±0.0078	-1.2120±0.3263	2006	0.0588±0.0180	2.9974±0.9178	-0.0802±0.0109	-3.3243±0.4535
Sri Lanka	0.0102±0.0026	1.9198±0.4955	2012	0.0227±0.0032	5.0066±0.6998	-0.0346±0.0125	-4.5187±1.6306
Sweden	-0.0165±0.0085	-1.4335±0.7371	2010	0.0047±0.0157	0.4572±1.5157	-0.1017±0.0336	-8.0913±2.6696
Syrian Arab Republic	0.0188±0.0061	1.1265±0.3665	2012	0.0487±0.0069	3.2961±0.4683	-0.1024±0.0161	-4.7261±0.7427
Thailand	0.0185±0.0041	1.3299±0.2967	2001	-0.0844±0.0270	-5.1037±1.6331	0.0283±0.0054	2.0382±0.3893
Togo	-0.0025±0.0040	-0.1975±0.3190	2011	0.0159±0.0053	1.3835±0.4578	-0.0315±0.0243	-2.4742±1.9129
Trinidad and Tobago	0.0048±0.0030	0.7763±0.4876	2011	0.0121±0.0049	2.1233±0.8502	-0.0341±0.0128	-4.2440±1.5982
Tunisia	0.0075±0.0020	1.0234±0.2715	2012	0.0122±0.0027	1.7361±0.3808	-0.0419±0.0109	-4.2392±1.1033
Turkey	0.0152±0.0038	1.1898±0.2942	2012	0.0166±0.0057	1.3080±0.4521	-0.0136±0.0223	-0.8418±1.3730
Turkmenistan	0.0080±0.0018	1.3365±0.3058	2012	0.0126±0.0026	2.2023±0.4633	-0.0207±0.0092	-2.5887±1.1523
Ukraine	0.0230±0.0056	1.1157±0.2737	2000	-0.0999±0.0573	-4.3258±2.4805	0.0247±0.0072	1.1630±0.3410
United Arab Emirates	0.0408±0.0043	1.9971±0.2082	2008	0.0594±0.0101	3.0777±0.5209	-0.0076±0.0108	-0.2738±0.3884
United Rep. of Tanzania	0.0019±0.0025	0.2627±0.3447	2009	0.0120±0.0039	1.8099±0.5831	-0.0247±0.0092	-2.9026±1.0848
United States Virgin Islands	-0.0063±0.0028	-1.1100±0.5002	2010	0.0082±0.0051	1.6927±1.0481	-0.0431±0.0074	-7.0744±1.2163
Uruguay	0.01300±0.0035	2.1241±0.5704	2001	-0.0345±0.0231	-4.313±2.8919	0.0226±0.0047	3.915±0.8233
Viet Nam	0.0331±0.0036	4.5861±0.4982	2002	-0.0215±0.0188	-2.3865±2.0850	0.0409±0.0053	4.8399±0.6269
Western Samoa	-0.0043±0.0016	-2.9344±1.0942	2011	0.0006±0.0026	0.5205±2.1668	-0.0264±0.0064	-17.4793±4.2234
Yemen	0.0002±0.0021	0.0255±0.3355	2012	0.0053±0.0028	0.9131±0.4802	-0.0393±0.0086	-5.4864±1.2043

Table 3: The same as Table 1 but for megacities and large urban agglomerations.

Population hot spot/Country	Whole period			Before the reversal		After the reversal	
	Abs. trend	Rel. trend	Reversal	Abs. trend	Rel. trend	Abs. trend	Rel. trend
Algiers/Algeria	0.1067±0.0116	3.7546±0.4074	-	-	-	-	-
Athens/Greece	-0.1389±0.0168	-1.8511±0.2237	2010	-0.132±0.0335	-1.7603±0.447	0.035±0.0471	0.7368±0.9919
Atlanta/U.S.	-0.1877±0.0326	-1.9143±0.3322	2005	0.136±0.1209	1.6073±1.4295	-0.2712±0.0572	-3.1238±0.6591
Baghdad/Iraq	0.4167±0.0194	16.9512±0.7872	-	-	-	-	-
Bangalore/India	0.0563±0.0147	2.3736±0.6188	2000	-0.126±0.0812	-4.527±2.9187	0.0623±0.0198	2.4822±0.7882
Bangkok/Thailand	0.1027±0.0363	1.3366±0.4731	2000	-0.5126±0.2235	-5.455±2.3784	0.1551±0.047	2.0616±0.625
Beijing/China	1.3639±0.1846	6.3824±0.8637	2011	2.3336±0.254	15.0678±1.6398	-1.2832±0.7816	-2.7203±1.6568
Boston/U.S.	-0.6011±0.0732	-3.5023±0.4268	2002	0.1483±0.2827	0.9363±1.7853	-0.4863±0.1282	-3.8831±1.024
Buenos Aires/Argentina	-0.0413±0.0361	-0.4606±0.4019	2002	-0.6614±0.2381	-5.8305±2.0989	0.1378±0.0461	1.974±0.6599
Cairo/Egypt	0.2209±0.016	3.8884±0.2812	-	-	-	-	-
Chengdu/China	0.7192±0.0819	11.6631±1.3279	-	-	-	-	-
Chicago/U.S.	-0.4966±0.0533	-2.5189±0.2702	-	-	-	-	-
Chongqing/China	0.863±0.143	28.1051±4.6582	2011	1.2461±0.2767	223.2413±49.5666	-0.4668±0.6464	-2.2276±3.0848
Damascus/Syria	0.1039±0.0167	2.6515±0.4257	2012	0.1962±0.0189	5.8739±0.5662	-0.171±0.0602	-2.9206±1.0281
Delhi/India	0.1981±0.0295	3.0992±0.4618	-	-	-	-	-
Dhaka/Bangladesh	0.2928±0.0222	16.5686±1.258	-	-	-	-	-
Guangzhou/China	-0.0041±0.155	-0.0149±0.5593	-	-	-	-	-
Ho Chi Minh City/Vietnam	0.104±0.0118	6.0077±0.6825	-	-	-	-	-
Hong Kong	-0.1403±0.0719	-0.8636±0.4424	2004	0.6006±0.3238	4.5684±2.4632	-0.4253±0.1337	-2.4391±0.7669
Houston/U.S.	-0.1922±0.0385	-1.7269±0.346	-	-	-	-	-
Hyderabad/India	0.0736±0.01	3.6592±0.4981	-	-	-	-	-
Istanbul/Turkey	-0.1183±0.0612	-0.8412±0.4351	-	-	-	-	-
Jakarta/Indonesia	0.0543±0.0379	0.5536±0.3864	2010	-0.0552±0.0671	-0.5237±0.6366	0.6451±0.0971	7.955±1.1971
Jeddah/Saudi Arabia	0.1074±0.0212	1.9974±0.3951	2006	-0.0945±0.0455	-1.4672±0.7062	0.2892±0.0494	5.514±0.9424

Johannesburg/South Africa	-0.1095±0.0493	-0.6881±0.3097	2010	-0.0833±0.0924	-0.5267±0.5842	0.3505±0.108	2.8627±0.8819
Kabul/Afghanistan	0.1626±0.0108	59.1318±3.9214	-	-	-	-	-
Karachi/Pakistan	0.1457±0.0132	5.2117±0.4705	-	-	-	-	-
Khartoum/Sudan	0.0125±0.0005	1.0543±0.4192	2002	-0.0736±0.0361	-4.7861±2.3473	0.0349±0.0046	3.3235±0.4371
Kinshasa/ Congo Dem. Rep.	0.002±0.0142	0.0861±0.5987	2005	-0.107±0.044	-3.5497±1.4579	0.0785±0.0211	4.4886±1.2062
Kolkata/India	0.115±0.0101	3.9462±0.3476	-	-	-	-	-
Lagos/Nigeria	0.0986±0.0155	5.0244±0.7892	-	-	-	-	-
Lahore/India	0.2477±0.0319	7.0208±0.9033	2006	-0.2831±0.1796	-4.4953±2.8511	0.3106±0.0382	6.3906±0.7868
Lima/Peru	0.2048±0.0351	11.6431±1.9953	-	-	-	-	-
London/U.K.	-0.3299±0.0618	-1.7508±0.3279	-	-	-	-	-
Los Angeles/U.S.	-1.3409±0.1068	-3.0652±0.2441	2000	3.392±1.0294	10.2779±3.1192	-1.6087±0.1215	-3.8522±0.2909
Madras/India	0.0994±0.0111	4.1378±0.4618	-	-	-	-	-
Manila/Philippines	-0.1915±0.0414	-2.1756±0.4702	2009	-0.5284±0.0546	-4.9194±0.508	0.4866±0.0635	13.7662±1.7965
Melbourne/Australia	-0.052±0.022	-0.7551±0.319	-	-	-	-	-
Mexico City/Mexico	0.1705±0.0937	0.769±0.4226	-	-	-	-	-
Mumbai/India	0.1324±0.0155	3.2392±0.3794	-	-	-	-	-
Nagoya/Japan	-0.2919±0.0862	-1.4545±0.4292	-	-	-	-	-
Nairobi/Kenya	0.0544±0.0081	7.0624±1.0563	-	-	-	-	-
New York/U.S.	-0.702±0.0899	-2.2804±0.2922	-	-	-	-	-
Osaka/Japan	0.0597±0.0652	0.434±0.4741	2004	0.6195±0.2964	5.6022±2.6807	-0.3963±0.102	-2.1992±0.5659
Paris/France	-0.3628±0.0534	-1.9942±0.2935	-	-	-	-	-
Philadelphia/U.S.	-0.4594±0.0829	-2.3181±0.4184	-	-	-	-	-
Po Valley/Italy	-0.5378±0.0715	-2.2338±0.2972	-	-	-	-	-
Rhein-Ruhr/Germany	-0.2739±0.0546	-1.4319±0.2854	-	-	-	-	-
Rio de Janeiro/Brazil	-0.0515±0.0403	-0.5932±0.4648	2006	-0.3246±0.1396	-3.1932±1.3737	0.2083±0.0505	3.2112±0.7788
Riyadh/Saudi Arabia	0.2506±0.033	2.8057±0.369	-	-	-	-	-
San Francisco/U.S.	-0.1811±0.0182	-1.8484±0.1856	2000	0.4305±0.2047	5.7477±2.7329	-0.2823±0.0221	-2.7484±0.2153
Santiago/Chile	0.3821±0.045	6.7049±0.7905	2001	-0.4556±0.339	-5.2588±3.9133	0.5314±0.0571	8.9297±0.9588
Sao Paulo/Brazil	0.1778±0.0612	1.5499±0.5335	-	-	-	-	-
Seoul/Korea	-0.1644±0.1654	-0.4773±0.4804	-	-	-	-	-
Shanghai/China	0.5892±0.0897	2.7416±0.4176	2008	1.2375±0.1843	6.9126±1.0293	-0.3565±0.2454	-1.0754±0.7403
Shenyang/China	0.9094±0.0797	16.2605±1.4244	2011	1.2764±0.1153	38.5851±3.4841	-0.8018±0.368	-3.2729±1.5023
Shenzhen/China	-0.2418±0.1057	-1.1426±0.4996	2004	1.1553±0.4633	7.6024±3.0484	-0.8052±0.1728	-3.3769±0.7248
Sydney/Australia	-0.0155±0.0288	-0.2052±0.3805	-	-	-	-	-
Taipei/Taiwan	-0.0222±0.0505	-0.2457±0.5592	2005	0.3101±0.1729	4.2073±2.3458	-0.2798±0.1127	-2.5731±1.0366
Tehran/Iran	0.8143±0.055	8.58±0.5793	-	-	-	-	-
Tianjin/China	1.7816±0.1703	14.8844±1.4228	2011	2.6934±0.2402	42.6832±3.8066	-1.5974±0.4331	-3.3685±0.9134
Tokyo/Japan	0.0274±0.1295	0.1188±0.5607	2005	1.2691±0.5074	7.0772±2.8294	-0.5473±0.1592	-2.0107±0.5849
Washington/U.S.	-0.2128±0.0522	-1.6797±0.4117	-	-	-	-	-
Wuhan/China	0.5741±0.0544	7.0464±0.6676	2012	0.7595±0.0776	10.8972±1.1135	-0.4586±0.2236	-2.3492±1.1456

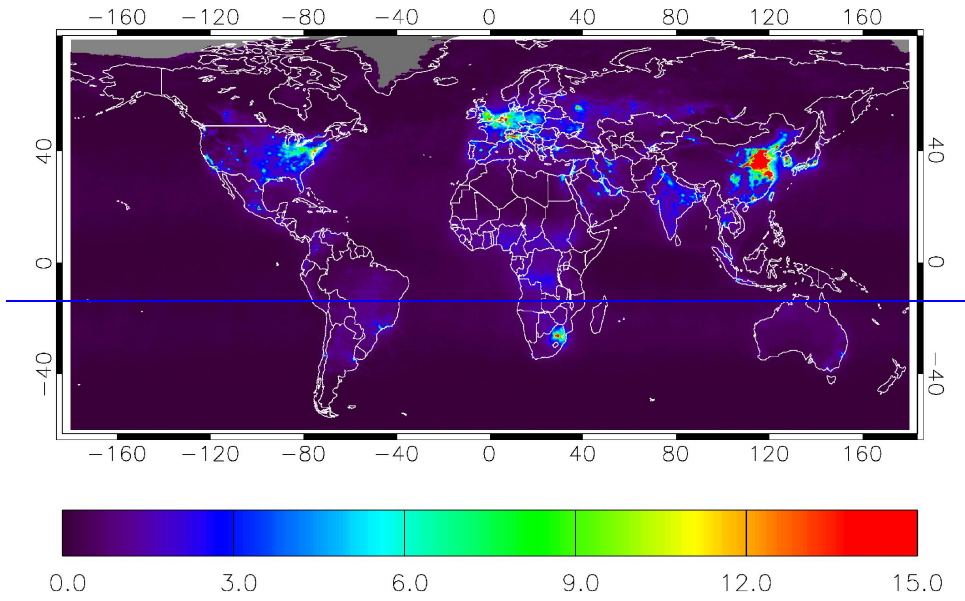


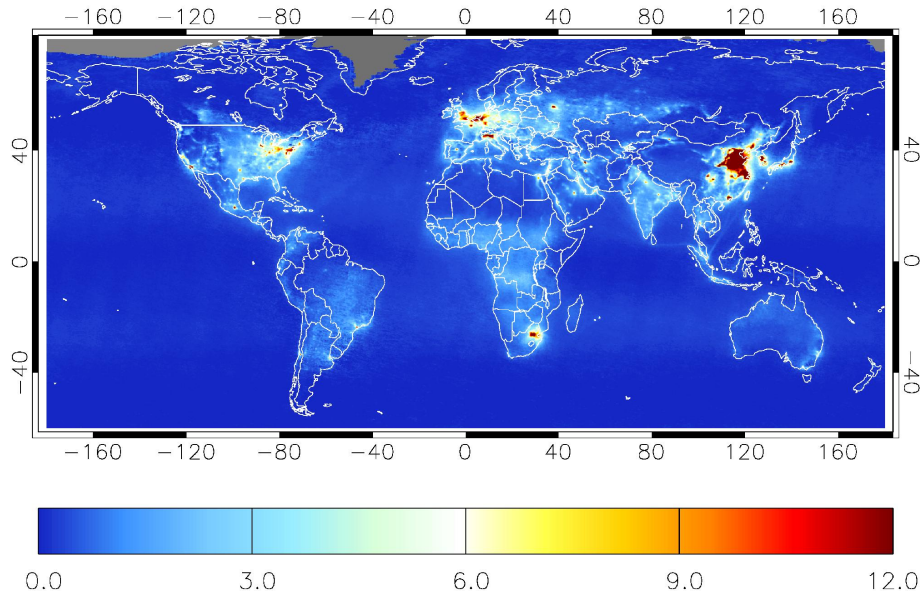
Formatted: Centered

Figure 1: GOME tropospheric NO₂ VCD (in 10¹⁵ molecules cm⁻²) patterns for the whole GOME period from the original (VCD_{G₀}) data (a), from the corrected in step 1 (VCDG_{C1}) data (b), from the corrected in step 2 (VCDG_{C2}) data (c) and from the corrected in step 3 (VCDG_{C3}) data (d).

Formatted: Subscript

Formatted: Subscript





Formatted: English (U.S.), Do not check spelling or grammar

Figure 12: Tropospheric NO₂ VCD (in 10¹⁵ molecules cm⁻²) patterns as seen using the self-consistent GOME, SCIAMACHY and GOME-2 dataset for the combined period (4/1996-9/2017).

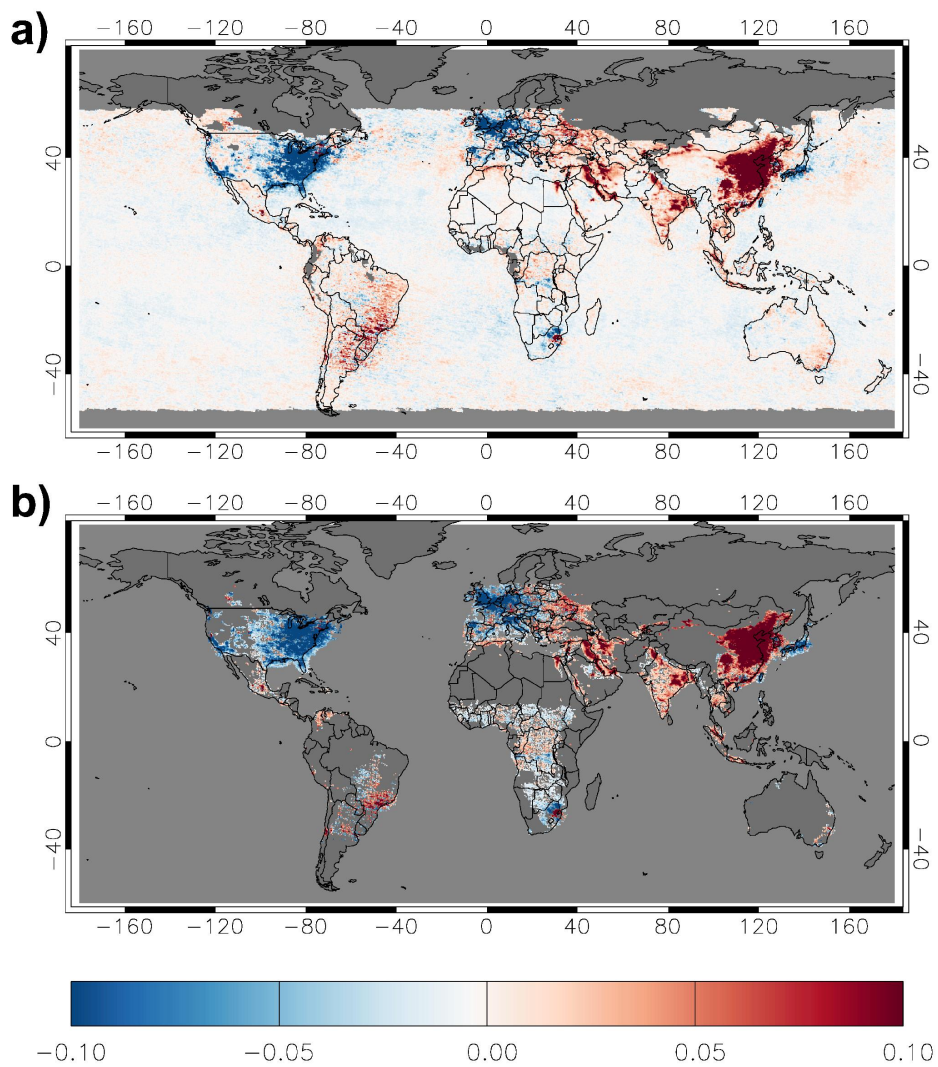
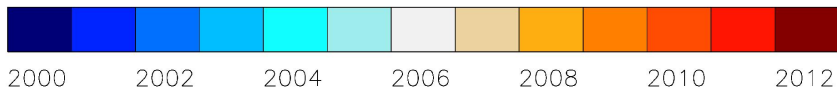
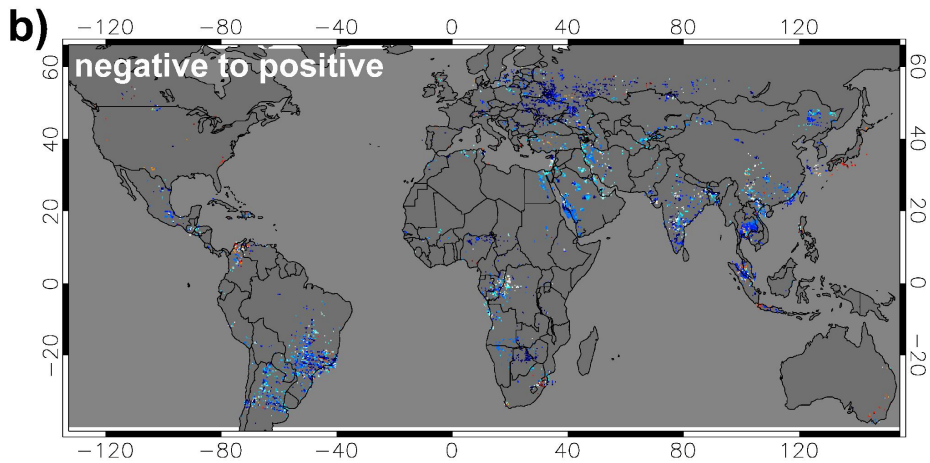
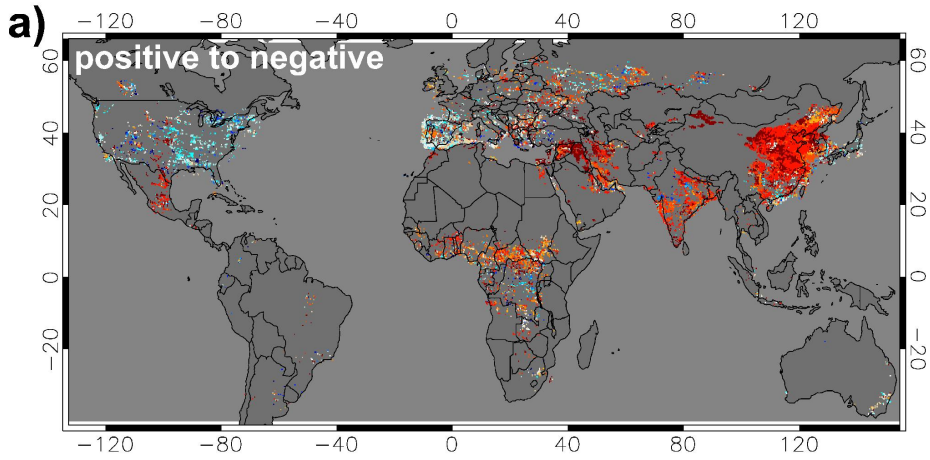


Figure 23: (a) Satellite-based trends of tropospheric NO₂ VCD (in 10^{15} molecules $\text{cm}^{-2} \text{yr}^{-1}$) for the period 4/1996-9/2017. Only trends calculated for timeseries with at least 8 months per year are taken into consideration. (b) Same as (a) but for statistically significant trends at the 95% confidence level and for grid cells with a long term tropospheric NO₂ VCD mean of at least 1×10^{15} molecules cm^{-2} .



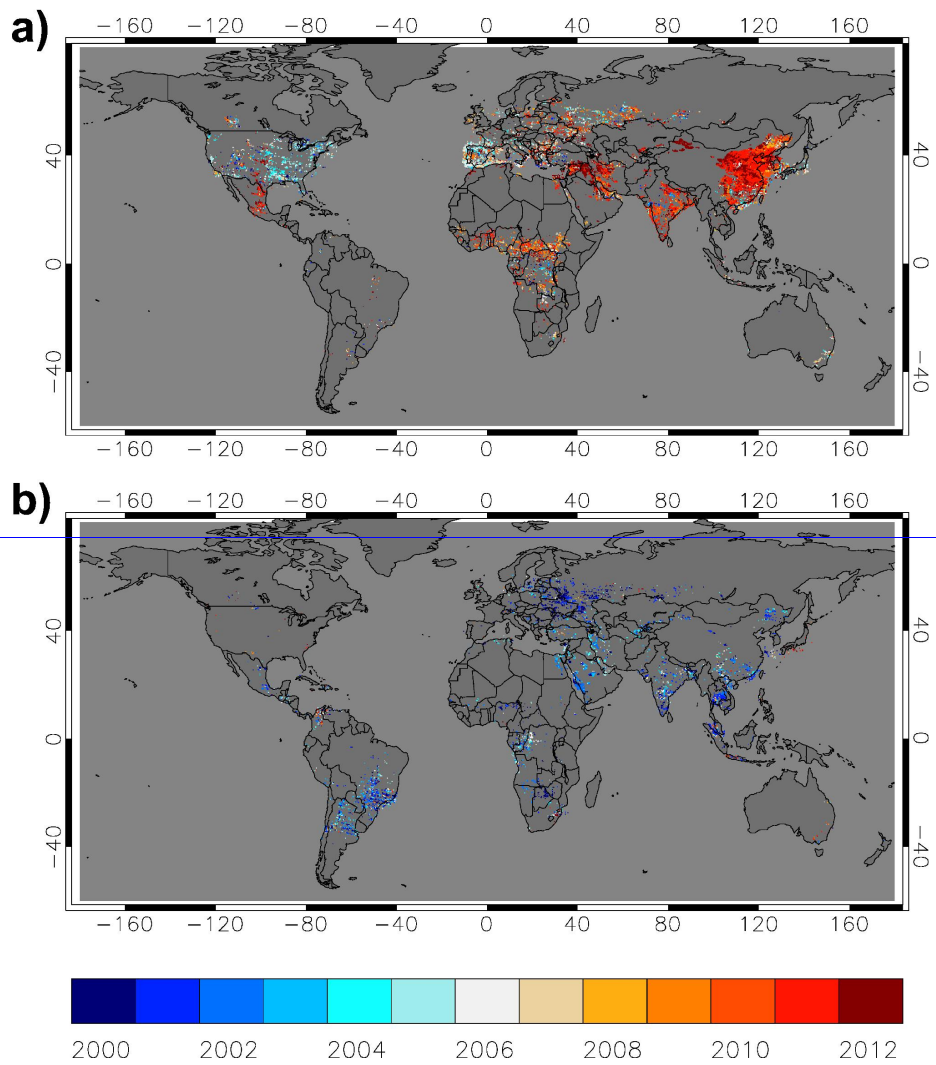
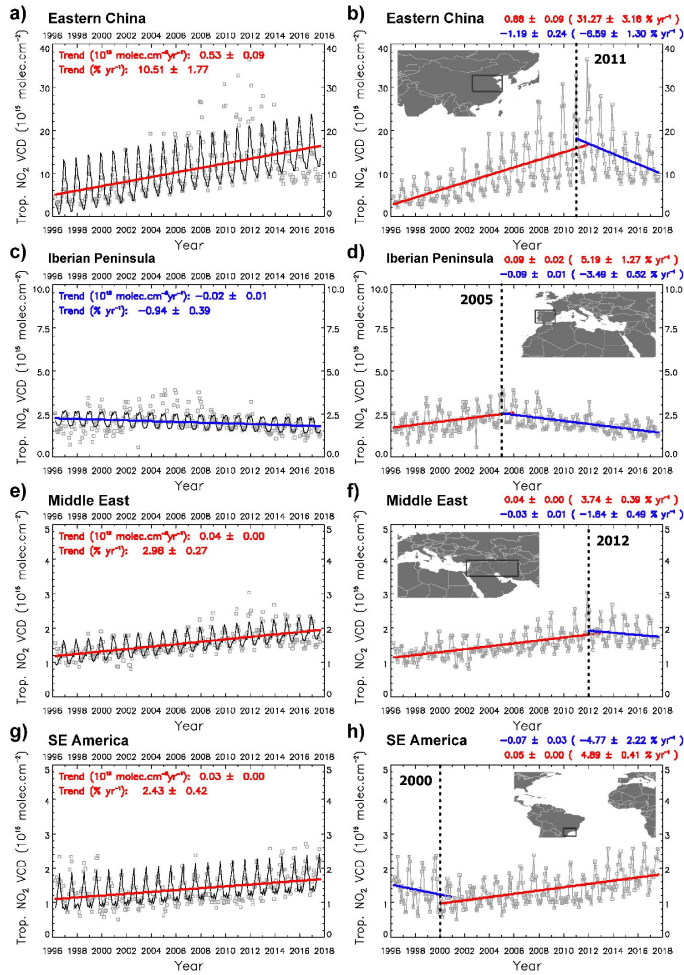


Figure 34: Year of tropospheric NO₂ VCD trend reversal from positive to negative (a) and from negative to positive (b). Only grid cells with a statistically significant trend at the 95% confidence level for the period before or after the year of reversal and with a long term tropospheric NO₂ VCD mean of at least 1×10^{15} molecules cm⁻² are shown.



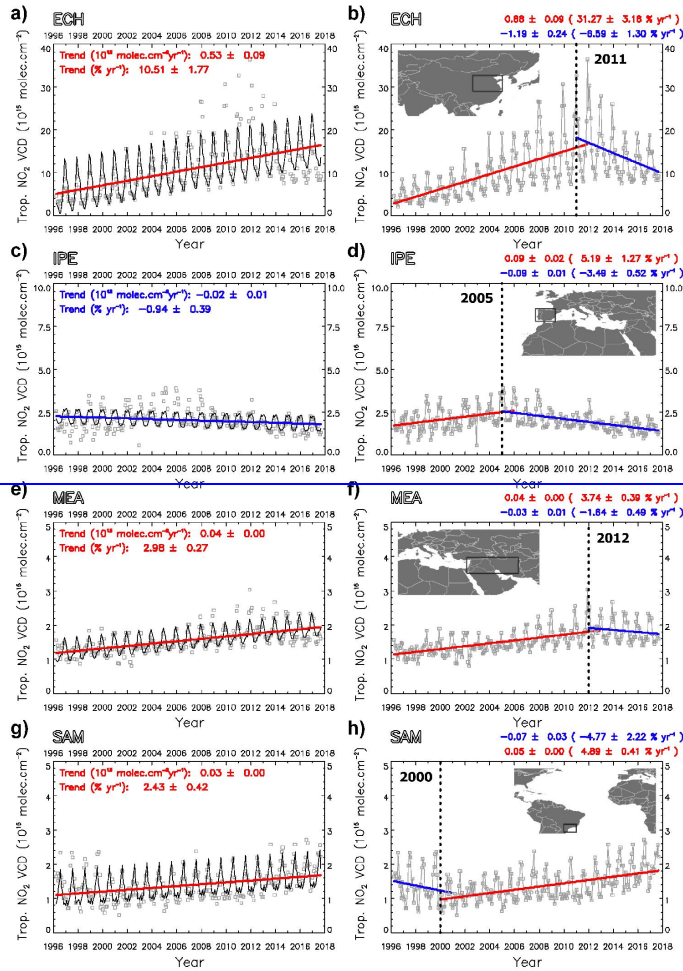


Figure 45: (Left column) satellite-based timeseries (grey colored points) of tropospheric NO₂ VCD for the period 4/1996-9/2017 for the eastern China (a), the Iberian Peninsula (c), the Middle East (e) and the south-eastern America (g). The black line depicts the fitted timeseries and the thick line depicts the trend (solid for statistically significant trends and dashed for statistically insignificant trends at the 95% confidence level / red color for positive trends and blue color for negative trends). The absolute trends (in 10¹⁵ molecules cm⁻² yr⁻¹) and the trends relative to the fitted mean of the first year (in % yr⁻¹) with the corresponding uncertainties (±1σ) are given on the plots. (Right column) satellite-based timeseries (grey colored points and lines) of tropospheric NO₂ VCD for the same regions. The thick lines, similarly to the left column panels, depict the trend for the sub-period before and the sub-period after the detected trend reversal (the year of reversal is included in both sub-periods). The year of the trend reversal is indicated with a thick dotted black line. The absolute trends and the trends relative to the fitted mean of the first year of the sub-periods (in parentheses) with the corresponding uncertainties are given on the plots (upper and lower lines correspond to the first and the second sub-period, respectively). The regions of interest are also shown on the panels.

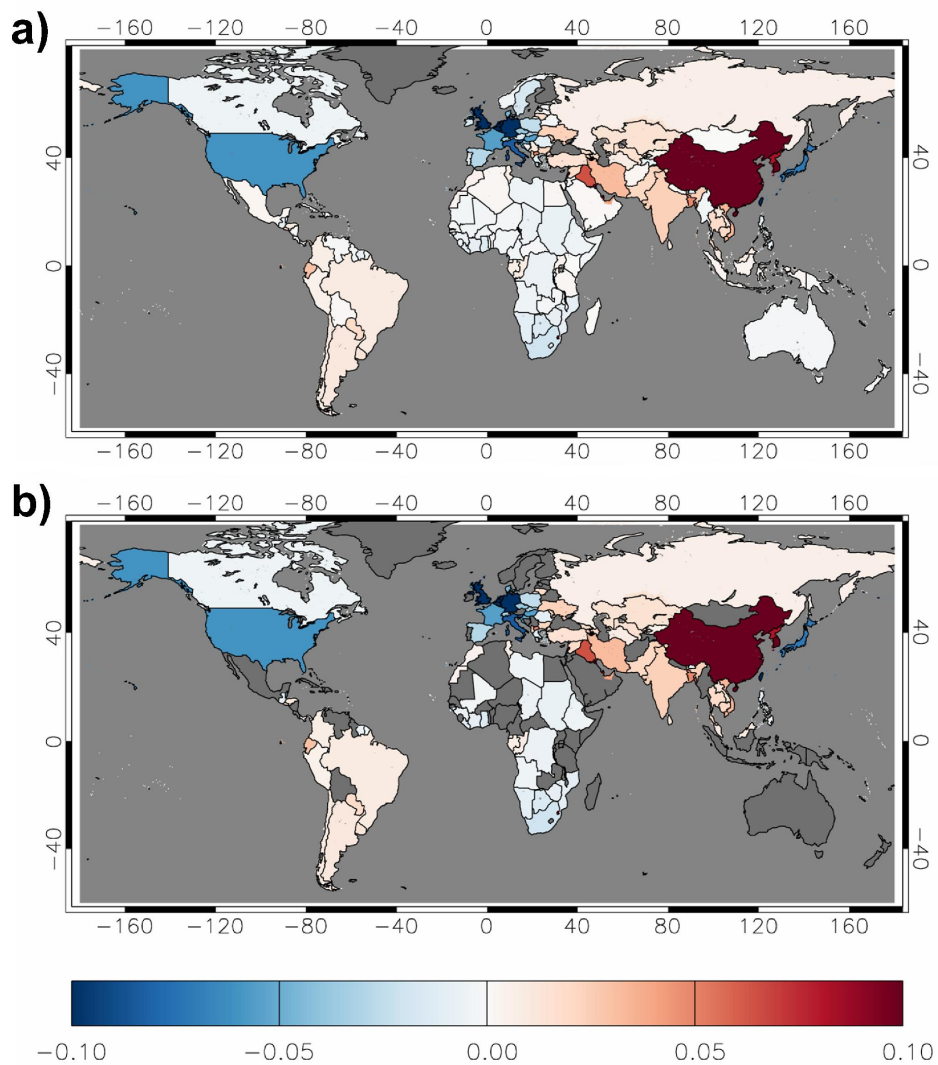
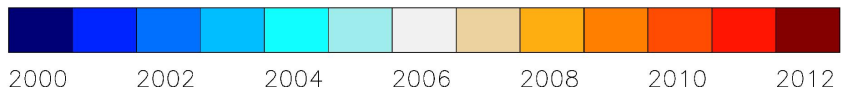
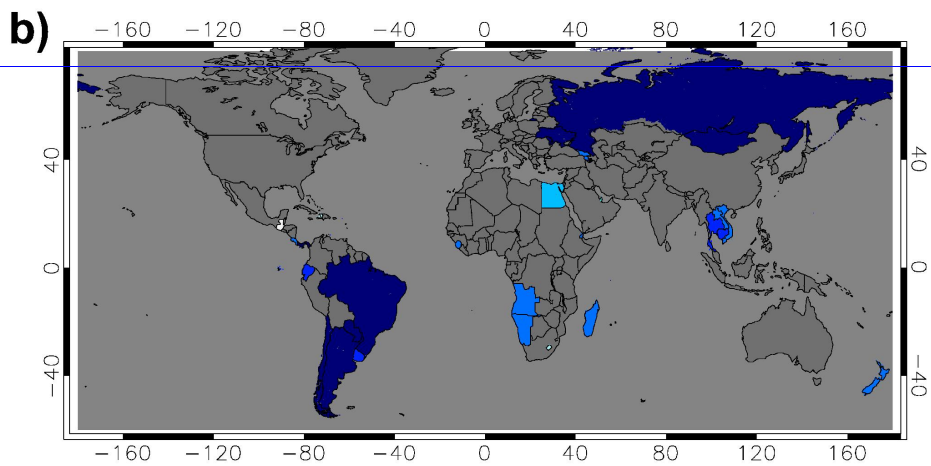
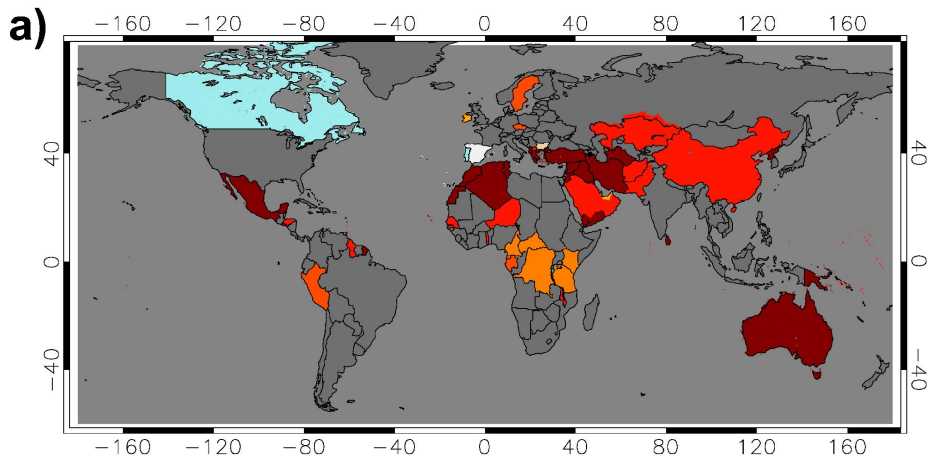


Figure 56: (a) Satellite-based trends of tropospheric NO₂ VCD (in 10¹⁵ molecules cm⁻² yr⁻¹) on a country basis for the period 4/1996-9/2017. Only trends calculated for timeseries with at least 8 months per year are taken into consideration. (b) Same as (a) but for statistically significant trends at the 95% confidence level.



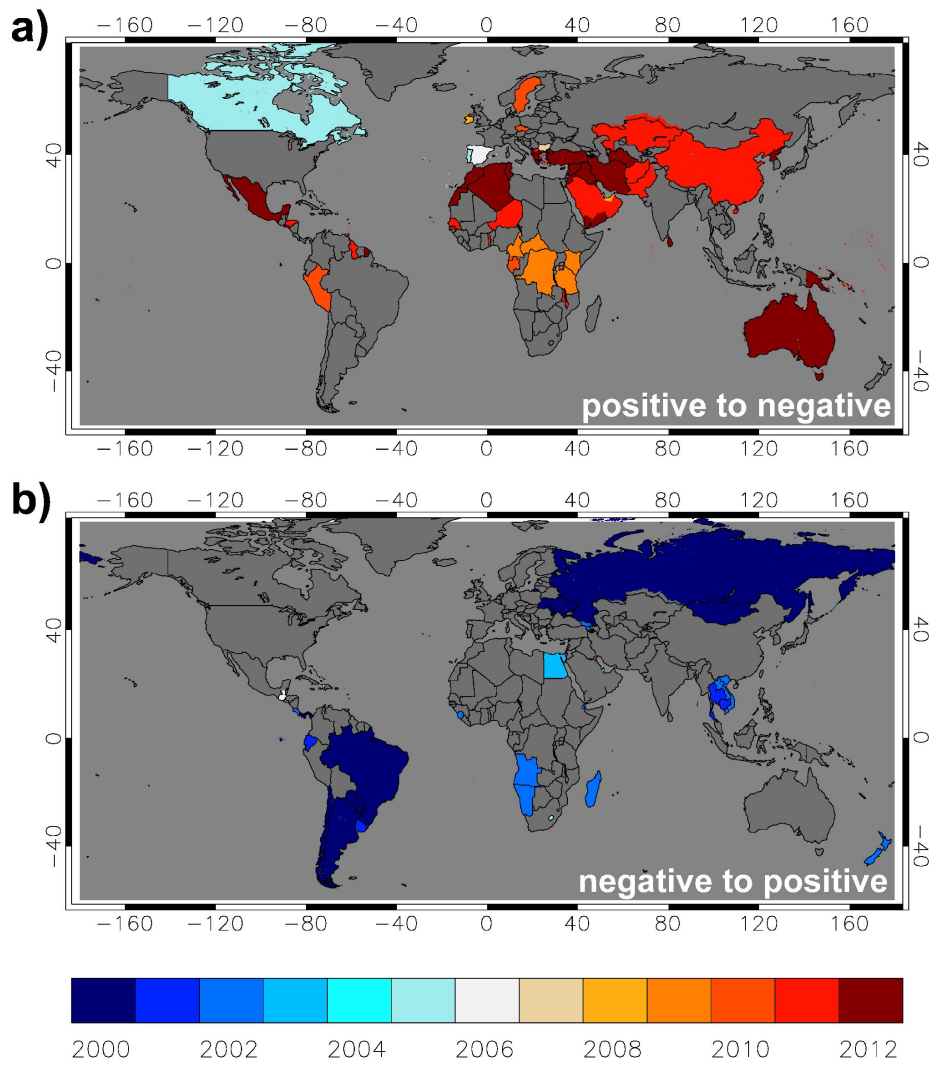
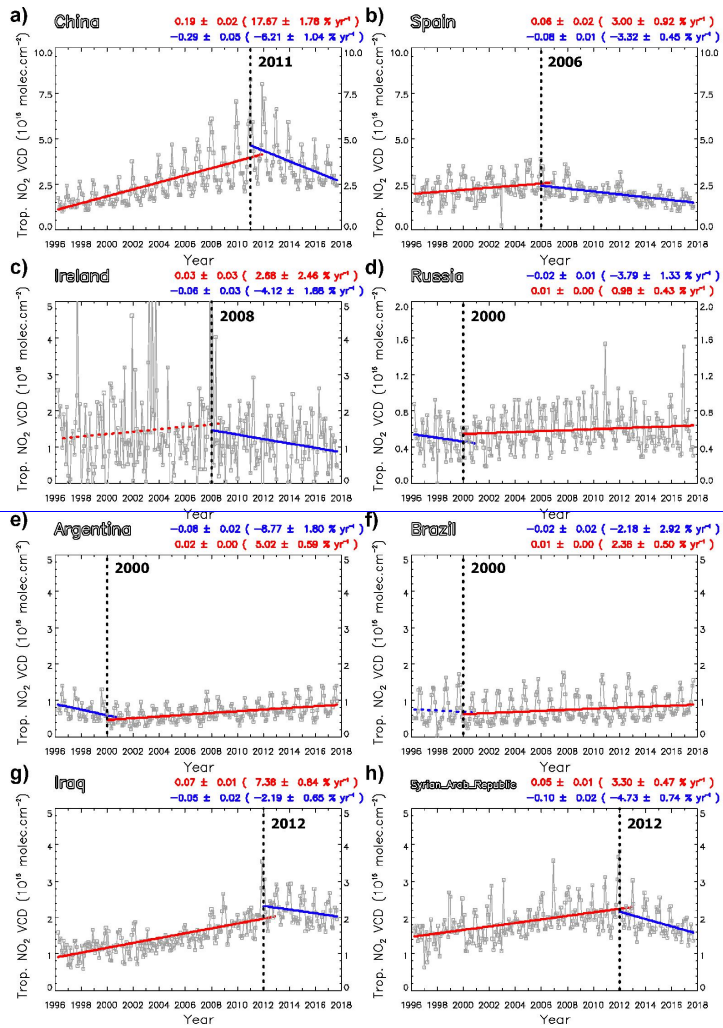


Figure 67: Year of tropospheric NO₂ VCD trend reversal from positive to negative (a) and from negative to positive (b) on a country level. Only countries with a statistically significant trend at the 95% confidence level for the period before or after the year of reversal are shown.



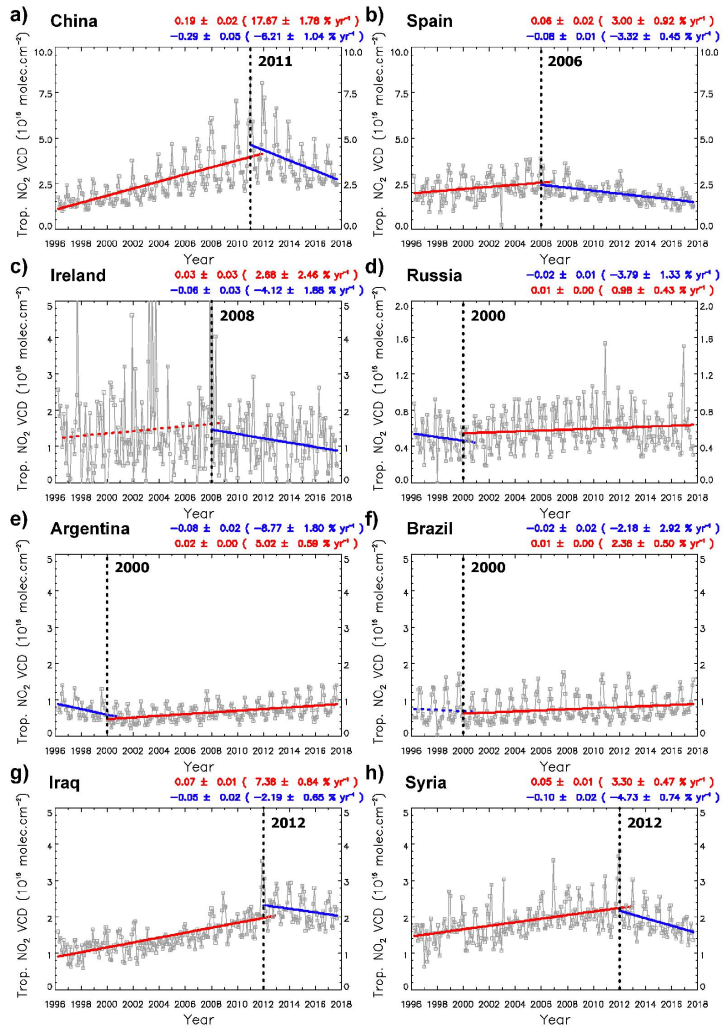


Figure 78: Satellite-based timeseries (grey colored points and lines) of tropospheric NO₂ VCD for the period 4/1996-9/2017 for China (a), Spain (b), Ireland (c), Russia (d), Argentina (e), Syria (f), Iraq (g) and Brazil (h). The thick lines depict the trend (solid for statistically significant trends and dashed for statistically insignificant trends at the 95% confidence level / red color for positive trends and blue color for negative trends) for the sub-period before and the sub-period after the detected trend reversal (the year of reversal is included in both sub-periods). The year of the trend reversal is indicated with a thick dotted black line. The absolute trends (in 10¹⁵ molecules cm⁻² yr⁻¹) and the trends (in % yr⁻¹) relative to the fitted mean of the first year of the sub-periods (in parentheses) with the corresponding uncertainties (±1σ) are given on the plots (upper and lower lines correspond to the first and the second sub-period, respectively).

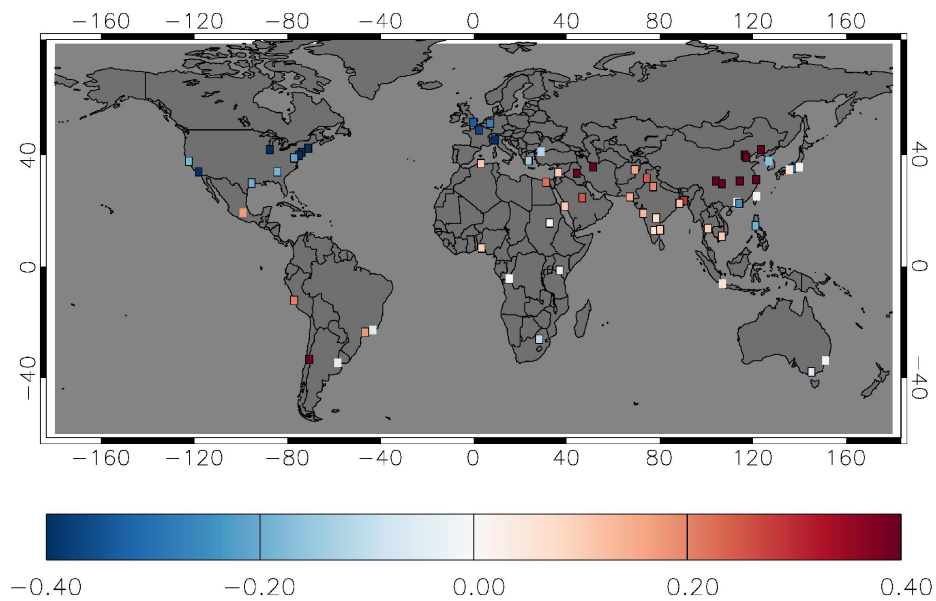
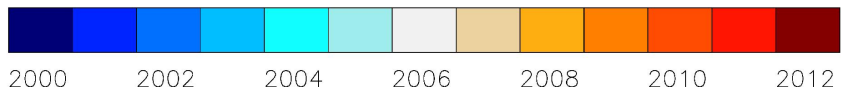
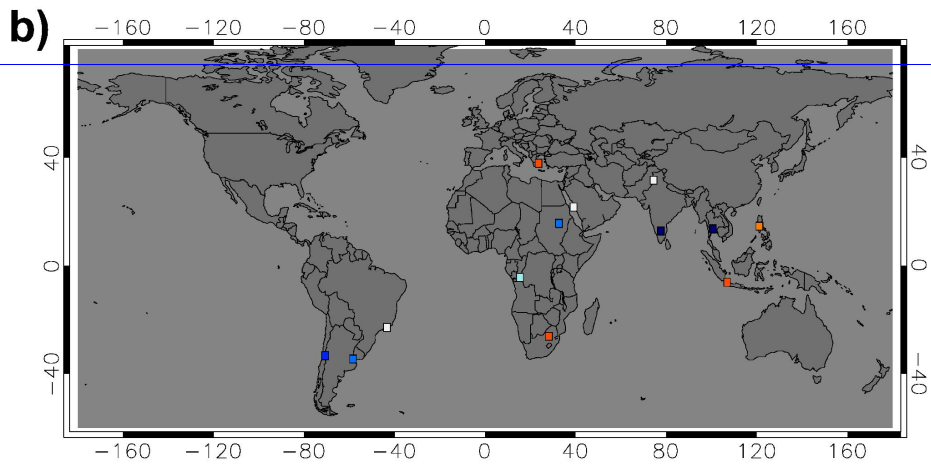
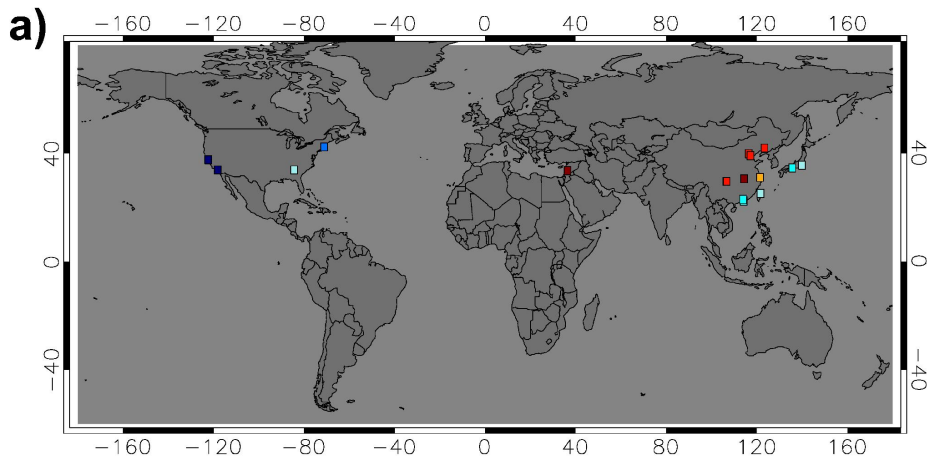


Figure 89: Satellite-based trends of tropospheric NO₂ VCD (in 10¹⁵ molecules cm⁻² yr⁻¹) for megacities and large urban agglomerations of the world for the period 4/1996-9/2017. The spots with a statistically significant trend at the 95% confidence level are marked with a black outline.

5

10

15



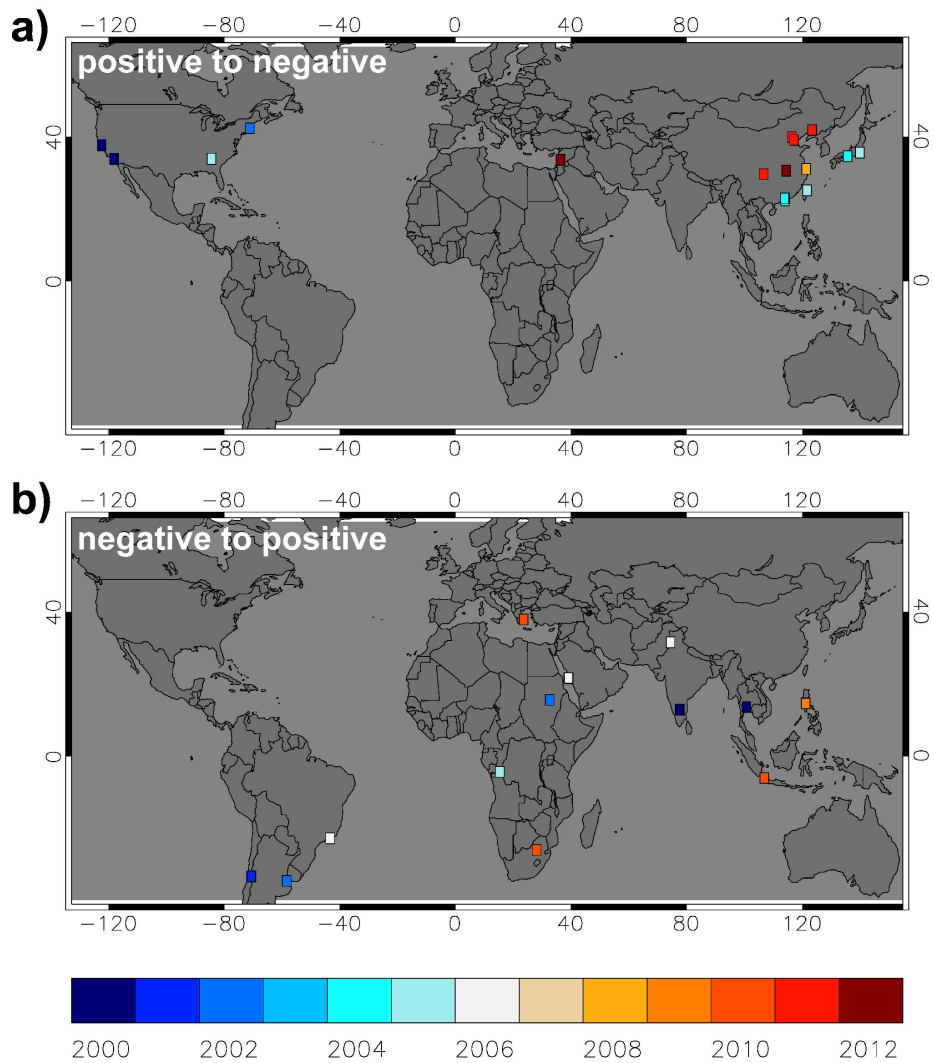
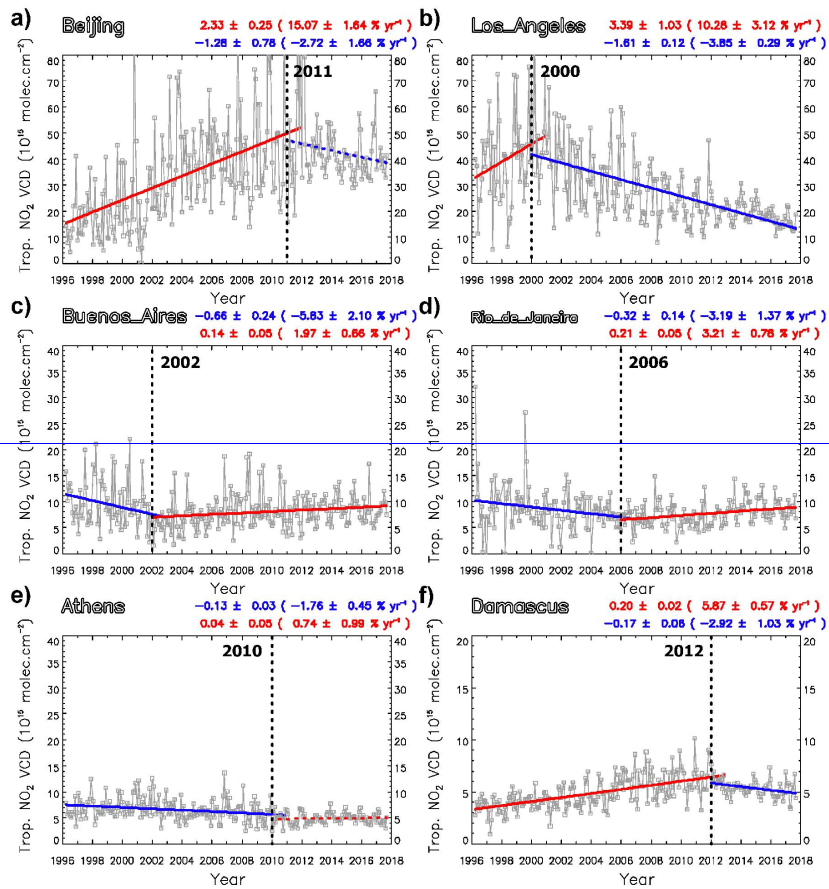


Figure 109: Year of tropospheric NO₂ VCD trend reversal from positive to negative (a) and from negative to positive (b) for megacities and large urban agglomerations of the world. Only spots with a statistically significant trend at the 95% confidence level for the period before or after the year of reversal are shown.



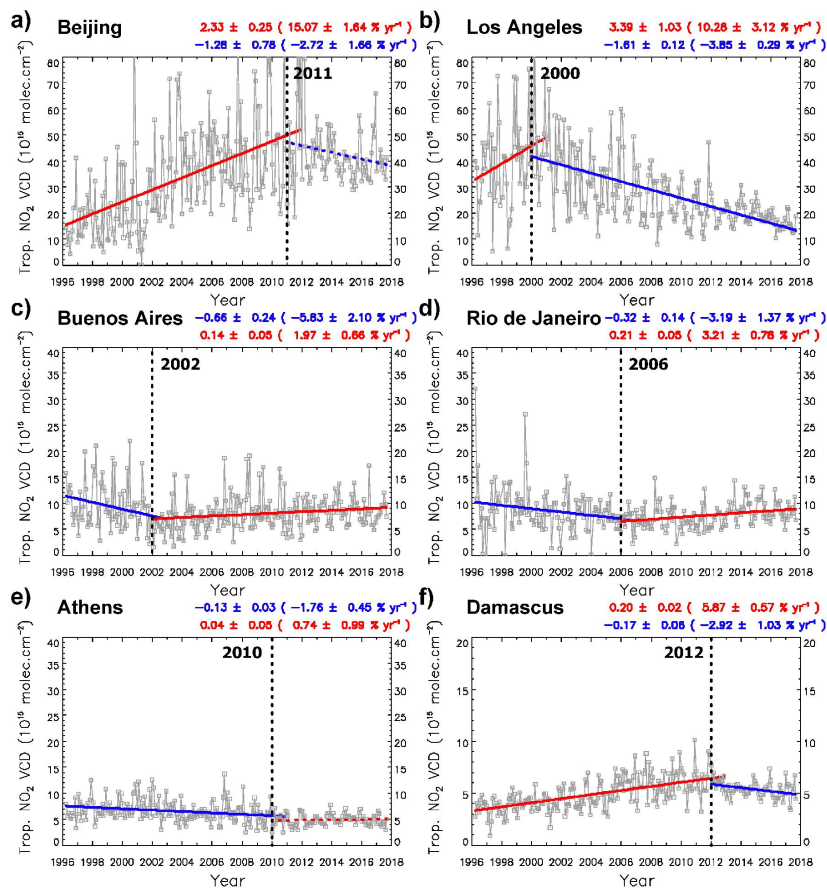


Figure 1011: The same as Fig. 7-8 but for (a) Beijing/China, (b) Los Angeles/U.S., (c) Buenos Aires/Argentina, (d) Rio de Janeiro/Brazil, (e) Athens/Greece and (f) Damascus/Syria.